Transcriptional profile of the mononuclear phagocyte system in the lungs

Inauguraldissertation

zur Erlangung des Grades eines Doktors der Humanbiologie

des Fachbereichs Medizin

der Justus-Liebig-Universität Gießen

vorgelegt von

Zbigniew Jan Zasłona

aus Warschau, Polen

Gießen 2009

Aus dem Zentrum für Innere Medizin
des Klinikums der Justus-Liebig-Universität Gießen
Direktor: Prof. Dr. W. Seeger

Gutachter: Prof. Dr. Jürgen Lohmeyer

Gutachter: Prof. Dr. Klaus Preissner

Tag der Disputation:

23.03.2010

I. Table of Contents

II. List of Figures

III. Abbreviations

A	absorption
Ab	antibody
AEC	alveolar epithelial cells
AMΦ	alveolar macrophages
APC	allophycocyanin
APS	ammonium persulfate
ATP	adenosine triphosphate
BAL(F)	bronchoalveolar lavage (fluid)
bp	base pairs
CCL	CC chemokine ligand
CD	cluster of differentiation
cDNA	complementary DNA
CFSE	carboxyfluorescein succinimidyl ester
Cx3cr1	chemokine (C-X3-C) receptor 1
Cy	cyanine
DC	dendritic cells
dNTP	deoxynucleotide triphosphate
dH_2O	distilled water
DTT	dithiothreitol
ECM	extracellular matrix
EDTA	ethylenediaminetetraacetic acid
ELISA	enzyme-linked immunosorbent assay
FACS	fluorescent-activated cell sorting
FCS	fetal calf serum
FITC	fluorescein-iso-thiocyanate
Flt3L	fms-like tyrosine kinase-3 ligand
FSC	forward scatter
FW	forward
gapdh	glyceraldehyde-3-phosphate dehydrogenase

GM-CSF	granulocyte-macrophage colony stimulating factor
GO	gene ontology
gzm	granzyme
HMBS	hydroxymethylbilane synthase
HBSS	Hank's balanced salt solution
htr2	serotonin receptor type 2
IgG	immunoglobulin G
il	interleukin
iMΦ	lung interstitial macrophages
ko	knock out
LPS	lipopolysaccharide
Ly6C	lymphocyte antigen 6 complex
MΦ	macrophages
mAb	monoclonal antibody
MCSF	macrophage colony-stimulating factor
MDP	macrophage and dendritic cell precursor
MHC II	major histocompatibility complex type II
MIP-2	macrophage inflammatory protein 2
MMLV	Moloney murine leukemia virus
MMP	matrix metalloproteinase
MPS	mononuclear phagocyte system
mRNA	messenger RNA
n.d.	not detected
NK	natural killer
n.s.	not significant
nt5e	Ecto-5-prime-nucleotidase (CD73)
OVA	ovalbumin
PBMo	peripheral blood monocytes
$PBS^{-/-}$	phosphate-buffered saline without Ca^{2+} and Mg^{2+}
PCR	polymerase chain reaction
pDC	plasmacytoid DC

PE	phycoerythrin
PMN	polymorphonuclear leukocyte
ptges	prostaglandin E synthase
qPCR	quantitative polymerase chain reaction
rAMΦ	resident alveolar macrophages
rpm	revolutions per minute
RPMI-1640	Roswell Park Memorial Institute, culture medium 1640
RT	room temperature
RT-PCR	reverse transcription-polymerase chain reaction
RV	reverse
SD	standard deviation
SDS	sodium dodecyl-sulfate
SEM	standard error of the mean
Siglec-H	sialic acid binding immunoglobulin-like lectin H
sphk1	sphingosine kinase 1
spp1	secreted phosphoprotein 1 (osteopontin)
SSC	side scatter
Tris	tris(hydroxymethyl)aminomethane
TGF-β	transforming growth factor-beta
TLR	Toll-like receptor
TNF-α	tumour necrosis factor-alpha
wt	wild type
5-HT	5-hydroxytryptamine (serotonin)

1. Introduction

1.1 The mononuclear phagocyte system

Phagocytic cells were in the past classified as the reticuloendothelial system, but this system did not distinguish between endothelial cells and macrophages (MΦ), so now the mononuclear phagocyte system (MPS) classification includes only MΦ and their monocyte and lineage precursors [1]. Developing MΦ are first found in the yolk sack, as identified by morphological characteristics, as well as macrophage markers. Studies in zebrafish have demonstrated that precursor MΦ from yolk differentiate, and emigrate into the head mesenchyme and the associated circulation [2]. Later in development, hematopoiesis in the fetal liver becomes a source of MΦ which resemble MΦ found in adults. Initially hematopoiesis in the liver generates large numbers of MΦ, which are present in most organs [1] (Fig. 1).

The tissue microenvironment can clearly influence the phenotype of tissue resident MΦ. The heterogeneity reflects the specialization of function that is adopted by MΦ in different anatomical locations [1]. Alveolar MΦ with high expression of scavenger and pattern recognition receptors [3], gut MΦ from the *lamina propria* with high bactericidal activity but very weak proinflammtory cytokine production [4] or Borowicz-Kupffer cells from the liver with high capacity for phagocytosis of complement system coated pathogens [5] all have different locations, and very different functions, but probably the same precursors.

Many studies indicate that although monocytes can be precursors for the replenishment of tissues resident MΦ, many MΦ might be derived by local proliferation, rather than from recruited peripheral monocytes. This local proliferation may play considerable role under steady state setting, but under inflammatory conditions, repopulation of tissue resident MΦ in inflamed tissues is certainly more dependent on the recruitment of precursor cells from the blood [1]. The question, however whether tissue MΦ are derived from a particular lineage dedicated only to be precursors for macrophages or rather from a more randomly selected circulating monocyte pool has not been clarified.

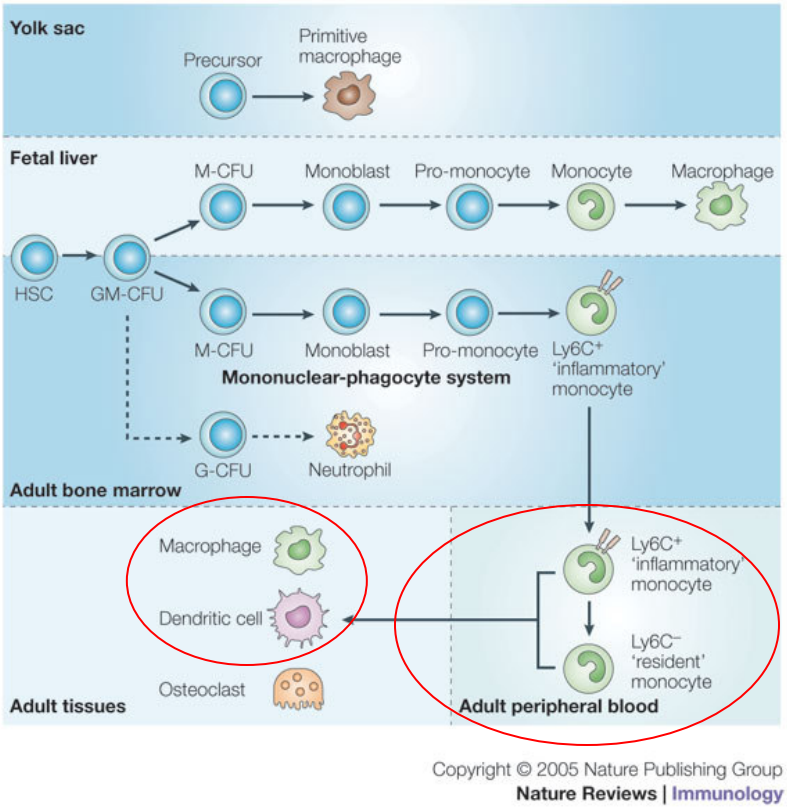

Figure 1. The development and members of the mononuclear phagocyte system. Adapted from Gordon and Taylor 2005 [1]. M-CSF-macrophage colony stimulating factor, HSC-hematopoietic stem cell, GM-CFU-granulocyte/macrophage colony forming unit, M-CFU-macrophage colony forming unit, G-CFU-granulocyte colony forming unit. In red circles highlighted cells investigates in the study.

1.1.1 Monocytes

Monocytes represent 10% of all leukocytes in human blood, and 4% of all leukocytes in mouse blood. Studying their function in biological processes is a difficult mission, because monocytes permanently survey the body environment and react to a variety of stimuli [6]. The best known function of monocytes is the ability to be a systemic reservoir of myeloid precursor cells for the renewal of some tissue MΦ and antigen presenting dendritic cells (DC) [7]. This differentiation of monocytes into DC, however, was studied primarily under inflammatory conditions. Another important role for monocytes is maintaining blood homeostasis, partly through the elimination of apoptotic cells and scavenging of toxic compounds [8], since monocytes are equipped with a wide spectrum of scavenger receptors that recognize microorganisms but also lipids of dying cells [9].

Monocytes can produce large amounts of inflammatory mediators that participate in the defense against pathogens [9] and in the pathogenesis of several inflammatory diseases, such as arthritis and atherosclerosis [10].

Mouse peripheral blood monocytes (PBMo) are identified in blood based on FSC/SSC (forward/site scatter) profile and the expression of CD115, F4/80 and CD11b. Mouse monocytes consist of two main subsets. The "inflammatory" subset expresses Ly6C ($GR1^+$), CCR2, L-selectin (CD62) and low level of CX3CR1 [7]. Inflammatory monocytes are selectively recruited to inflamed tissue [11] and lymph nodes [12] and produce high amounts of tumor necrosis factor (TNF)-α and Interleukin (IL)-1 during infection or tissue damage [9, 13]. A second subset of monocytes, often called "resident" monocytes is characterized by lack of expression of Ly6C ($GR1^-$), CCR2 and L-selectin, and by high expression of CX3CR1, LFA-1 and CD43 [7, 14]. This subset has a longer half-life than inflammatory monocytes, and is found in resting, as well as in inflamed tissues.

1.1.2 Monocytes are precursors for lung macrophages and lung dendritic cells

According to present knowledge, most investigators believe that monocytes, many subsets of MΦ and DC originate from a common myeloid precursor [15]. Among myeloid precursors, the macrophage and dendritic cell precursor (MDP) was identified as a subset of bone marrow proliferating cells that gives rise to monocytes, which are an intermediate cell type for DC and MΦ, but also generates some of DC subpopulations directly [6, 15, 16] (Fig. 2).

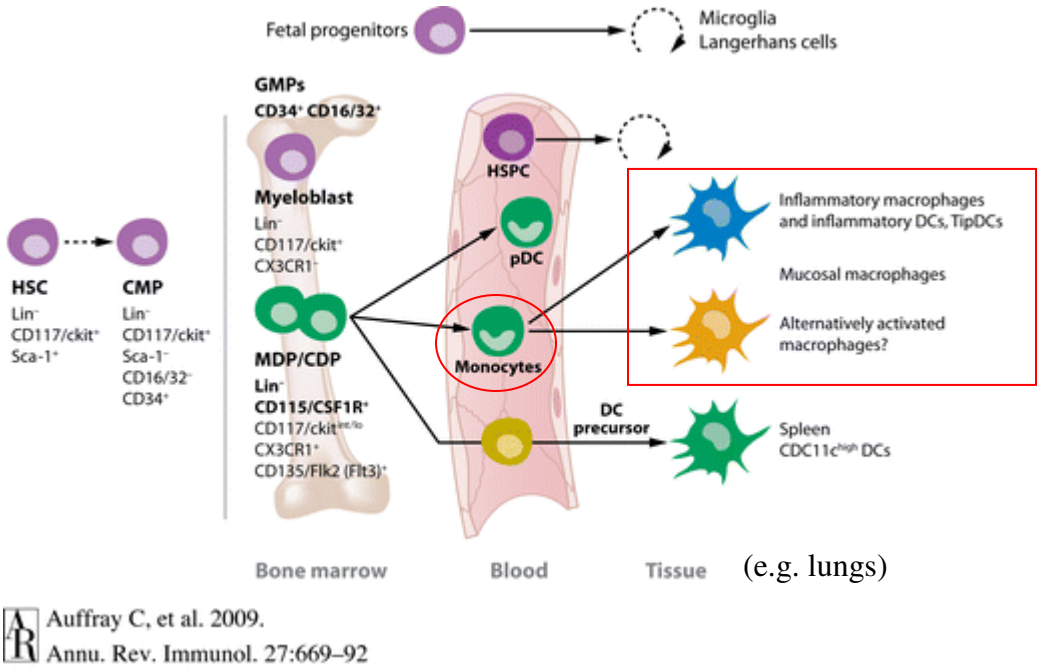

Auffray C, et al. 2009.
Annu. Rev. Immunol. 27:669–92

Figure 2. Differentiation of the macrophage and dendritic cell progenitor and origin of macrophage and dendritic cells subsets. Adapted from Auffray *et al.* 2009 [6]. DC-dendritic cells, HSC-hematopoietic stem cell, CMP-common myeloid precursor, GMP-granulocyte/macrophage precursor, MDP-macrophage and DC precursor, CDP-common DC precursor, pDC-plasmacytoid dendritic cell. In red frames highlighted cells investigated in the study.

Peripheral blood monocytes can emigrate from the blood through the endothelial barrier into various tissues under both non-inflammatory, steady-state conditions and in response to inflammatory stimuli. After extravasation, PBMo rapidly undergo phenotype changes and differentiate into cells of the organ resident MPS. In the lung, the $GR1^+$ population of PBMo can replenish MΦ and DC [17, 18] (Fig. 3). This highly coordinated process implicates close linkage between monocyte trafficking and cellular differentiation, which shapes the phenotype of the extravasated cells.

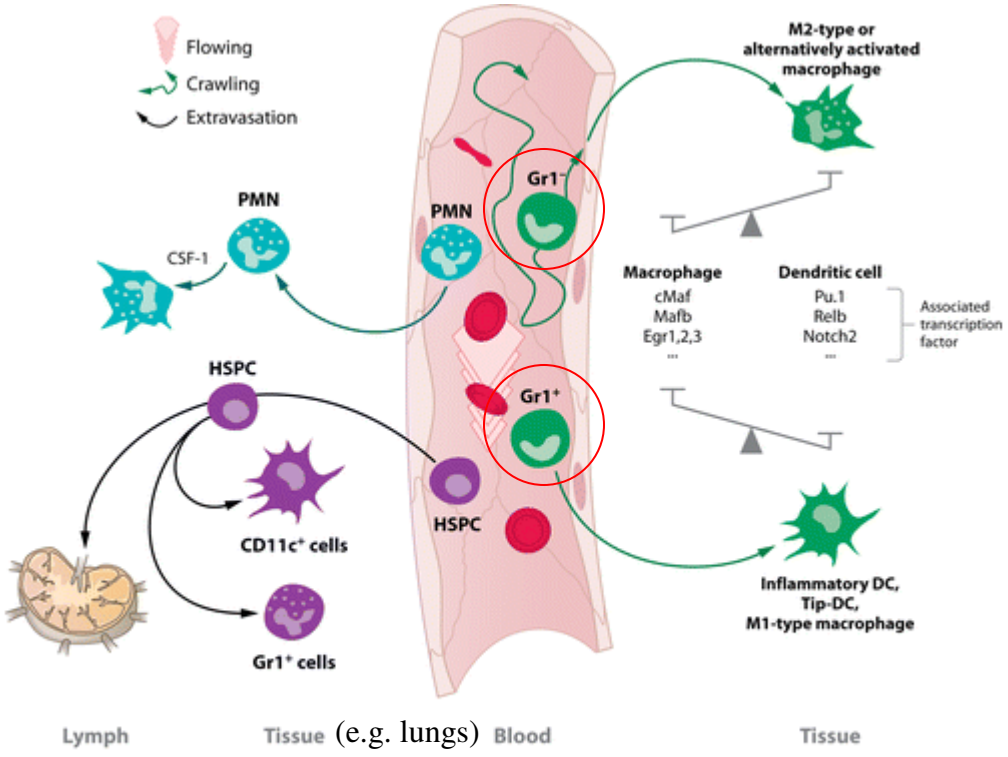

Auffray C, et al. 2009.
Annu. Rev. Immunol. 27:669–92

Figure 3. Tissue macrophages and dendritic cells can arise from GR1⁺ monocytes, but also from hematopoietic stem and progenitor cells (HSPC) and granulocytes (PMN); adapted from Auffray *et al.* 2009 [6]. In red circles highlighted cells investigates in the study.

Monocyte differentiation has been extensively studied *in vitro*. Monocytes cultured in medium containing macrophage colony-stimulating factor (M-CSF) differentiate into MΦ, while in the presence of granulocyte macrophage colony-stimulating factor (GM-CSF) and IL-4, monocytes differentiate into DC [19, 20]. Although recent *in vivo* investigations have demonstrated that subsets of PBMo can be precursors for DC and MΦ [7, 18], the detailed fate of PBMo once they leave the circulation has not been comprehensively addressed. Moreover, while cell recruitment under inflammatory conditions has been extensively studied, the tissue migration and differentiation of mononuclear phagocytes under non-inflammatory conditions remain poorly understood.

1.1.3 Alveolar macrophages

Under steady state conditions, alveolar macrophages (AMΦ) represent the majority (95%) of leukocytes in the lower respiratory tract. Through the presence of surface

receptors for numerous ligands and through their large number of secretory products, lung MΦ can respond to environmental factors [21]. Alveolar macrophages are avidly phagocytic and ingest all types of inhaled particles that reach the alveolar space [22]. Alveolar macrophages are key players in controlling pulmonary immune responses [23] and depletion of AMΦ leads to a significant increase in the inflammatory response to an intratracheally administered antigen [24]. The main role of AMΦ under steady state conditions is to maintain the airspace quiescent and preserve the ability of the lung to perform gas exchange. Additionally, AMΦ posses the power to reduce the activity, proliferation and functions of $CD4^+$ T-cells [25] and can downregulate the antigen presentation capacity of pulmonary DC [26]. In addition, AMΦ also play an important role in inflammatory processes through the release of oxygen radicals and proteolytic enzymes. However, when AMΦ are exposed to large numbers of pathogens or pathogen-derived products and components, such as LPS, AMΦ can initiate a strong inflammatory response involving the release of cytokines including TNF-α, IL-1β or IL-6, as well as the chemokines CCL2 and CCL5, thereby recruiting monocytes and neutrophils [27]. Through the release of several cytokines and growth factors, AMΦ may also influence both matrix damage and repair processes [28].

1.1.4 Lung dendritic cells

Mouse lung DC all express CD11c and exhibit low autofluorescence, in contrast to the highly autofluorescent aMΦ [29]; having different anatomical locations in the lung, DC reside in conducting airways, lung parenchyma and the alveolar compartment and pleura [30]. The trachea and large conducting airways contain intraepithelial DC expressing CD103, but not CD11b (which is a myeloid cell marker), while in the sub-mucosa of the conducting airways $CD103^-$ and $CD11b^+$ DC can be found [31]. In the lung interstitium, both mentioned lung DC subpopulations are found. The plasmacytoid DC (pDC) are $CD11b^-$ but express Siglec-H. Although pDC are present in small amounts in different airway compartments, the vast majority reside in central lymphoid organs [32]. During lung inflammation there is a recruitment of $CD11b^+$ DC expressing Ly6C, illustrating their recent descent of monocytic precursors [33].

The main task of DC is the continuous surveillance of antigen exposed sites, and deciding whether to present sampled antigen in an immunogenic or tolerogenic way. These circumstances are especially important in the lung, where the interface between epithelial cells and the external environment is the largest in the body, and where strong immune responses may have devastating effects on fragile gas exchange structures [34].
Even in the absence of inflammation DC or their precursors are continuously recruited from the blood into the lung [34]. Holt and coworkers [35] were the first to demonstrate that pulmonary DC are constantly replenished by steady state bone marrow output. Inflammatory stimuli in the inhaled air have a profound impact on these steady state dynamics. Dendritic cell recruitment after inhalation of pathogenic material is very rapid, in some cases, ahead of neutrophil influx [36], and is an integral part of the early phase of the innate immune response, with the potential to progress toward a powerful adaptive defense [34].

1.1.5 Lung macrophages and dendritic cells have different functions and location in the lung

In the lung, cells of the MPS are key players in host defense and immunological homeostasis. While lung MΦ are generally present in both the lung interstitium and alveolar airspaces, DC are located primarily within the interstitium, with only a minor proportion found in the respiratory tract surface areas [34, 37] (Fig.4). In addition to their different localization, lung MΦ and DC fulfill distinct and specialized roles in the immune response, which correlate with their different migration properties and cellular phenotypes. In the absence of inflammatory stimuli, DC have a much shorter half-life in the lung compared to AMΦ [38]. Furthermore, DC do not exhibit impressive phagocytic activity, but rather process antigens which are then presented to T cells upon stimulation, causing antigen specific T cell priming. To ensure a successful antigen presentation to T cells, DC must migrate to the regional lymph nodes. In contrast, lung MΦ are considered to form resident cell populations both in the interstitium (interstitial macrophages, iMΦ) and in the alveolar airspace (resident alveolar macrophages, rAMΦ), where they function as major sentinel and phagocytic populations in the lung, for

invading pathogens [39]. Alveolar macrophage and DC precursors must migrate from the bloodstream through endothelial and epithelial barriers into the alveolar compartment. This journey requires the expression of genes involved in communication with barrier structures and rapid adjustment to different oxygen concentrations and osmotic pressures.

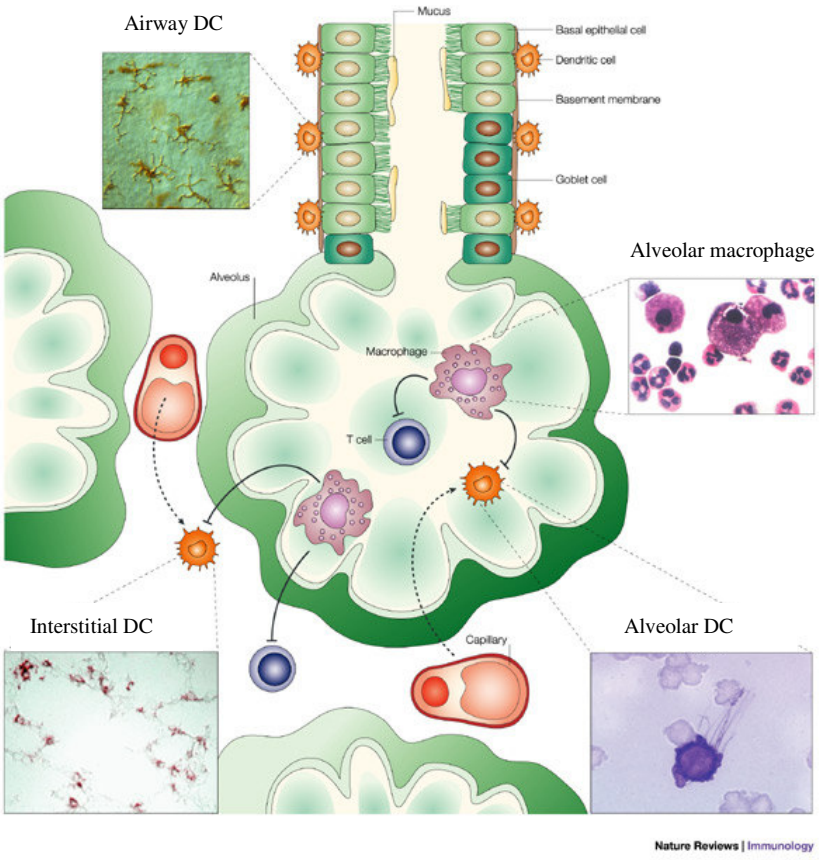

Figure 4. Localization of dendritic cells and macrophages in the lung. Adapted from Lambrecht and Hammad 2003 [40]

1.1.6 Genes involved in the trafficking of mononuclear phagocytes

Trafficking of monocytes into the lung tissue and their differentiation into lung rAMΦ and DC is proposed to be regulated by the expression of specific gene clusters, which promote cell-cell interaction, migration and matrix degradation, and the acquisition of tissue specific cellular phenotypes. Traffic related gene clusters include chemokines, integrins, and tissue-degrading matrix metalloproteinase (MMP) enzymes, for all of which members have been demonstrated to be functionally important. A complete

picture, however, of the gene clusters that are regulated during *in vivo* migration and differentiation of PBMo under non-inflammatory conditions has not yet been obtained. Currently, adaptive changes of cellular phenotypes cannot be directly assessed by cell fate mapping during the slow trafficking of PBMo to the lung tissue under steady-state conditions. An alternative approach to gain a better insight into the genetic programs that drive the PBMo migration and differentiation processes would be comparison of the transcriptomes of PBMo with their lung tissue mononuclear phagocyte progeny.

1.2 Serotonin

1.2.1 Serotonin as a neurotransmitter

Serotonin (5-hydroxytryptamine, 5-HT) is one of the most extensively studied neurotransmitters. It is a monoamine neurotransmitter found in large amounts in the gastrointestinal tract of animals. About 80% of the total serotonin is located in the enterochromin cells in the gut, and is stored in platelets, which express the serotonin reuptake transporter (SERT). In the gut, the 5-HT activity is restricted primarily to the regulation of intestinal movements [41]. Serotonin is also synthesized in serotonergic neurons in the central nervous system, where it has various functions, including the regulation of mood, appetite, sleep, muscle contraction, and some cognitive functions including memory and learning [41]. Serotonin is also involved in the regulation of diverse cellular processes, such as cell growth and division, cytokine synthesis and chemotaxis [41].

1.2.2 Serotonin and the immune system

Serotonin, apart from being well known for a role in vasoconstriction, has been implicated in diverse biological processes such as tissue regeneration [42], platelet activation [43], and recently in the immune system regulation [44]. Platelets release 5-HT

upon activation in response to vascular wall injury, or LPS [45] or allergen challenge [46]. Increased levels of 5-HT in inflammatory processes are well documented [44].

Many components of the innate and adaptive immune system have the capability to produce, sequester and respond to 5-HT. Activated T-cells [47] and MΦ [48] express Thp1, rate limiting enzyme for 5-HT biogenesis, while DC [47], mast cells [49], monocytes [50] and MΦ [51] express SERT.

Serotonin has a well documented effect on cytokine release from blood cells. Dendritic cells stimulated with 5-HT increase production of IL-1β and IL-8 and reduce production of IL-12 and TNF-α [52]. In human PBMo and human monocytes stimulated with LPS, a similar pattern of cytokine release was observed [53, 54]. In addition to cytokine release 5-HT has been also implicated in the upregulation of phagocytosis by peritoneal MΦ [55].

1.2.3 Serotonin receptors in the lung

The broad spectrum of 5-HT action is mediated by a large family of serotonin receptors, including ionotropic cation channels ($5\text{-}HT_3$) and six types of metabotropic G-protein coupled receptors [56]. To the present day, particularly important for the lungs are $5\text{-}HT_2$ receptors, which are involved in a pathogenesis of pulmonary fibrosis [57] and pulmonary hypertension [58].

The serotonin receptor $5\text{-}HT_2$ class includes $5\text{-}HT_{2A}$, $5\text{-}HT_{2B}$, $5\text{-}HT_{2C}$ receptors, which are coupled to G proteins. Activation of a receptor initiates signaling cascade resulting in the formation of inositol phosphates and elevation of intracellular calcium levels. Many inflammatory processes, such as cytokine release, oxidative burst, and interferon responses are calcium dependent [59]. While $5\text{-}HT_{2A}$ and $5\text{-}HT_{2B}$ receptors have been studied on alveolar epithelial cells, the expression of 5-HT receptors and the effects of 5-HT on freshly isolated rAMΦ remain elusive.

1.3 Granzymes

1.3.1 The Granzyme family

Granzymes are a subfamily of serine proteases, expressed primarily in NK cells and $CD8^+$ cytotoxic T-cells. There are 10 granzyme genes in mice (gzmA, gzmB-G, gzmK, gzmM, gzmN) and five genes in humans (gzmA, gzmB, gzmK, gzm H and gzmM) [60]. Although the first molecular target identified for granzymes was an extracellular protein [61], the capacity of granzymes to induce target cell death is now considered as their main function, and is most extensively studied.

Since granzyme expression is restricted primarily to cytotoxic lymphocytes, the role of granzyme has been mainly investigated in host defense and the eradication of virally infected and malignant cells. Major component of cytotoxic granules produced by cytotoxic lymphocytes are granzymes A and B and perforin, which is essential for granule release. Cytotoxic cells kill target cells by releasing granules, which cause rapid induction of apoptosis by DNA damage, disruption of mitochondrial membrane potential, and prevents the cell from repairing the damage it has caused [62].

1.3.2 Non-apoptotic roles of granzymes A and B in immune cells

Recently, many have clarified that, while intracellular targets for granzymes are important and have attracted much attention, new non-death related functions for granzymes should be proposed and investigated [63-66] (Fig. 5). Apart from the induction of cell death, granzymes are important for diverse biological processes, such as stimulation of proinflamatory cytokines, remodeling of the extracellular matrix (ECM) or inactivation of intracellular pathogens. Recent reports demonstrate that granzyme A and B expression is not restricted to cytotoxic and lymphoid cells. Granzyme B was found in human plasmacytoid dendritic cells [67], human blood basophils [68], and human and mouse mast cells [69, 70]. It is also clear from *in vitro* data that granzyme B can participate in ECM remodeling by cleavage of vitronectin, fibronectin and laminin [71]. Granzyme B can also cleave viral proteins, which can cause, for example, attenuation of

herpes simplex virus-1 reactivation without killing the infected cells [72]. Granzyme A, apart from cleaving ECM proteins [73], can also induce a proinflammatory cytokine response, to such a extent that gzmA knockout animals resist the lethal effects of LPS [74].

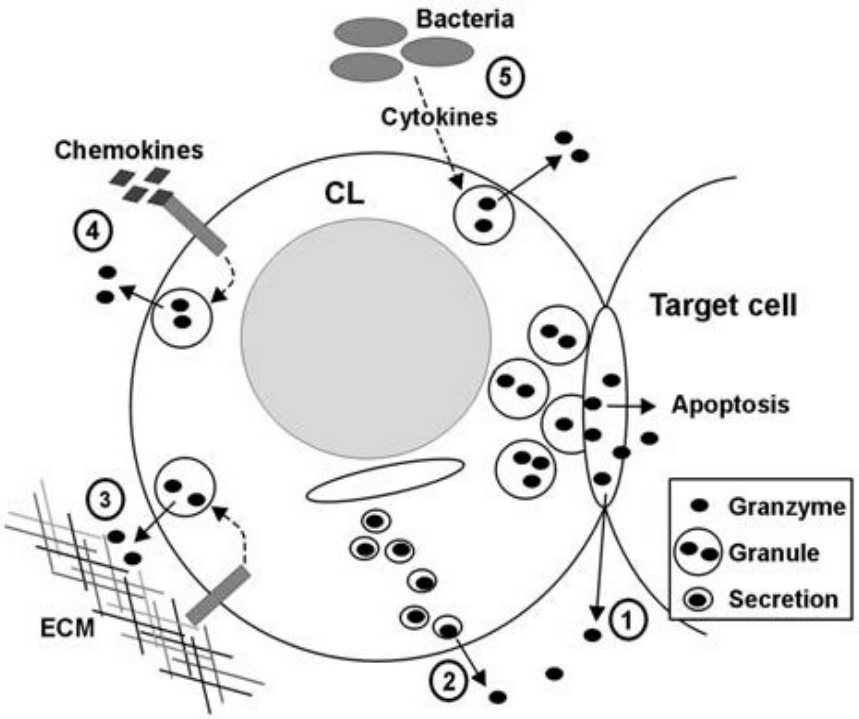

Figure 5. **Mechanisms of granzyme escape into the extracellular environment**. Adapted from Buzza and Bird 2006 [64]. (1) Escape from immunological synapses during target cell killing, (2) constitutive granzyme secretion (3) integrin mediated granzyme release by contact with extracellular matrix (ECM) proteins (4) local action of chemokines can induce granzyme release (5) bacteria and bacterial components such as LPS as well as proinflammatory cytokines induce granzyme release

1.4 Aim of the study

Lung macrophages and lung dendritic cells are believed to originate from the same monocytic-like precursor cell from the blood. The structure and functions of these two cell types are clearly different, however, because of a lack of one specific marker, it is not easy to discriminate between these two cell types in the lung, and study their functions separately.

In the presented study differences between lung alveolar macrophages and lung dendritic cells were explored, starting with transcriptomic tools to learn more about macrophage and dendritic cell biology, as well as to highlight genes that might be crucial for the respective unique phenotypes.

To investigate this problem in an unbiased manner, a whole scale genome approach was conducted in which alveolar macrophages, dendritic cells and putative precursor monocytes were compared. Candidate genes were then verified for functional relevance.

2. Materials and Methods

2.1 Animals

Wild-type C57BL/6 mice were purchased from Charles River (Sulzfeld, Germany). Animals deficient for the 5-HT_{2C} receptor were generated by Dr. Laurence H. Tecott (Department of Psychiatry, University of California, San Francisco, USA) [75] and obtained from Dr. Pete Clifton (Department of Psychology, University of Sussex, Falmer, Brighton, UK). Animals were kept under conventional conditions and used at 6-12 weeks of age. All animal experiments were approved by the local authorities.

2.2 Isolation of peripheral blood monocytes, lung macrophages and lung dendritic cells

Mice were sacrificed by an overdose of isoflurane by inhalation (Forene®, Abbott). Blood was collected from the *vena cava caudalis* and aseptically transferred to 15 ml tubes. Clotting was prevented by addition of ethylenediaminetetraacetic acid (EDTA). Erythrolysis was performed with 10 ml 0.8% ammonium chloride lysis buffer. Erythrolysis was stopped by addition of 5 ml of RPMI-1640 medium supplemented with 10% FCS and L-glutamine, and cells were centrifuged (400 × *g*, 10 min, 4 °C). The pellet was resuspended in 10 ml ammonium chloride buffer, and the procedure was repeated. Cells were then washed in 5 ml RPMI-1640 medium supplemented with 10% FCS and L-glutamine, resuspended in PBS/2 mM EDTA/0.5% FCS, and stained for flow cytometry. Macrophages and DC from lungs were isolated as recently described in detail [37, 76]. Briefly, lungs were perfused with 20 ml of sterile HBSS until free of blood by visual inspection, then removed and transferred into Petri dishes containing 0.7 mg/ml collagenase A (Roche; Germany) and 50 µg/ml DNAse I (Serva; Germany) in RPMI-1640 medium. Lungs were minced and cut into small pieces, agitated on a shaker (30 min, RT) and then incubated at 37 °C for 30 min in a humidified atmosphere

containing 5% CO_2. Cell aggregates were dispersed by repeated passage through a syringe, and filtered through a 200 µm and a 40 µm cell strainer (BD Biosciences), to obtain single cell suspension. Subsequently, cells were rinsed with HBSS and PBS/2 mM EDTA/0.5% FCS, followed by incubation with an excess concentration of nonspecific IgG (Octagam, Octapharma, Germany) to reduce nonspecific antibody binding. After washing with PBS/2 mM EDTA/0.5% FCS, cells were stained with magnetic bead-conjugated anti-CD11c antibodies (Miltenyi Biotec) followed by a magnetic separation according to the manufacturer's instructions. Subsequently, the cell population (containing CD11c positive cells) was stained with CD11c-PE conjugated antibodies (BD Pharmingen) and sorted. To obtain rAMΦ, bronchoalveolar lavage fluid (BALF) was performed with 500 µl aliquots of sterile PBS/2 mM EDTA (pH 7.2) until a BALF volume of 5 ml was recovered following previously described protocols [77]. The BALF was centrifuged (400 × g, 10 min, 4 °C); the cell pellet was resuspended in PBS/2 mM EDTA/0.5% FCS, stained with CD11c PE conjugated antibodies (BD Pharmingen) and subjected to sorting.

2.3 Intratracheal LPS installation

Mice were sedated with xylazine hydrochloride (2.5 mg/kg, intramuscular injection) and ketamine hydrochloride (50 mg/kg), followed by fur/skin disinfection and subsequent shaving of the area above the trachea. A small incision was made and surrounding tissue bluntly dissected to expose the trachea. An Abbocath catheter was inserted in the trachea and subsequently LPS (10 µg/mouse) dissolved in sterile PBS in a total volume of 70 µl was slowly instilled, under stereomicroscopic control. Subsequently, the skin was sutured and mice were left to recover from anesthesia and then returned to their cages, with free access to food and water.

2.4 Pappenheim-stained cytocentrifuge preparations

For identification of flow-sorted subpopulations in samples Pappenheim staining of cytocentrifuge preparations were used. Briefly, cytospins were prepared from every flow sorted sample, containing 30000-50000 cells in 100 µl, and subsequently stained for 5 min in May-Grünwald stain, washed with distilled water and stained for 10 min in 5%

of Giemsa Azur-Eosin-Methylen Blue solution. Total rAMΦ, lung DC and PBMo were determined by differential cell counts using overall morphological criteria, including differences in cells size and shape of nuclei, the purity of the cells was always >95%.

2.5 Gene expression analysis

2.5.1 RNA isolation

After sorting, cells were frozen at -80 °C in RLT lysis buffer (Qiagen) supplemented with 1% β-mercaptoethanol (Sigma). The RNA from highly purified cell populations was isolated using an RNeasy Micro Kit (Qiagen) according to the manufacturer instructions. RNA from cell cultures, where there was no limitation with cell number, was isolated from the RNeasy Mini Kit (Qiagen). Quantification and purity of RNA was determined with an Agilent Bioanalyzer 2100 (Agilent Biosystems). Only those RNA preparations exceeding absorbance ratios of $A_{260/280\ nm} > 1.90$ and of a total amount of RNA greater than 200 ng were used for cDNA synthesis.

2.5.2 cDNA synthesis

After isolation, purified mRNA was transcribed into cDNA by reverse transcriptase (RT)-reaction. To perform cDNA synthesis, RNA was heated for 5 min at 70 °C, immediately thereafter transferred onto ice, and RT mix was added. The total reaction volume was 25 µl. The mixture was then incubated for 1 h at 37 °C, heated on 94 °C for 7 min to inactivate the enzyme. The obtained cDNA was then either used for real-time PCR or stored at -20 °C until further use.

RT mix:

- 5× 1st stand buffer 5 µl
- dithiothreitol (DDT) 2.5 µl (250 nmol)
- Rnase Inhibitor 0.5 µl (20 U)
- dNTPs 1 µl (2.5 nmol)
- random hexamers 1.5 µl (150 ng)
- RT (MMLV) 1 µl (150 U)

2.5.3 Real time quantitative PCR

Quantitative gene expression analysis was performed by real time quantitative PCR (qPCR), using Platinum SYBR®Green qPCR SuperMix-UDG (Invitrogen, UK). The ROX reference dye was used to normalize the fluorescent signal between reactions. PCR reactions were performed in 25 µl volume by using the qPCR mix.

qPCR mix:

- SYBR®Green mix 13 µl
- $MgCl_2$ 1 µl (50 nmol)
- FW primer 0.5 µl (5 pmol)
- RV primer 0.5 µl (5 pmol)
- dH_2O 5 µl
- cDNA 5 µl

Cycling conditions were as follows: 95 °C for 5 min, 45 cycles of 95 °C for 10 s, 60 °C for 30 s and 72 °C for 10 s. Formation of a single specific PCR product was confirmed by melting curve analysis and agarose gel electrophoresis.

The *actb, gapdh* and *hmbs* genes served as reference genes for different real-time PCR reactions, depending on the type of the experiment performed. Relative changes in gene expression were determined with the ΔCt method using the following formula: ΔCt = Ct reference – Ct target.

The primers used for qPCR were designed with the help of the online program Primer3 (http://frodo.wi.mit.edu/primer3/). All primer sequences used throughout the study are listed in the *Appendix* section (7.3).

2.5.4 Microarray experiment

Microarray experiment (outline illustrated in Fig. 6), namely cDNA synthesis, RNA amplification, labeling and purification reaction, as well as hybridization were performed according to the manufacturer's instructions (Agilent Technologies, CA, USA).

Briefly, isolated RNA was transcribed to cDNA as described above. Freshly transcribed cDNA was incubated for 5 min on ice, spun down and added to Transcription Master Mix. Samples were mixed gently and incubated for 2 h at 40 °C.

Transcription Master Mix

- dH_2O 15.3 µl
- 4× Transcription buffer 20 µl
- 0.1M DTT 6 µl
- NTP mix 8 µl
- 50% PEG 6.4 µl
- RNaseOUT 0.5 µl
- Inorganic pyrophosphatase 0.6 µl
- T7 RNA polymerase 0.8 µl
- Cy 3-CTP or Cy 5-CTP 2.4 µl

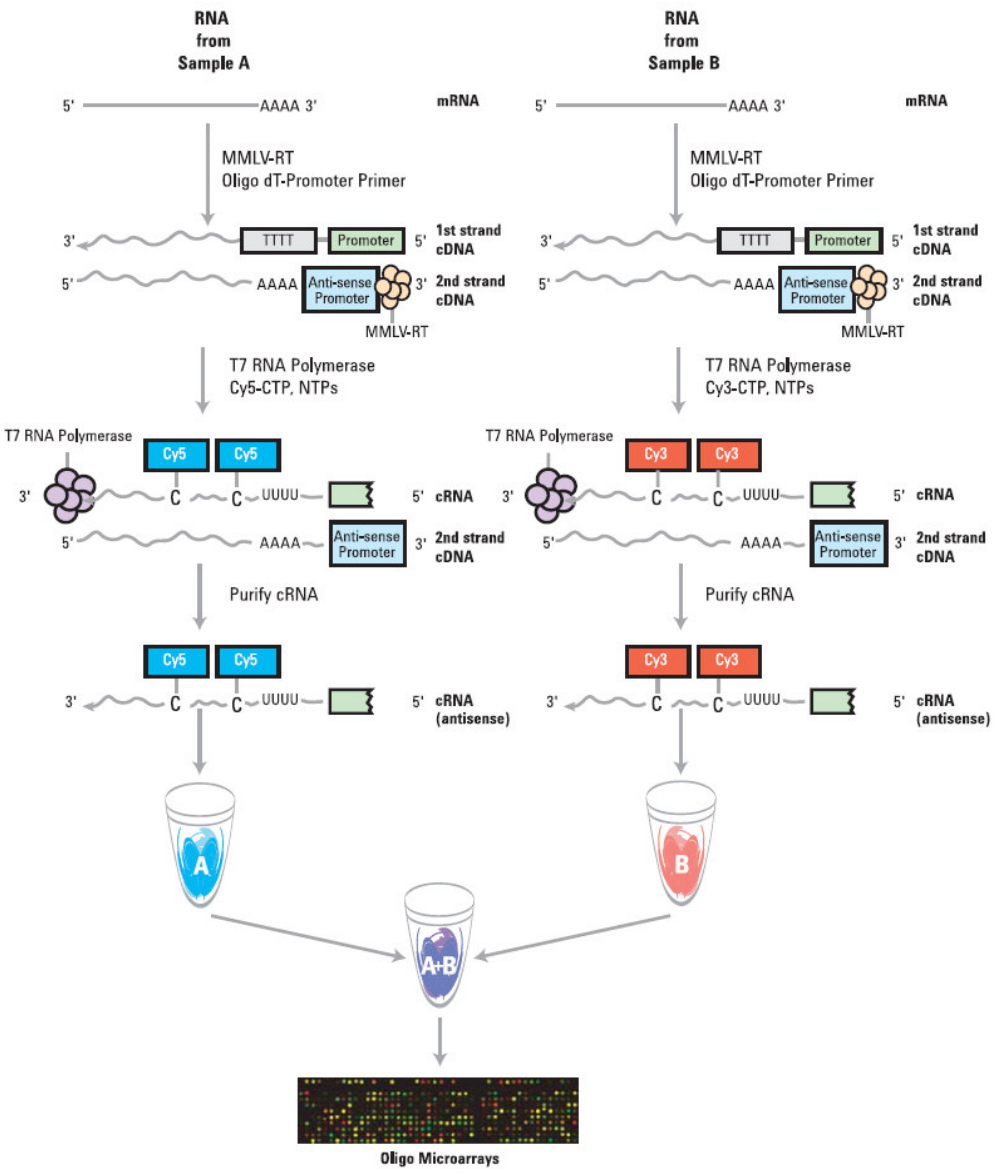

Figure 6. Generation of labeled RNA for two-color microarray experiment. Adapted from the Agilent Technologies protocol "Two color microarray-based gene expression analysis" version 5.7. cDNA-complementary DNA, cRNA-complementary RNA, Cy-cyanine, MMLV-moloney murine leukemia virus, RT-reverse transcription . One RNA sample was labeled with Cy5 (A) and second with Cy3 (B). Samples were mixed and spotted on the microarray to perform hybridization.

Labeled RNA was transferred into spin columns from RNeasy kit (Qiagen) and purified according to the manufacturer's instructions. After the purification procedure concentration, quality (RNA absorbance ratio measured at 260/280 nm) and degree of incorporation of fluorescent dyes (Cyanine 3-labeled and Cyanine 5-labeled concentration) was recorded by spectrophotometer (Agilent Bioanalyzer 2100, Agilent, Germany). Samples were added to the Fragmentation buffer (Agilent Technologies) and incubated for 30 min at 60 °C to fragment labeled RNA. Samples were immediately thereafter transferred to the Hybridization buffer (Agilent Technologies) and subsequently slowly dispensed on the gasket slide that was covered with array forming a sandwich that was closed in a chamber in which hybridization took place for 17 h at 60 °C. Next day the chamber was dissembled and array was washed two times and dried by submerging in acetonitrile. Array slides were scanned directly to minimize the impact of environmental oxidants on signal intensities. Data from the scanned array was extracted to measured gene expression in the experiments by the Agilent Feature Extraction software.

2.6 Protein expression analysis

2.6.1 Western blot

Cells were lysed with lysis buffer containing 20 mM Tris (pH 7.5), 150 mM NaCl, 1 mM EDTA (pH 8.0), 1 mM EGTA (pH 8.0), 0.5% NP-40, 2 mM sodium orthovanadate (pH 10.0), and protease inhibitor cocktail (Roche, Mannheim, Germany). The lysates were kept on ice for 30 min, followed by centrifugation for 15 min at 13,000 rpm at 4°C. Proteins were separated by electrophoresis on 10% SDS PAGE under reducing and denaturating conditions. Subsequently proteins were transferred to polyvinylidene difluoride membranes (Micron Separations, Westborough, MA). After transfer membranes were incubated in blocking buffer (5% nonfat milk in PBS, 0.05% Tween 20) at room temperature for 1 hour. Primary antibodies were added, and membranes were incubated overnight at 4 °C, washed three times, and incubated with horseradish peroxidase-conjugated secondary antibody (Pierce, Rockford, IL). After subsequent three washes, an enhanced chemiluminescence system was used to visualize immune complexes (Amersham Pharmacia Biotech, Little Chalfont, Buckinghamshire, UK).

Loading Buffer

50 mM Tris Cl (pH 6.8), 100 mM DTT, 2% SDS (10%) glycerol, 0.1% bromophenol blue

Electrophoresis buffer mix

(5x Solution)

- 25 mM Tris 15.1 g
- 250 mM glycine 94 g
- 0.1% (v/v) SDS 50 ml (10%)
- dH_2O 1000 ml

Gel electrophoresis conditions

80 V, 40 mA for 2.5 h

Transfer Buffer (blotting)

- 25 mM Tris 3.02 g
- 192 mM glycine 14.4 g
- 20% methanol 200 ml
- dH_20 up to1000 ml

Wet blotting conditions

100 V, 265 mA 1 h, with mixing, at 4 °C

Washing Buffer

0.05% Tween 20 (2.5 ml) in PBS

Blocking Buffer

5% Milk powder diluted in Washing Buffer

Developing mix

Mix reagents 2 ml Solution A, to 50 µl Solution B per membrane for 3 min.

2.6.2 Flow cytometric analysis and flow sorting

For staining for flow cytometric analysis and flow sorting, single cell suspensions were resuspended in PBS/2 mM EDTA/0.5% FCS. Cell numbers were assessed using a Neubauer chamber. Fc-receptor-mediated and non-specific antibody binding was blocked by addition of excess of non-specific immunoglobulin (Octagam®, Octapharma, Germany).

Staining was performed at 4 °C in the dark for 20 min. After staining, cells were washed twice in PBS/2 mM EDTA/0.5% FCS. Biotinylated primary antibodies were further incubated for 5 min with APC-conjugated streptavidin (BD Pharmingen) followed by two

additional washes with PBS/2 mM EDTA/0.5% FCS. Cell sorting was performed with a FACSVantage SE flow cytometer equipped with a DiVA sort option and an argon-ion laser at 488 nm excitation wavelength and a laser output of 200 mW (BD Biosciences). A FACSCanto flow cytometer (BD Biosciences) was used for flow cytometric characterization of cell populations. The BD FACSDiVa software package was used for data analysis (BD Biosciences). Purity of sorted cells was ≥ 98% as determined by flow cytometry and differential cell counts of Pappenheim (May-Grünwald-Giemsa)-stained cytospins.

The following monoclonal antibodies were used at appropriate dilutions for staining: CD11c-PE and -APC (HL3, BD Pharmingen), CD11b-FITC, -APC, and -PE (M1/70, BD Pharmingen), CD115-PE (604 B5 2EII, Serotec), GR-1-PE-Cy7 and -PE (RB6-8C5, Biolegend), F4/80-PE (CI:A3-1, Serotec), biotinylated I-A/I-E (2G9, BD Pharmingen), CD3-PE (17A2, BD Pharmingen), CD19-PE (1D3, BD Pharmingen), NK-1.1-PE (PK136, BD Pharmingen), CD80-PE (1G10, BD Pharmingen), CD86-PE (GL1, BD Pharmingen), B220-PE (RA3-6B2, BD Pharmingen), CD49d-PE (R1-2, Biolegend), CD103-PE (2E7, Biolegend), CD61-PE (2C9G2, Biolegend), Integrin β7 (FIB504, Biolegend).

2.6.3 Enzyme-linked immunosorbent assay

Cytokine levels of CCL2 in cell culture supernatants were measured using commercially available sandwich enzyme-linked immunosorbent assay (ELISA) kit following the instructions of the manufacturer (R&D Systems, Minneapolis, MN). Standards, control, and samples were pipetted into the wells, incubated for 2 h at room temperature (RT), followed by five washing steps with an ELISA autowasher. After 2 h of incubation with the conjugate solution and repetitive washing, substrate solution was added to each well for 30 min, and then the reaction was stopped. The optical density was measured using a microplate reader set at 450 nm; the sample values were read off the standard curve. The detection limit for CCL2 was 2 pg/ml.

2.6.4 Fluorescent substrate activity assay

Granzyme B activity was measured from flow-sorted cells cultured for 24 h in the presence or absence of LPS. For the measurement cell culture supernatant, as well as cell lysates were collected. Granzyme B fluorescent substrate (Calbiochem, Germany) was added to samples for 30 seconds after which the reaction was stopped by addition of hydrochloride acid to stop granzyme activity. Fluorescent activity was measured using a microplate spectrophotometer (Becton Dickinson, USA) set at wavelength tailored to each substrate.

3. Results

3.1 Immunophenotypic identification and high purity isolation of peripheral blood monocytes, lung dendritic cells and lung macrophages

For high purity sorting, PBMo were identified as SSC^{low}, $CD11b^{pos}$, M-CSF receptor/$CD115^{pos}$ cells, following previously reported protocols [14] (Fig. 7A). The cells defined by this approach homogenously expressed the monocyte marker F4/80, and were partially positive for GR-1 and CD11c, with low levels or absence of MHC class II expression, thereby exhibiting the typical phenotype of PBMo (Fig. 7C) [14]. In contrast, no expression of T cell, B cell or NK cell markers (CD3, CD19, and NK1.1, respectively) was detected (Fig. 7B).

For high purity separation of MΦ and DC from lung homogenates, in a first step the $CD11c^{pos}$ cell fraction was isolated from lung homogenates using magnetic bead separation as outlined in the *Materials and Methods* section. Within this cell population, lung DC were identified as $CD11c^{pos}$, low autofluorescent cells in the FL1 channel, while lung rMΦ were discriminated as $CD11c^{pos}$, high FL1 autofluorescent cells (Fig. 8A). Further phenotyping of accordingly gated subsets revealed the characteristic marker profiles of lung DC and rMΦ, with lung DC displaying a MHC II^{high} $CD80^{low}$ $CD86^{low}$ $F4/80^{low}$ phenotype and lung rMΦ displaying a MHC II^{low} $CD80^{low}$ $CD86^{neg}$ $F4/80^{pos}$ phenotype (Fig. 8B), which were in line with previously published results [37, 76]. Lung DC primarily exhibited an immature phenotype, as defined by high expression of MHC class II and intermediate expression of the co-stimulatory molecules CD80 and CD86 (Fig. 8B). Expression neither of CD115 nor of neutrophil, T cell, B cell, or NK cell markers was detected (Fig. 8B). The purity of sorted cells used for the microarray experiments (PBMo, lung DC and lung MΦ) was assessed by flow cytometry and Pappenheim-stained cytospins (Fig. 8C) and was always ≥ 98%. As sample processing may alter the gene expression profile of primary cells [78], every effort was made to minimize processing time and, where possible, all procedures were performed on ice.

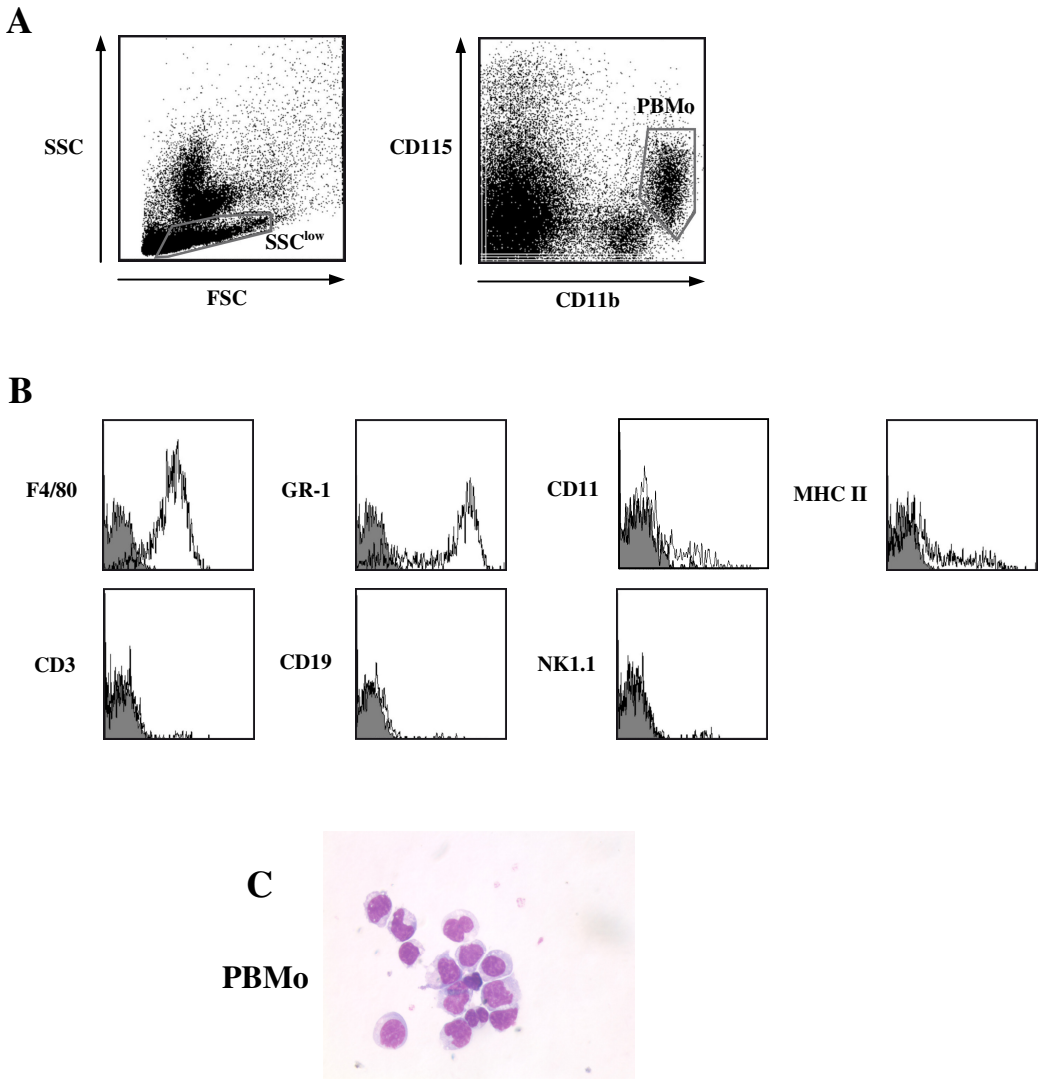

Figure 7. **Identification and characterization of peripheral blood monocytes by flow cytometry**. (**A**) Peripheral blood was obtained from untreated mice as described, subjected to erythrolysis, and analyzed by flow cytometry. Peripheral blood monocytes (PBMo) were identified as low side scatter (SSC) cell population showing a cell surface expression of CD11b and CD115. (**B**) The cell surface antigen distribution profile of PBMo was characterized by flow cytometry. PBMo were gated as displayed in (A). Open histograms indicate specific fluorescence of the respective antigen; shaded histograms represent control stained cells. Note that all cells displayed F4/80 expression, but were negative for GR-1, CD3, CD19, B220/CD45R, and NK1.1, thus excluding contamination by neutrophils, T cells, B cells, or NK cells, respectively. Displayed data are representative of three independent experiments. (**C**) Pappenheim staining of sorted PBMo. Displayed data are representative of 5-6 independent sorting experiments per group.

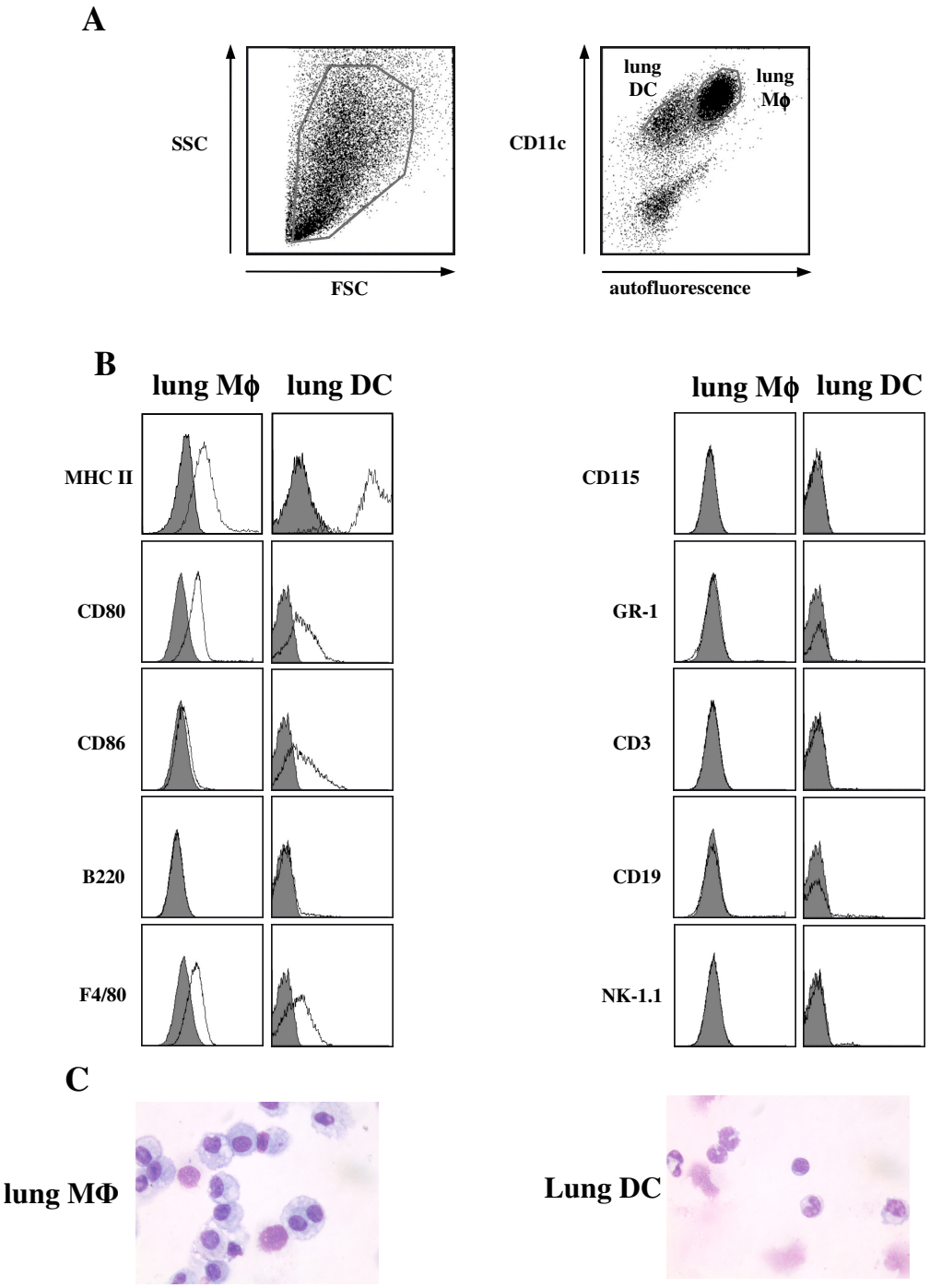

Figure 8. **Identification and characterization of lung macrophages and dendritic cells by flow cytometry.** (**A**) CD11c positive cells were obtained from lung homogenate by magnetic bead isolation, stained for CD11c, and analyzed by flow cytometry. Lung dendritic cells (DC) and lung macrophages (MΦ) were differentiated by CD11c expression and autofluorescence with lung DC displaying a low autofluorescence and lung MΦ displaying a high autofluorescence in the FL1 channel. (**B**) The cell surface antigen distribution profiles of lung MΦ and lung DC were analyzed by flow cytometric analysis. Lung MΦ and DC were gated as displayed in (A). Open histograms indicate specific fluorescence of the respective antigen; shaded histograms represent control stained cells. Displayed data are representative of three independent experiments. (**C**) Pappenheim staining of sorted lung DC and MΦ. Displayed data are representative of 5-6 independent sorting experiments per group.

3.2 Differentially expressed genes between peripheral blood monocytes, lung dendritic cells and lung macrophages

After cell sorting and RNA isolation, gene expression profiles of PBMo, lung DC and lung MΦ were compared by microarray experiment on a whole genome scale. For each comparison, four hybridizations were performed (Fig. 9).

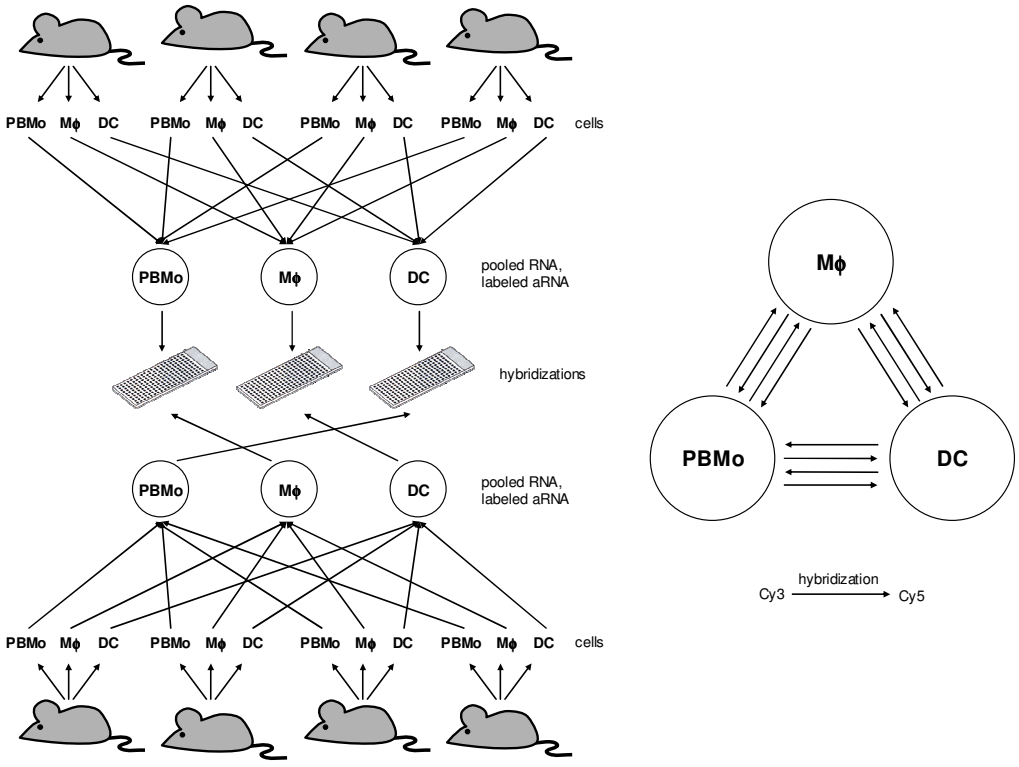

Figure 9. **Microarray experiment design (RNA material pooling strategy and dye switch diagram).** From each mouse peripheral blood monocytes (PBMo), lung dendritic cells (DC) and lung macrophages (MΦ) were isolated. Four mice were used per one array hybridization. In total 12 hybridizations were performed with each four comparing PBMo with MΦ, PBMo with DC, and MΦ with DC. To avoid label factor (for example interaction of certain gene with a dye) in microarray experiment dye switch was performed. In four comparisons between groups, each time two samples were dyed with Cy3 and two times with Cy5.

After cell sorting and RNA isolation, gene expression profiles of PBMo, lung DC and lung MΦ were compared by microarray experiment on a whole genome scale. For each comparison, four hybridizations were performed (Fig. 9). Genes that exhibited a greater

than two-fold change in expression were considered as being differentially expressed, as described in the *Materials and Methods* section. Among the genes differentially expressed between lung MΦ and PBMo, 1530 genes were up-regulated, and 1440 genes were down-regulated. Comparing lung DC and PBMo, 1271 genes were up-regulated, and 341 were down-regulated. Furthermore, 832 genes were found to be up-regulated and 1565 genes down-regulated between lung MΦ and DC. An analysis of the correlation of the M values for the regulated genes from the different hybridizations showed a high correlation with an average Pearson correlation coefficient of 0.95, indicating a high consistency between the four hybridizations per group. In a pathway analysis, using *Pathway-Express from Onto-Tools*, the cell adhesion molecule pathway was the most differentially regulated pathway in all comparisons. The antigen presentation and processing pathway was the second most differentially regulated pathway comparing lung MΦ versus DC and DC versus PBMo (Fig. 11, 12, 13).

To further analyze and structure the microarray data, and to address the question of which gene clusters and cellular pathways are regulated during the extravasations and lung tissue differentiation process of mononuclear phagocytes, particular attention was paid to genes involved in cell trafficking, namely integrins, MMPs, chemokines and chemokine receptors, as well as interleukins and interleukin receptors (Table 1). In order to visualize the results, volcano plots were created with depicted genes belonging to each cluster (Fig. 10). The highlighted genes were validated on independently sorted samples by qRT-PCR and demonstrated the same expression trends as the microarray results (Fig.14, 15, 16). It must be noted, however, that the log intensity ratios (for example the coefficients displayed in Table 1) obtained from the microarray experiments do not directly equal the ΔCt values obtained from the qRT-PCR validation. This is a well-known phenomenon, and taking place due to factors such as the preamplification procedure itself and the limited dynamic range of fluorescence detection [79, 80]. Due to this fact, ΔCt values obtained from the qRT-PCR analysis were often found to be higher than the coefficients for the same genes obtained from the microarray analysis. Likewise, by qRT-PCR analysis, there were significant expression differences detectable in certain genes that had not been detected by the microarray experiments (Table 1 and Fig. 14, 15, 16).

Table 1 The most strongly and significantly regulated genes belonging to the selected clusters

gene symbol	gene description	coefficient		
	chemokine/chemokine receptor	MΦ vs PBMo	DC vs PBMo	MΦ vs DC
Cxcl1	chemokine (C-X-C motif) ligand 1, [NM_008176]	5,69	4,45	ND
Cxcl2	chemokine (C-X-C motif) ligand 2, [NM_009140]	4,76	ND	ND
Cx3cl1	chemokine (C-X3-C motif) ligand 1, [NM_009142]	4,09	4,37	ND
Ccl6	chemokine (C-C motif) ligand 6, [NM_009139]	2,70	ND	2,6
Ccl17	chemokine (C-C motif) ligand 17, [NM_011332]	2,68	4,38	ND
Ccrl2	chemokine (C-C motif) receptor-like 2, [NM_017466]	2,35	ND	ND
Ccl3	chemokine (C-C motif) ligand 3, [NM_011337]	2,25	ND	ND
Cxcl10	chemokine (C-X-C motif) ligand 10, [NM_021274]	2,06	ND	ND
Ccl2	chemokine (C-C motif) ligand 2, [NM_011333]	2,04	2,44	ND
Ccl9	chemokine (C-C motif) ligand 9, NM_011338]	-2,07	ND	ND
Cxcl4	chemokine (C-X-C motif) ligand 4, [NM_019932]	-2,38	ND	-2,8
Cx3cr1	chemokine (C-X3-C) receptor 1, [NM_009987]	-3,36	ND	-2,7
Ccl5	chemokine (C-C motif) ligand 5, [NM_013653]	-3,72	ND	-5,9
Cxcl7	chemokine (C-X-C motif) ligand 7, [NM_023785]	-4,68	-3,42	ND
Ccr2	chemokine (C-C motif) receptor 2, [NM_009915]	-4,70	-2,04	-2,7
Ccr7	chemokine (C-C motif) receptor 7, [NM_007719]	ND	4,61	-4,4
Cxcl16	chemokine (C-X-C motif) ligand 16, [NM_023158]	ND	4,17	-2,6
Ccl4	chemokine (C-C motif) ligand 4, [NM_013652]	ND	4,09	-3,3
Ccl12	chemokine (C-C motif) ligand 12, [NM_011331]	ND	2,72	ND
Cxcr3	chemokine (C-X-C motif) receptor 3, [NM_009910]	ND	2,55	-4,2
Cxcr4	chemokine (C-X-C motif) receptor 4, [NM_009911]	ND	2,51	-2,6
Ccr9	chemokine (C-C motif) receptor 9, [NM_009913]	ND	2,45	-2,5
Ccl7	chemokine (C-C motif) ligand 7, [NM_013654]	ND	2,26	ND
Cxcr6	chemokine (C-X-C motif) receptor 6, [NM_030712]	ND	ND	-2,6
	interleukin/interleukin receptor			
Il1a	interleukin 1 alpha, [NM_010554]	4,21	2,25	2,2
Il6	interleukin 6, [NM_031168]	4,18	ND	ND
Il18	interleukin 18, [NM_008360]	3,04	ND	2,6
Il17d	interleukin 17D, [NM_145837]	2,69	ND	ND
Il1b	interleukin 1 beta, [NM_008361]	2,18	3,84	ND
Il11ra1	interleukin 11 receptor, alpha chain 1, [NM_010549]	2,09	ND	ND
Il2rb	interleukin 2 receptor, beta chain, [NM_008368]	-3,14	ND	-5,1
Il12b	interleukin 12b, [NM_008352]	ND	3,92	-2,5
Il7r	interleukin 7 receptor, [NM_008372]	ND	2,87	-2,7
Il6	interleukin 6, [NM_031168]	ND	2,82	ND
Il18r1	interleukin 18 receptor 1, [NM_008365]	ND	ND	-3,3
	metallopeptidases			
Mmp19	matrix metallopeptidase 19, [NM_021412]	1,99	ND	2,0
Mmp13	matrix metallopeptidase 13, [NM_008607]	ND	3,81	ND
Adam23	disintegrin and metallopeptidase domain 23, [NM_011780]	ND	3,02	ND
Mmp14	matrix metallopeptidase 14, [NM_008608]	ND	2,61	-2,6
Adam8	disintegrin and metallopeptidase domain 8, [NM_007403]	ND	2,50	-3,7
Mmp12	matrix metallopeptidase 12, [NM_008605]	ND	2,39	ND
Mmp8	matrix metallopeptidase 8, [NM_008611]	ND	-2,74	ND
Adam19	disintegrin and metallopeptidase domain 19, [NM_009616]	ND	ND	-2,1
Mmp13	matrix metallopeptidase 13, [NM_008607]	ND	ND	-2,7
Adamts2	disintegrin-like and metallopeptidase with thrombospondin type 1 motif, 2 [NM_175643]	3,65	ND	ND
	integrins			
Itgax	integrin alpha X, [NM_021334]	2,39	2,25	ND
Itga2b	integrin alpha 2b, [NM_010575]	-2,02	ND	ND
Itgam	integrin alpha M, [NM_008401]	-2,11	ND	-2,1
Itga4	integrin alpha 4, [NM_010576]	-2,63	ND	-2,3
Itgb7	integrin beta 7, [NM_013566]	-3,76	ND	-3,5
Itgae	integrin, alpha E, epithelial-associated, [NM_008399]	ND	3,88	-3,1
Itgb3	integrin beta 3, [AK135584]	-3,64	ND	-2,78

Genes were selected to keep a false-discovery rate of 10%. The coefficient given for expression differences corresponds to log(2) of fold change with a coefficient >0 indicating upregulation and a coefficient <0 indicating downregulation of the respective gene. Lack of given value (indicated as ND) indicates either lack of differential regulation or absence of expression.

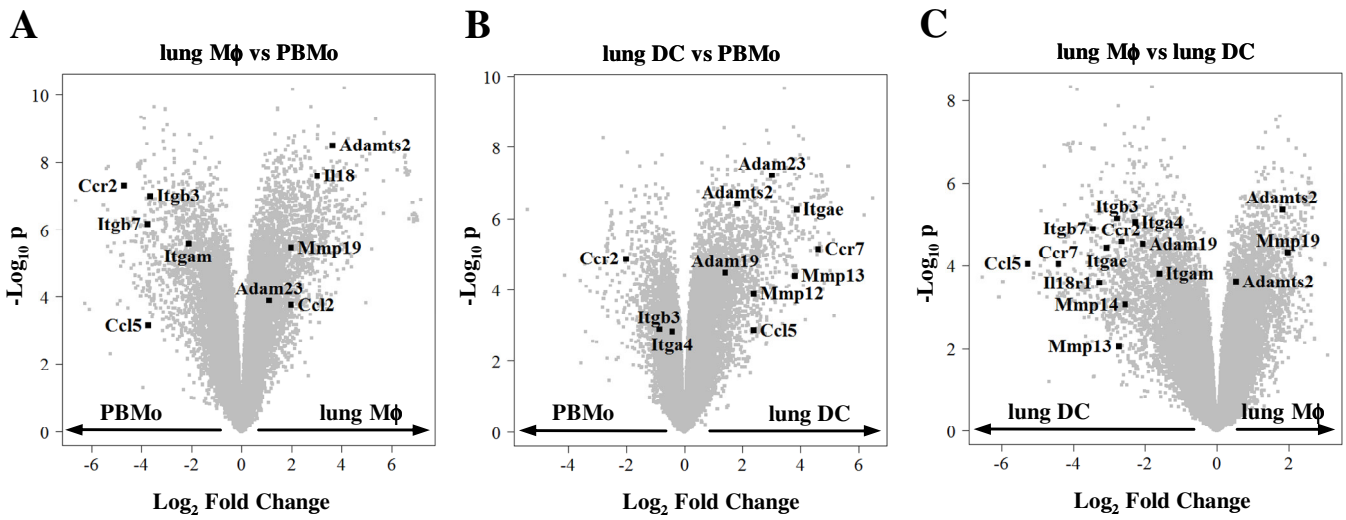

Figure 10. **Volcano plot representation of differentially regulated genes among lung dendritic cells, lung macrophages and monocytes**. Gene expression profiles of (**A**) lung macrophages (MΦ) versus peripheral blood monocytes (PBMo), (**B**) lung dendritic cells (DC) versus PBMo, and (**C**) lung MΦ versus lung DC were plotted according to the $\log_2$ fold change (X axis) and $\log_{10}$ unadjusted p-value (Y axis). The genes for which the expression has been validated by qRT-PCR are highlighted. Data are representative of four hybridizations per group.

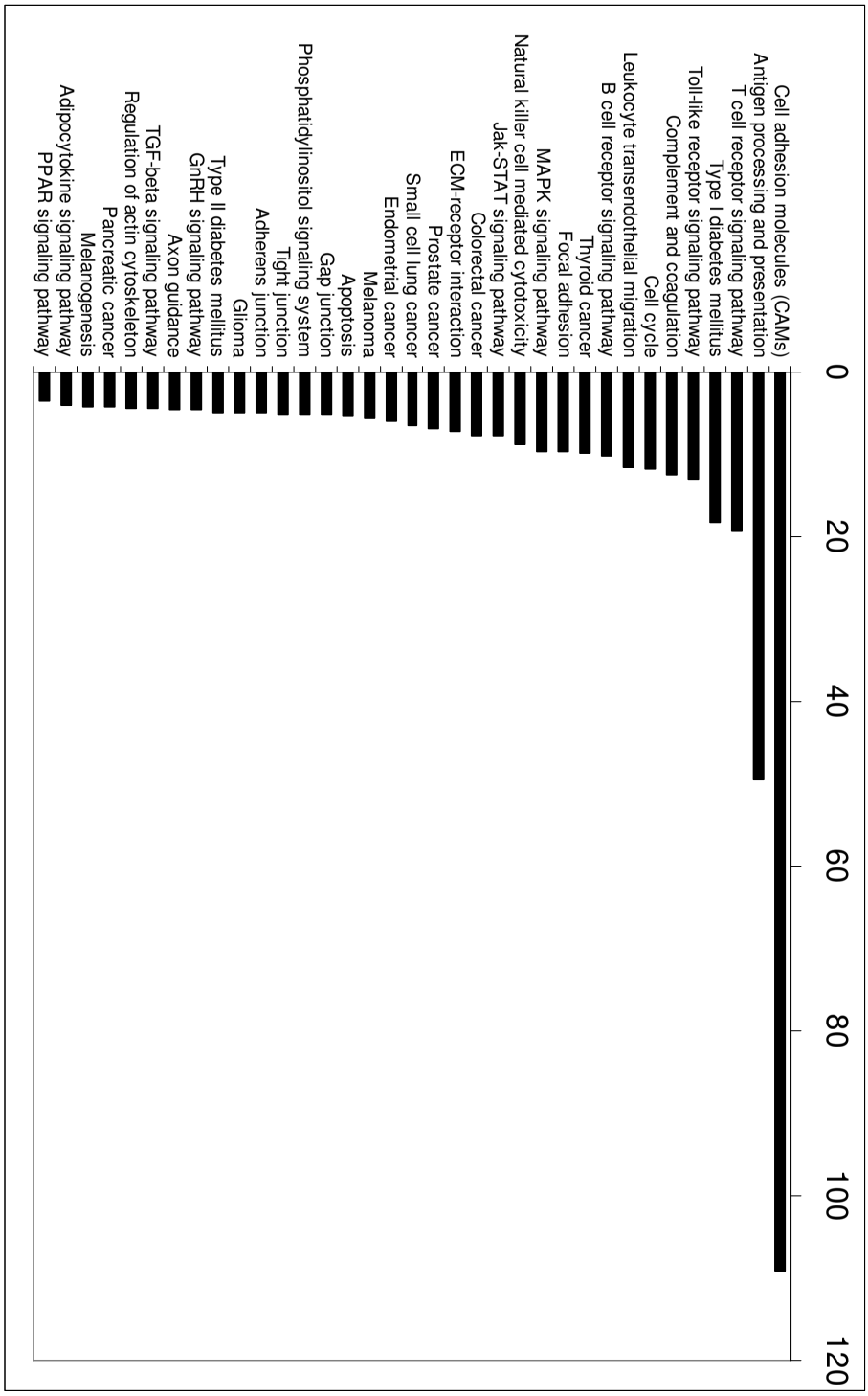

Figure 11. Gene ontology biological processes classification of differentially regulated genes between lung dendritic cells and monocytes. Gene Ontology analysis was performed online using Pathway-Express from Onto-Tools.

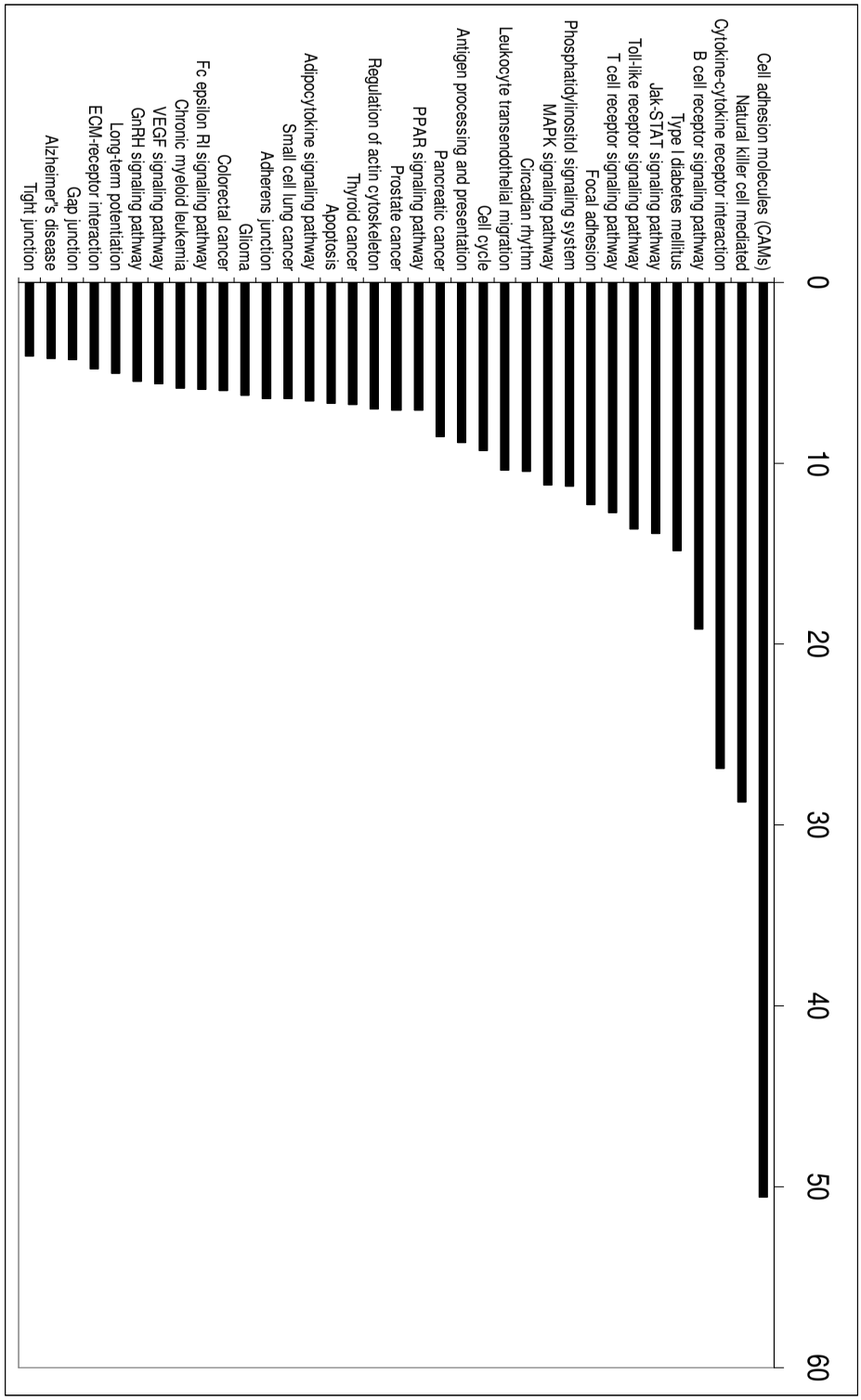

Figure 12. Gene ontology biological processes classification of differentially regulated genes between lung macrophages and monocytes. Gene Ontology analysis was performed online using Pathway-Express from Onto-Tools.

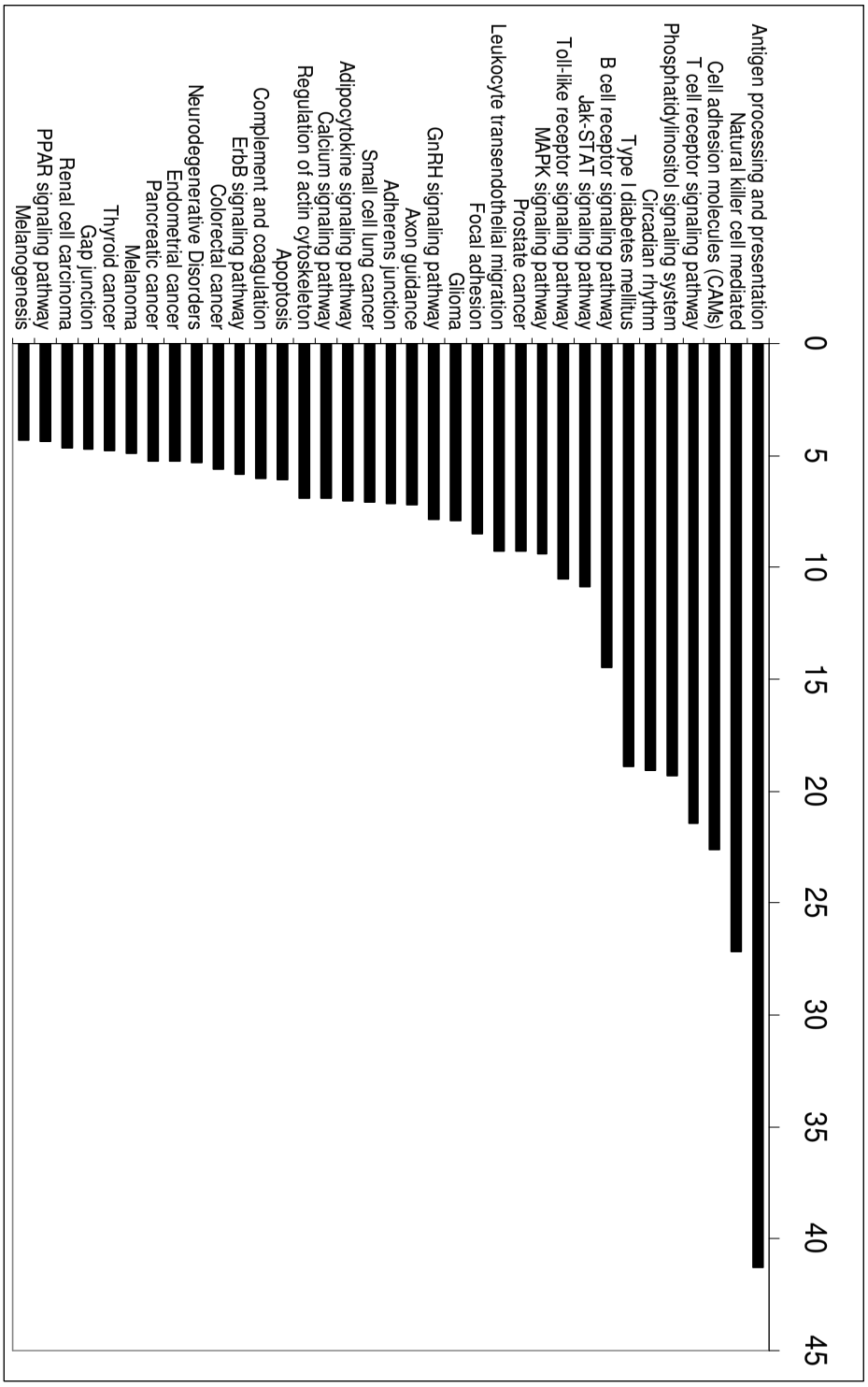

Figure 13. **Gene ontology biological processes classification of differentially regulated genes between lung macrophages and lung dendritic cells.** Gene Ontology analysis was performed online using Pathway-Express from Onto-Tools.

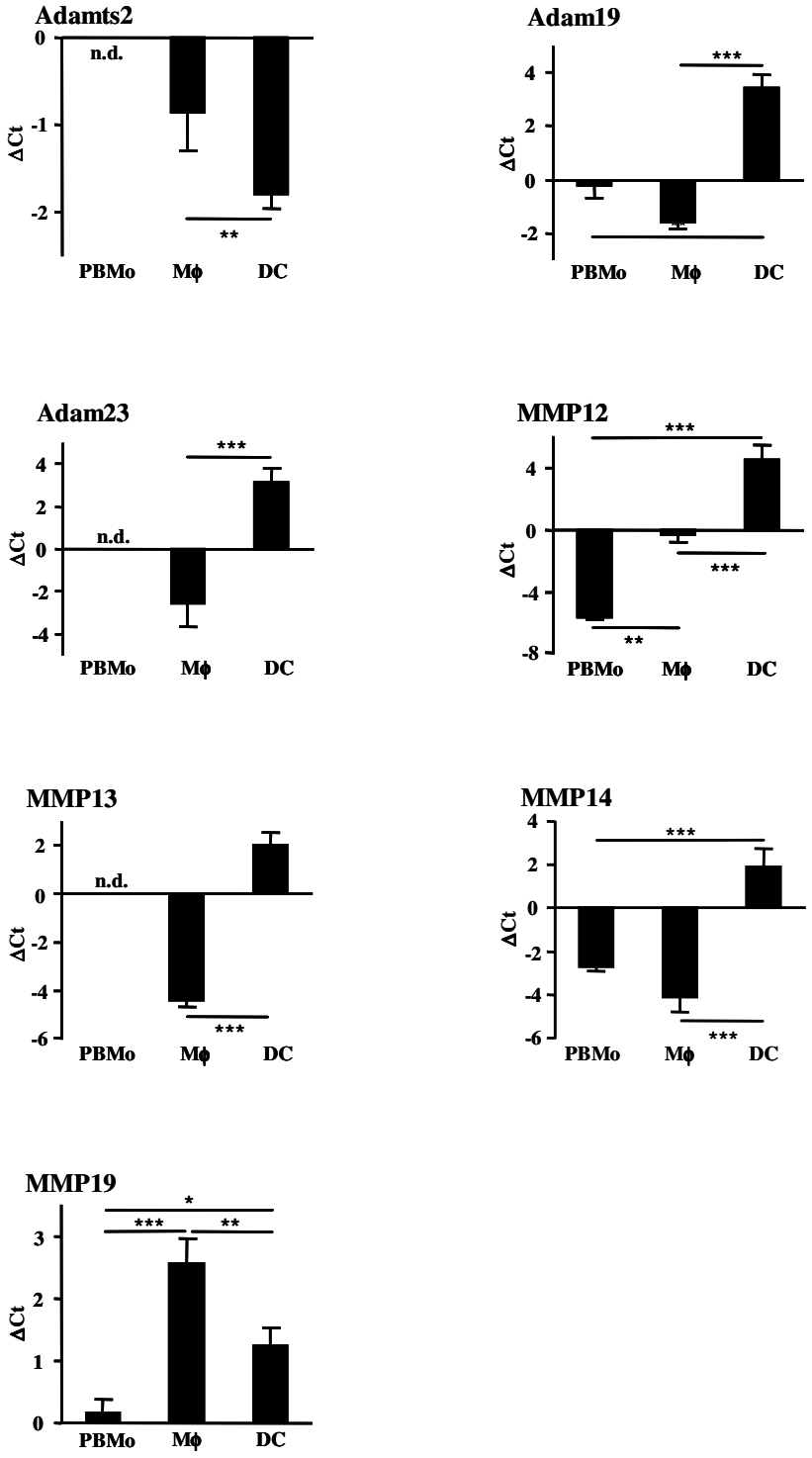

Figure 14. Validation of microarray-based expression pattern of metalloproteinase genes by qRT-PCR. Peripheral blood monocytes (PBMo), lung macrophages (MΦ) and dendritic cells (DC) were sorted as shown in Fig. 7A and 8A. The mRNA expression was assessed by qRT-PCR analysis for metalloproteinases. Data represent 3-4 independent experiments per group. * indicates $p<0.05$, ** indicates $p<0.01$, *** indicates $p<0.001$. A non-detectable gene expression is indicated by n.d. (not detected).

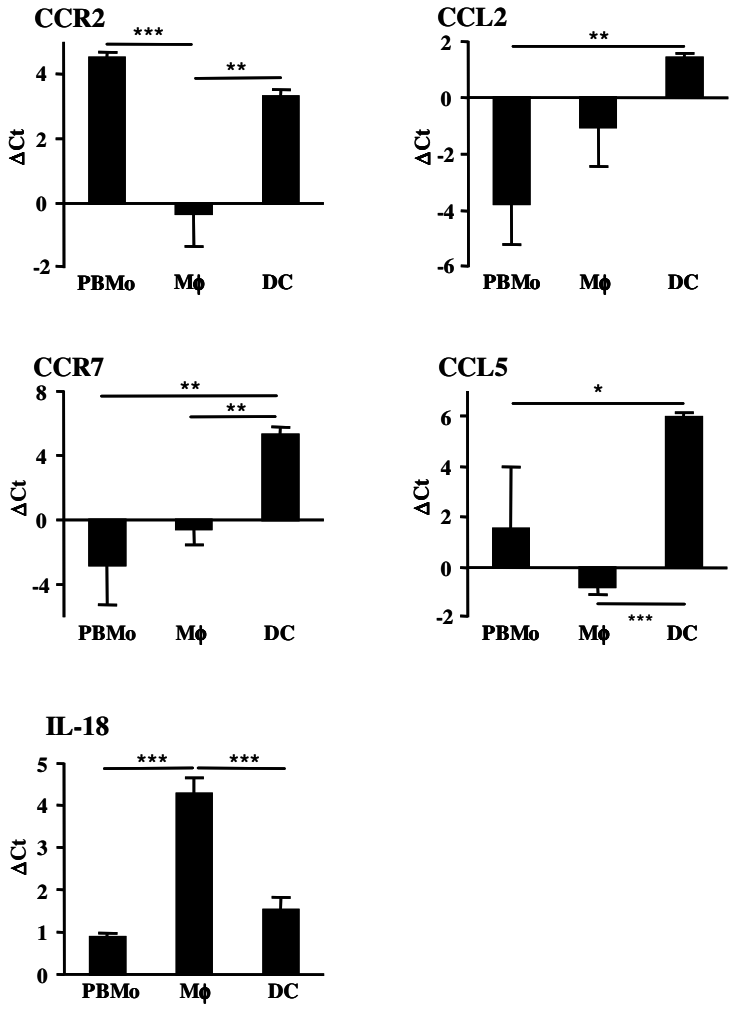

Figure 15. **Validation of microarray-based expression pattern of chemokine and interleukin genes by qRT-PCR.** Peripheral blood monocytes (PBMo), lung macrophages (MΦ) and dendritic cells (DC) were sorted as shown in Fig. 7A and 8A. The mRNA expression was assessed by qRT-PCR analysis for chemokines and interleukins. Data represent 3-4 independent experiments per group. *indicates $p<0.05$, **indicates $p<0.01$,*** indicates $p<0.001$

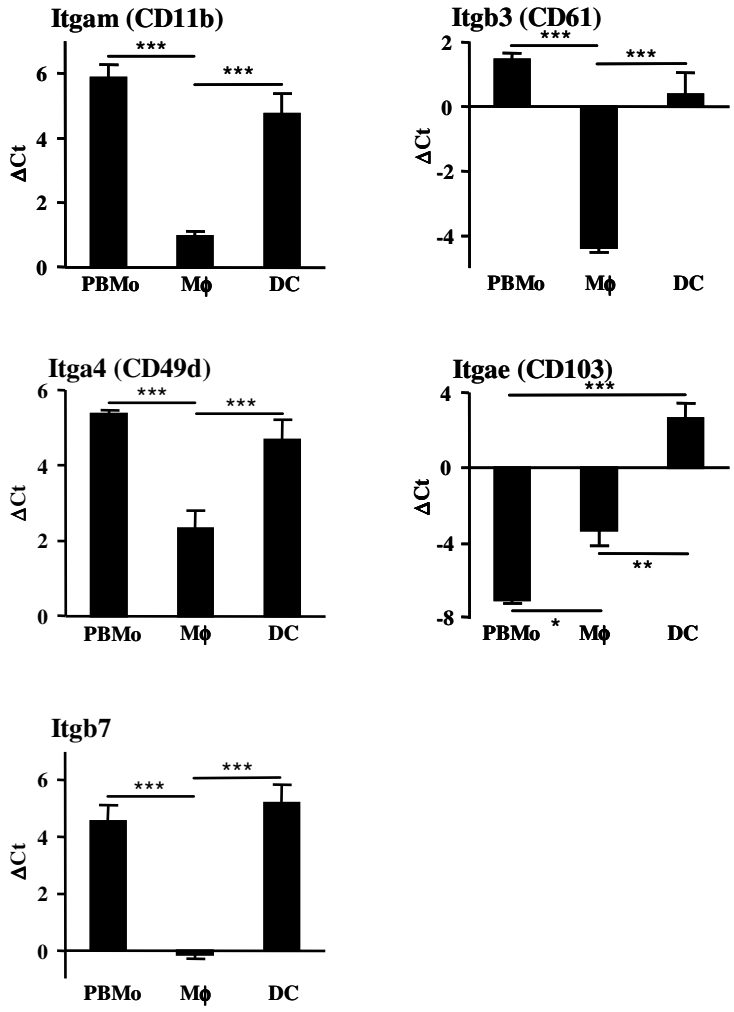

Figure 16. **Validation of microarray-based expression pattern of integrin genes by qRT-PCR**. Peripheral blood monocytes (PBMo), lung macrophages (MΦ) and dendritic cells (DC) were sorted as shown in Fig. 6A and 7A. The mRNA expression was assessed by qRT-PCR analysis for integrins. Data represent 3-4 independent experiments per group. * indicates $p<0.05$, ** indicates $p<0.01$, *** indicates $p<0.001$

3.3 Isolation and gene expression profiling of subpopulations of peripheral blood monocytes and lung macrophages

The microarray experiments described above were designed to compare the gene expression profiles of PBMo and their fully differentiated pulmonary progeny lung DC and lung MΦ on a genome-wide scale. This approach, however, does not detect potential differences in gene expression between intermediate differentiation stages or distinct subpopulations of circulating or lung tissue mononuclear phagocytes, which have been ascribed different migratory and differentiation properties. Thus, the two dominant subpopulations of PBMo, the "inflammatory" (GR-1^{pos}) and the "resident" (GR-1^{neg}) subsets, have been attributed with different biological functions, including recruitment under inflammatory versus steady-state conditions, and differentiation into functionally different DC and MΦ populations [7, 81]. To further identify possible differences in the expression profiles of the selected genes, GR-1^{high} and GR-1^{low} PBMo were sorted for qRT-PCR analysis based on the expression of CD11b, CD115 and GR-1, as depicted in (Fig. 17A). Like PBMo, lung MΦ can be divided into two major populations according to their anatomical location, the parenchymal or interstitial (iMΦ), and the resident alveolar macrophages (rAMΦ). Whether these populations represent functionally different subpopulations has long been a matter of debate. Recent reports, however, indicate a functional and developmental difference, with the iMΦ being proposed as precursor cells for rAMΦ [17]. For the separation of rAMΦ, BALF was obtained from mouse lungs, and rAMΦ were flow-sorted from the lavage by gating the high FL1 autofluorescent, CD11c^{pos} cell population (Fig. 17B). By lavaging it is possible to remove > 90% of the rAMΦ from mouse lungs [82]. In the current experiments, the lavage procedure depleted rAMΦ efficiently from the lungs, thus enriching the iMΦ subset, following an approach used by Landsman *et al*. [17, 18]. No additional rAMΦ could be obtained by serial lavage, indicating an efficient lavaging procedure. Enriched interstitial iMΦ and DC were then isolated from homogenates obtained from lavaged lungs (Fig. 17C) using the sorting strategy described above (Fig. 8A).

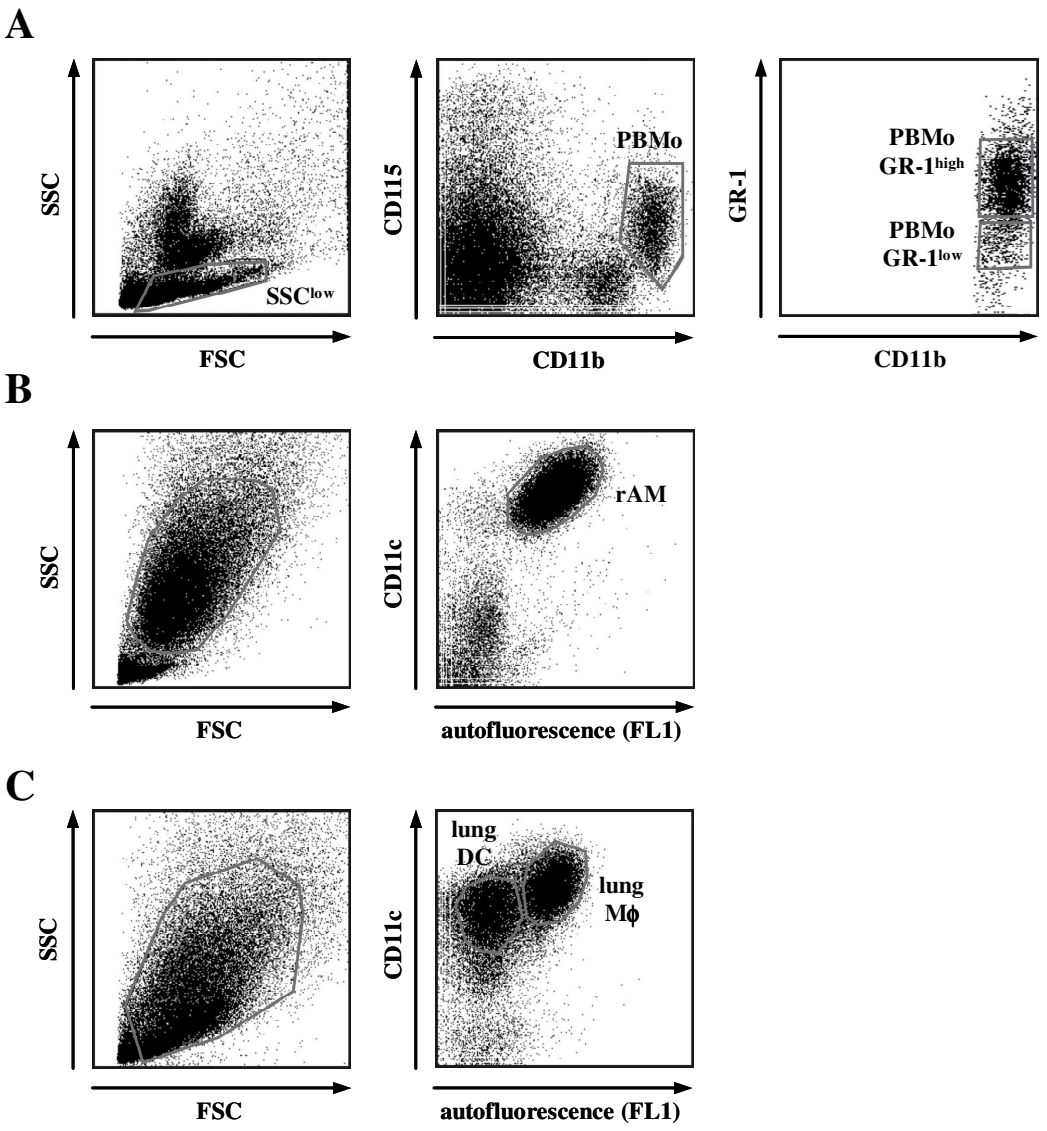

Figure 17 Isolation strategy of subpopulations of peripheral blood monocytes and lung macrophages. (**A**) Peripheral blood monocytes (PBMo) were flow-sorted from peripheral blood leukocytes by gating on the low SSC/CD11b^{pos}/CD115^{pos} population, as shown in Fig. 1. Additional gates were set on the GR-1-positive (PBMo GR-1^{high}) and GR-1-negative (PBMo GR-1^{low}) subsets of PBMo. (**B**) Resident alveolar macrophages (rAM) were flow-sorted from BAL fluid by gating on the high FSC/high SSC/CD11c^{pos}/high autofluorescent cell population. (**C**) After BAL, lungs were removed, and CD11c^{pos} cells were isolated from lung homogenates using magnetic beads as described. Subsequently, CD11c^{pos} cells from lung homogenates were flow-sorted for the low autofluorescent population representing lung DC and the high autofluorescent population representing MΦ as described. Note that the majority of rAM had been removed from lungs by lavage prior to homogenization, and that the flow-sorted MΦ mainly represent iMΦ. Displayed data are representative of 5-6 independent sorting experiments per group.

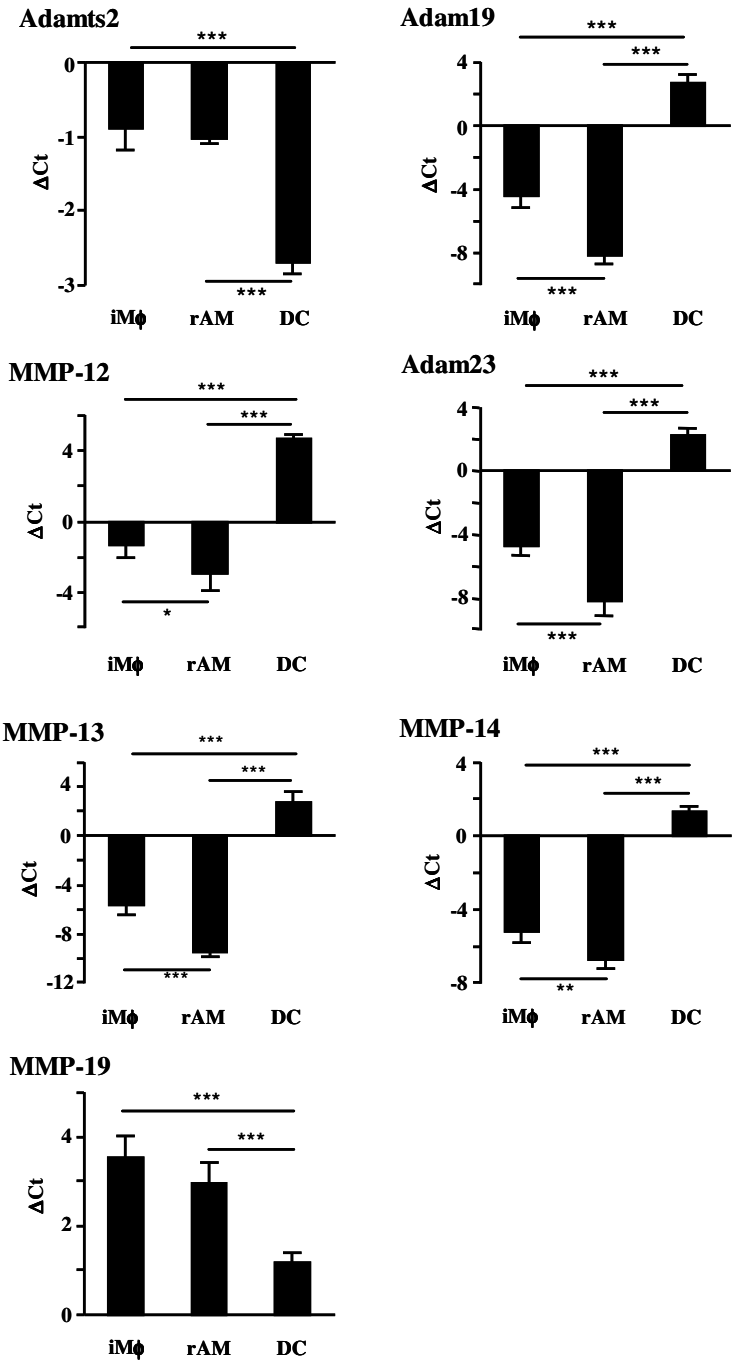

Figure 18. **Relative mRNA expression of metalloproteinase genes from lung dendritic cells and subpopulations of lung macrophages and peripheral blood monocytes by qRT-PCR**. Lung interstitial macrophages (iMΦ) and resident alveolar macrophages (rAM) as well as lung dendritic cells (DC) were sorted as shown in Fig. 17, and mRNA expression was assessed by qRT-PCR analysis. Data represent 3-4 independent experiments per group. * indicates $p<0.05$, ** indicates $p<0.01$, *** indicates $p<0.001$.

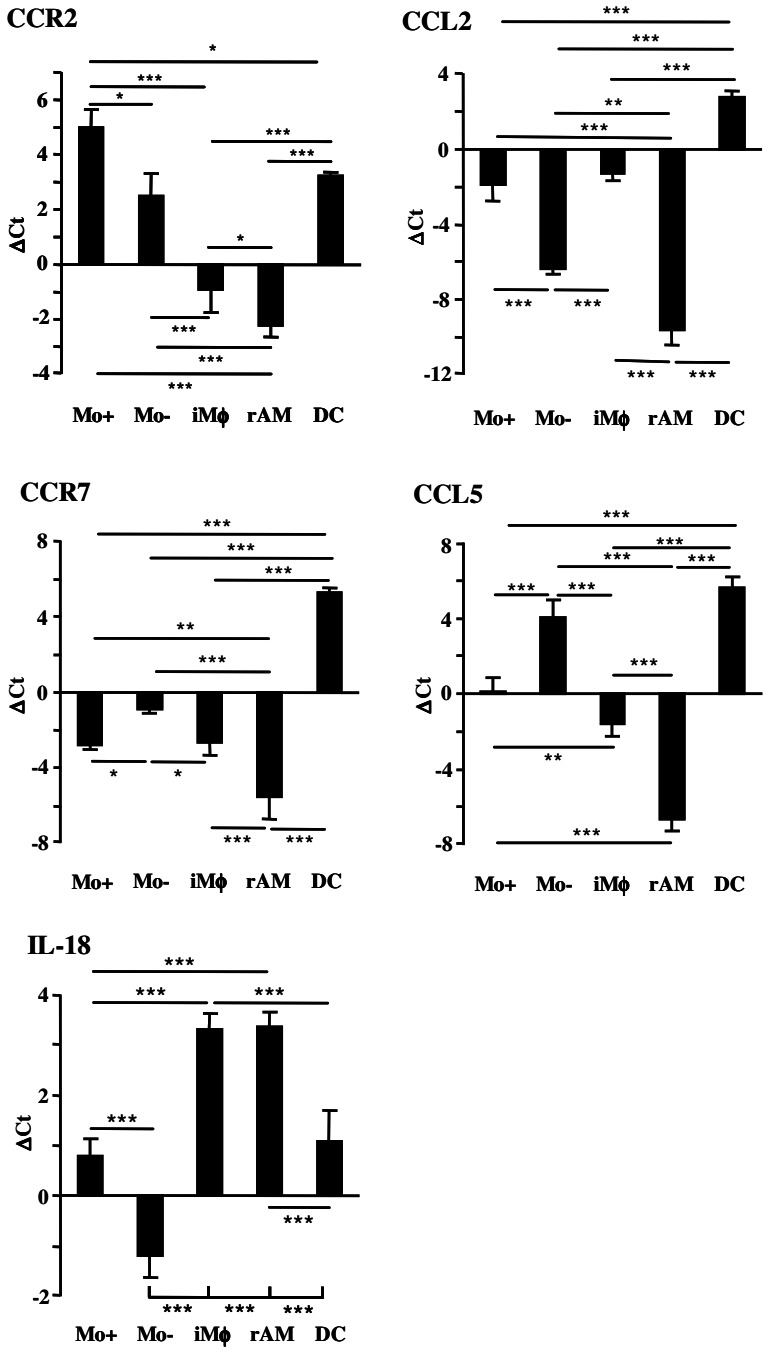

Figure 19. Relative mRNA expression of chemokine and interleukin genes from lung dendritic cells and subpopulations of lung macrophages and peripheral blood monocytes by qRT-PCR. GR-1^{high} (Mo+) and GR-1^{low} (Mo-) peripheral blood monocytes (PBMo), lung interstitial macrophages (iMΦ) and resident alveolar macrophages (rAM) as well as lung dendritic cells (DC) were sorted as shown in Fig. 17, and mRNA expression was assessed by qRT-PCR analysis. Data represent 3-4 independent experiments per group. * indicates $p<0.05$, ** indicates $p<0.01$, *** indicates $p<0.001$

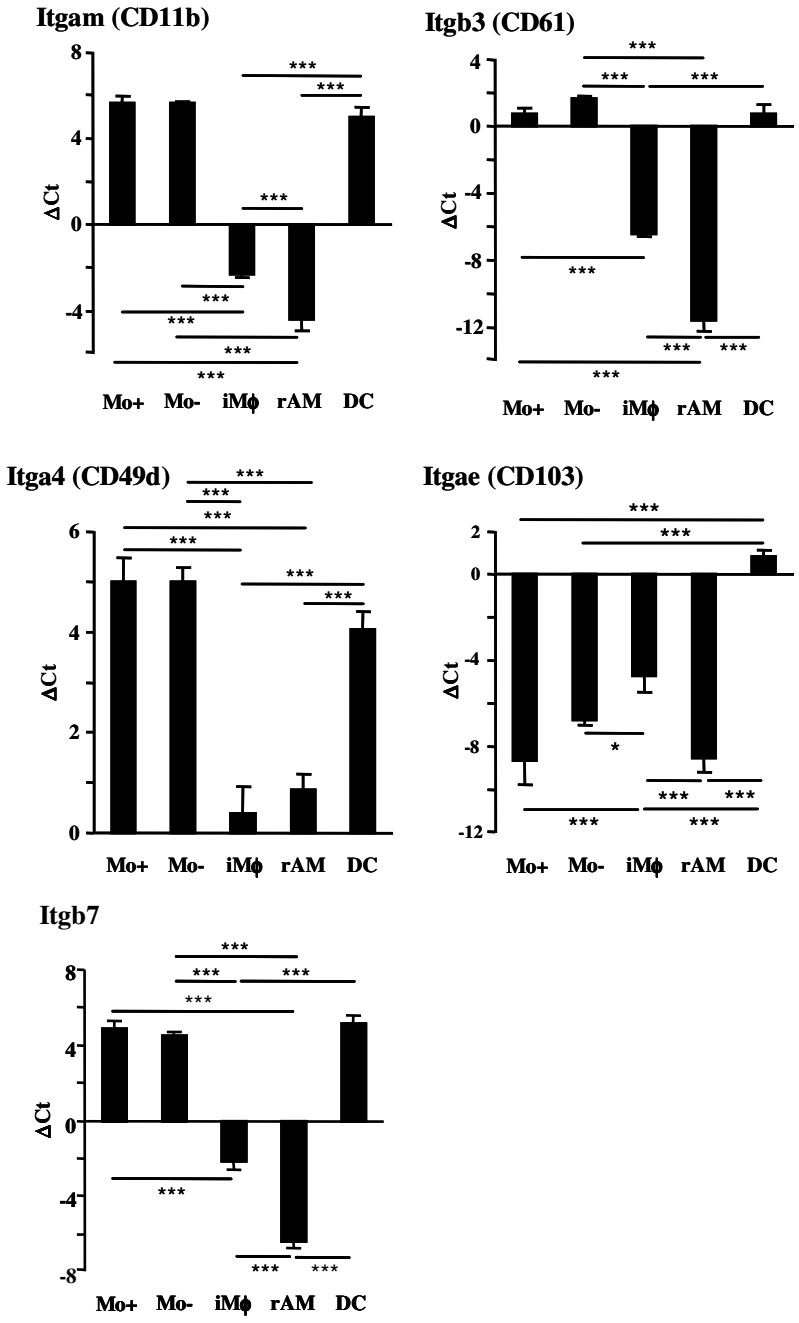

Figure 20. **Relative mRNA expression of integrin genes from lung dendritic cells and subpopulations of lung macrophages and peripheral blood monocytes by qRT-PCR**. GR-1^{high} (Mo+) and GR-1^{low} (Mo-) peripheral blood monocytes (PBMo), lung interstitial macrophages (iMΦ) and resident alveolar macrophages (rAM) as well as lung dendritic cells (DC) were sorted as shown in Fig. 17, and mRNA expression was assessed by qRT-PCR analysis. Data represent 3-4 independent experiments per group.* indicates $p<0.05$, ** indicates $p<0.01$, *** indicates $p<0.001$.

The differential expression of selected genes was further evaluated in the GR-1^{high} and GR-1^{low} subsets of PBMo, iMΦ and rAMΦ, as well as in lung DC, by qRT-PCR (Fig. 18, 19, 20). Differences in the mRNA expression of all selected genes were statistically significant, and demonstrated the same expression trends as the results obtained by microarray experiments (Fig. 18, 19, 20). Further information was obtained with respect to differences in gene expression between subpopulations of PBMo and lung MΦ. iMΦ and rAMΦ exhibited significantly different gene expression in 14 out of 17 analyzed genes and GR-1^{high} and GR-1^{low} subsets of PBMo differed in 5 out of 10 analyzed genes, suggesting a functional and/or developmental difference.

Expression levels of MMPs in PBMo subpopulation were very low or not detectable in qRT-PCR experiments, except for Mmp14, Mmp19 and Adam19 (Fig. 18). Expression of Mmp19 and Adamts2 did not differ between iMΦ and rAMΦ, but both genes exhibited elevated expression compared to DC. All other MMPs examined exhibited higher expression levels in DC in comparison to iMΦ and rAMΦ. The GR-1^{high} and GR-1^{low} PBMo subsets did not differ in integrin expression, but significant differences were observed in all other genes analyzed, especially with respect to chemokine and chemokine receptor expression, confirming and expanding previous reports. The expression profile of lung DC was essentially similar to the expression profiles of PBMo subpopulations, while subpopulations of lung MΦ significantly differed.

3.4 Confirmation of selected integrin expression by flow cytometry on subsets of peripheral blood monocytes, lung macrophages, and lung dendritic cells

To further assess whether transcript levels demonstrated the same protein expression pattern, the integrins examined by qRT-PCR on mononuclear phagocyte populations (Fig. 20) were also assessed for cell surface expression by quantitative flow cytometry (Fig. 21). The cell surface expression levels of the respective integrin molecules demonstrated the same expression trends as the observed mRNA levels in the mononuclear phagocyte subsets analyzed. In particular, iMΦ and rAMΦ lose expression of most selected integrins, except integrin αM, which was partially expressed by iMΦ,

but was not present in rAMΦ. In contrast, integrin β1, β2 and β3 expression remains high in lung DC. Integrin αE was expressed exclusively on a lung DC subset, and its expression pattern was identical to the expression of integrin β7, suggesting co-expression of integrins αE and β7 on subpopulation of DC, which has previously been described [83].

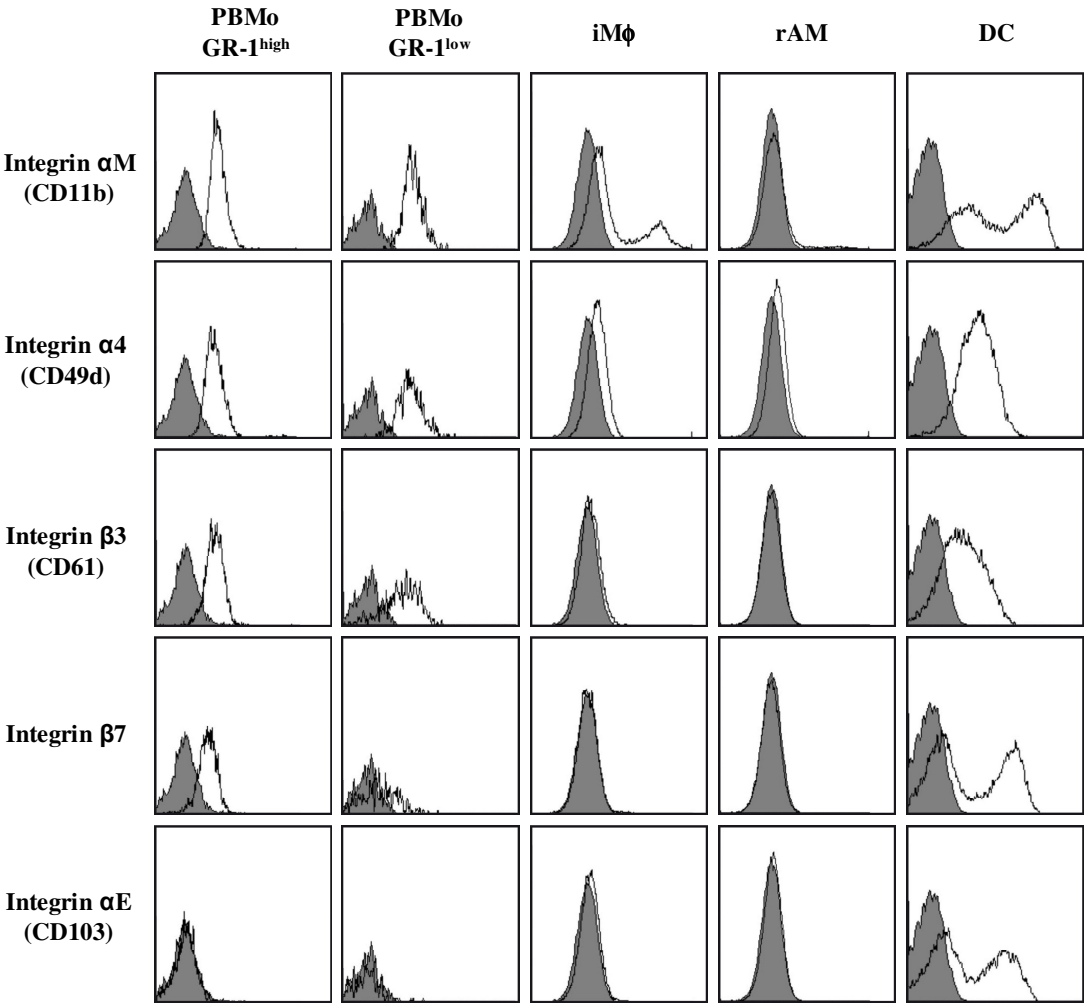

Figure 21. **Differentially regulated integrins from lung dendritic cells and supopulations of lung macrophages and peripheral blood monocytes assessed by flow cytometry**. GR-1-positive peripheral blood monocytes (PBMo) GR-1^{high} and GR-1-negative (PBMo GR-1^{low}) subsets of PBMo, lung interstitial (iMΦ) and alveolar (rAM) macrophages, and lung dendritic cells (DC) were isolated as described and analyzed by flow cytometry for the expression of the indicated integrins. Gates on the respective cell populations were set as illustrated in Fig. 17. Open histograms indicate specific fluorescence of the indicated antigen; shaded histograms represent control stained cells. Displayed data are representative of three independent experiments.

3.5 Serotonin receptor expression in the lung

3.5.1 Alveolar macrophages express the 5-HT$_{2C}$ receptor

The microarray data suggested the expression of 5-HT$_{2C}$ receptor on lung MΦ**.** This gene was significantly upregulated, based on microarray experiment data, on MΦ in comparison with DC and PBMo. This finding was validated by qPCR. To have an impression of how the expression of this receptor is distributed among lung cells a qPCR was performed including alveolar epithelial cells (AEC) (Fig. 22). The expression of serotonin 5-HT$_{2C}$ receptor was not detected in AEC and was significantly upregulated in lung MΦ in comparison with lung DC. Additionally there was a difference in the expression of 5-HT $_{2C}$ receptor between iMΦ and rAMΦ; with highest expression levels detected in iMΦ.

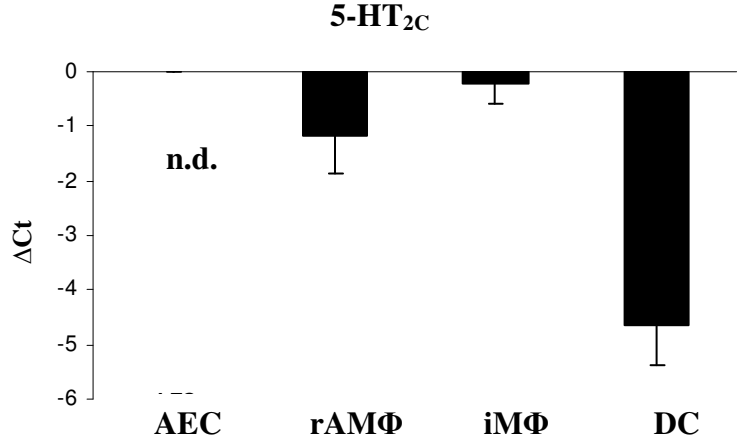

Figure 22. The expression of 5-HT$_{2C}$ receptor in lung cells examined by qRT-PCR. PBMo (peripheral blood monocytes), lung MΦ (macrophages), DC (dendritic cells) and AEC (alveolar epithelial cells) mRNA expression was assessed by qRT-PCR analysis for 5-HT$_{2C}$. Data are presented as mean ± SD of 4 independent experiments per group. All differences between gene expressions were statistically significant with $p < 0.05$ except where indicated by n.s. (not significant). A non-detectable gene expression is indicated by n.d. (not detected).

3.5.2 The serotonin receptors 5-HT$_{2A/2B}$ are expressed by alveolar epithelial cells

Amongst type 2 serotonin receptors apart from the 2C receptor there are two more members: 2A and 2B receptors. The mRNA expression of all type 2 serotonin receptor was examined by qPCR in lung cells (Fig. 23, 24). The serotonin receptors 5-HT$_{2A}$ and 5-HT$_{2B}$ were most upregulated on AEC and to a lesser extent on lung DC. Lung MΦ had

the lowest expression of compared cell types, but still detectable. To characterize the expression of 5-HT receptors in MΦ subsets and AEC, high purity cell sorting and qRT-PCR was employed, as recently described [84]. Alveolar and interstitial MΦ express high levels of mRNA coding for 5-HT_{2C} and lower quantities of 5-HT_{2A} and 5-HT_{2B} mRNAs. The serotonin receptors 5-HT_{2A} and 5-HT_{2B} are expressed by AEC, which do not express detectable mRNA levels of 5-HT_{2C} (Fig. 22).

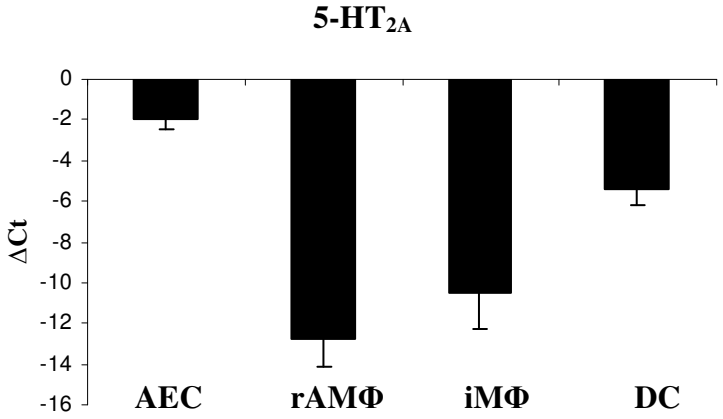

Figure 23. The expression of 5-HT_{2A} receptor in lung cells examined by qRT-PCR. PBMo (peripheral blood monocytes), lung MΦ (macrophages), DC (dendritic cells) and AEC (alveolar epithelial cells) mRNA expression was assessed by qRT-PCR analysis for 5-HT_{2A}. Data are presented as mean ± SD of 4 independent experiments per group. All differences between gene expressions were statistically significant with $p < 0.05$ except where indicated by n.s. (not significant).

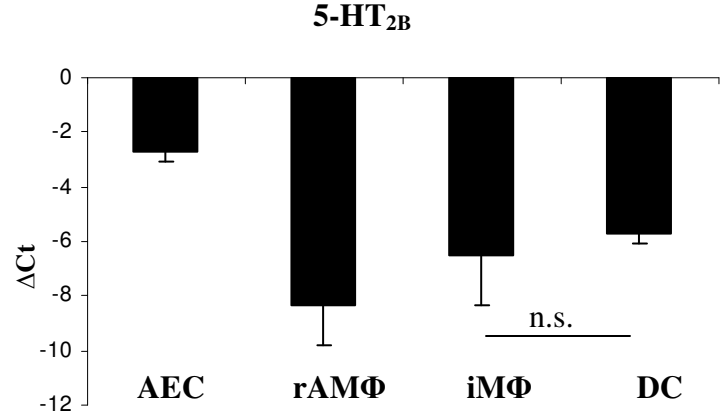

Figure 24. The expression of 5-HT_{2B} receptor in lung cells examined by qRT-PCR. PBMo (peripheral blood monocytes), lung MΦ (macrophages), DC (dendritic cells) and AEC (alveolar epithelial cells) mRNA expression was assessed by qRT-PCR analysis for 5-HT_{2B}. Data are presented as mean ± SD of 4 independent experiments per group. All differences between gene expressions were statistically significant with $p < 0.05$ except where indicated by n.s. (not significant).

3.6 Serotonin action in the lung

3.6.1 Serotonin increase CCL2 production by alveolar macrophages acting through the 5-HT_{2C} receptor

To test whether serotonin acts on rAMΦ and if 5-HT_{2C} has any function in rAMΦ the production of one of the most common macrophage chemokines (CCL2) was examined (Fig. 25). Indeed, stimulation with serotonin increased CCL2 release, and this effect was completely abrogated in ko animals which lacked 5-$HT_{2C.}$

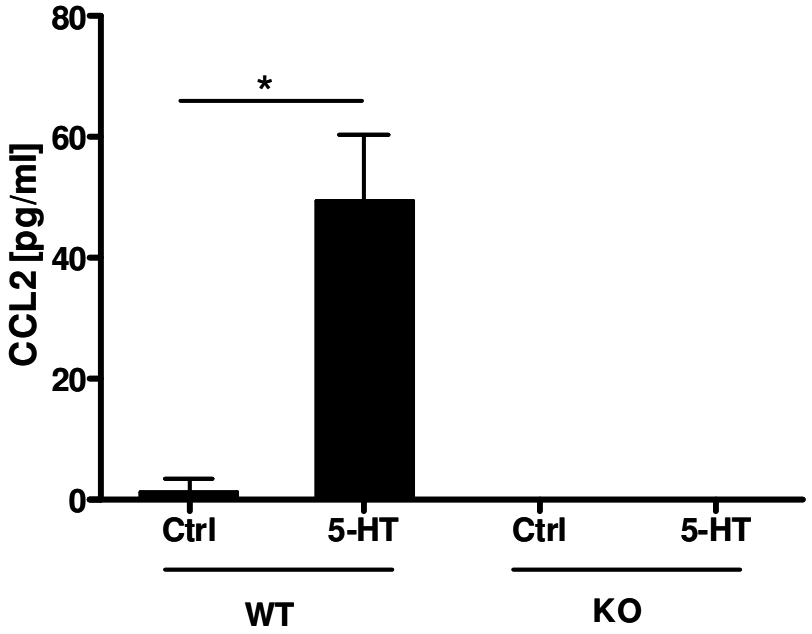

Figure 25. CCL2 protein production is increased in resident alveolar macrophages upon serotonin stimulation. Resident alveolar macrophages were stimulated with 10^{-5} M serotonin (5-HT) and cultured for 24 h. CCL2 was quantified by ELISA. Data represent 3-4 independent experiments per group. * indicates $p<0.05$. KO-knockout animals lacking 5-HT_{2C}, WT-wild type animals

There was a significant increase in levels of CCL2 in culture supernatants from rAMΦ cultured under basal conditions, compared to rAMΦ treated with 5-HT. The expression levels of CCL2 did not change upon 5-HT stimulation when experiments were performed on rAMΦ isolated from 5-HT_{2C} deficient animals, indicating an involvement of that receptor in the CCL2 secretion (Fig. 25). To investigate whether CCL2 production reflected a release of stored intracellular chemokine into the supernatant or if it is

accompany by transcriptional regulation qPCR was performed. After 4 h there was a significant increase in CCL2 mRNA expression in rAMΦ stimulated with 5-HT, while no difference in CCL2 mRNA expression was observed in 5-HT_{2C} deficient animals, once more proving a role of this receptor on rAMΦ response to 5-HT (Fig. 26).

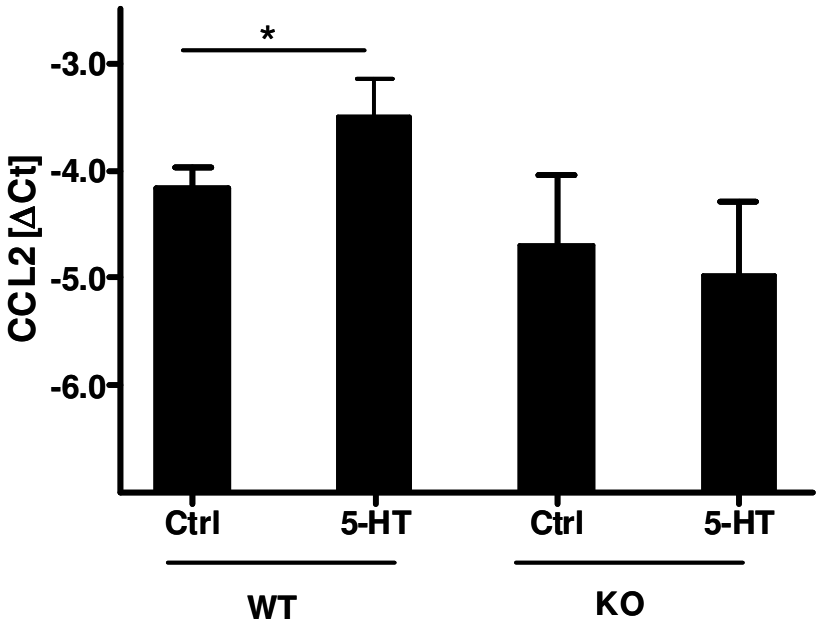

Figure 26. CCL2 mRNA production is increased in alveolar macrophages upon serotonin stimulation. Resident alveolar macrophages were stimulated with 10^{-5} M serotonin (5-HT) and cultured for 4 h. The CCL2 mRNA was measured quantified by qPCR. Data represent 3-4 independent experiments per group. * indicates $p<0.05$ KO-knockout animals lacking 5-HT_{2C}, WT-wild type animals

3.6.2 Microarray analysis reveal transcriptional changes in alveolar macrophages stimulated with serotonin acting exclusively through the 5-HT_{2C} receptor

To assess how 5-HT can change the transcriptional profile of rAMΦ, whole mouse genome microarray was used to address this question. Freshly isolated rAMΦ were stimulated with 5-HT and after 4 h, cells were collected and RNA was isolated, transcribed to cDNA and hybridized on the array. To understand if the action of 5-HT was mediated by the 5-HT_{2C} receptor, the same experiment setup was applied to mice lacking 5-HT_{2C}.

There were 53 genes regulated in wild type rAMΦ stimulated with 5-HT and non in mice lacking 5-HT_{2C} (Fig. 27). This clear result proved that 5-HT acts on rAMΦ at the transcriptional level, through the 5-HT_{2C} receptor, and provided a list of interesting genes that are regulated upon 5-HT stimulation.

Out of 53 genes regulated on the array, 39 were upregulated and 14 were downregulated. Many from upregulated genes were involved in cytokine activity (*spp1*), signal transduction involving G-protein coupled receptors (*sphk1*), biosynthetic processes (*nt5e*) or cell differentiation (*csf1*). Downregulated genes such as (*ptges*) are involved in anti-inflammatory response, ECM organization (*tgfbi*) or exhibit peptidase activity (*htra1*).

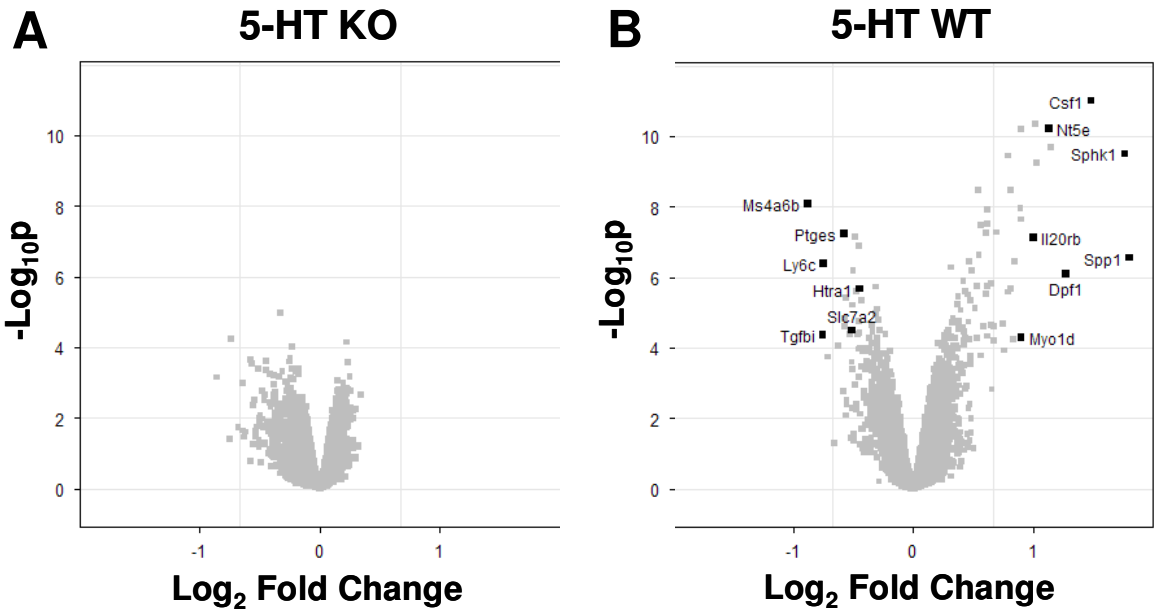

Figure 27. Volcano plots representing genes regulated in alveolar macrophages upon serotonin stimulation. Resident alveolar macrophages were isolated from 5-HT_{2C} deficient (KO) (A) and wild type (WT) (B) animals and treated with 10^{-5} M serotonin (5-HT) for 4 h. Some differentially regulated, arbitrarily chosen genes were marked.

3.6.3 Validation of candidate genes by real time quantitative PCR

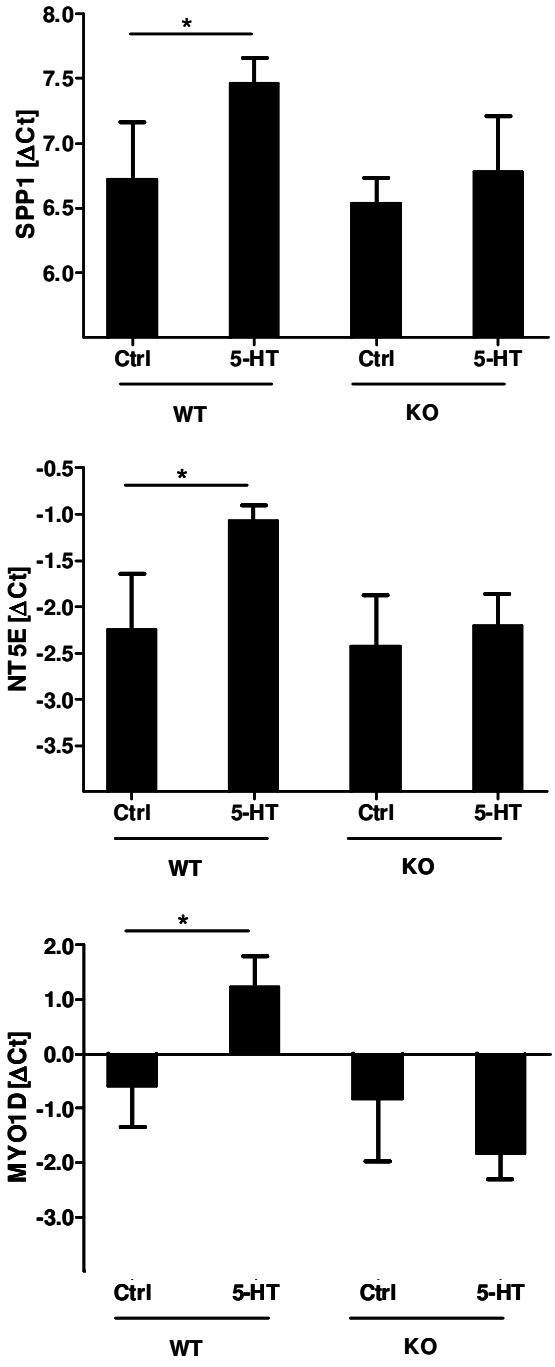

Figure 28. **Validation of spp1, nt5e and myo1d by qRT-PCR.** Resident alveolar macrophages were isolated from 5-HT_{2C} deficient (KO) (A) and wild type (WT) (B) animals and treated with 10^{-5} M serotonin (5-HT) for 4 h. The mRNA of selected genes was measured quantified by qPCR. Data represents 3-4 independent experiments per group. * indicates $p<0.05$

To validate the microarray results three genes (*spp1, nt5e, myo1d*) were chosen and their mRNA expression was assessed by qPCR. The expression profile was consistent with microarray results. There was an increase in mRNA expression of the genes listed above when wild type rAMΦ stimulated with 5-HT were compared with unstimulated control, and no difference was observed in the expression of rAMΦ from 5-HT_{2C} deficient animals stimulated with 5-HT compared with unstimulated control (Fig. 28).

3.6.4 Serotonin increase the production of MIP-2 in alveolar epithelial cells

To examine if 5-HT had any effect on AEC primary AEC on the third day of culture were stimulated with 5-HT. An increase in MIP-2 production was observed after 24 h, as well as after 48 h of culture. Since AEC do not express 5-HT_{2C} serotonin receptor MIP-2 increase in expression is mediated by other type of receptor(s).

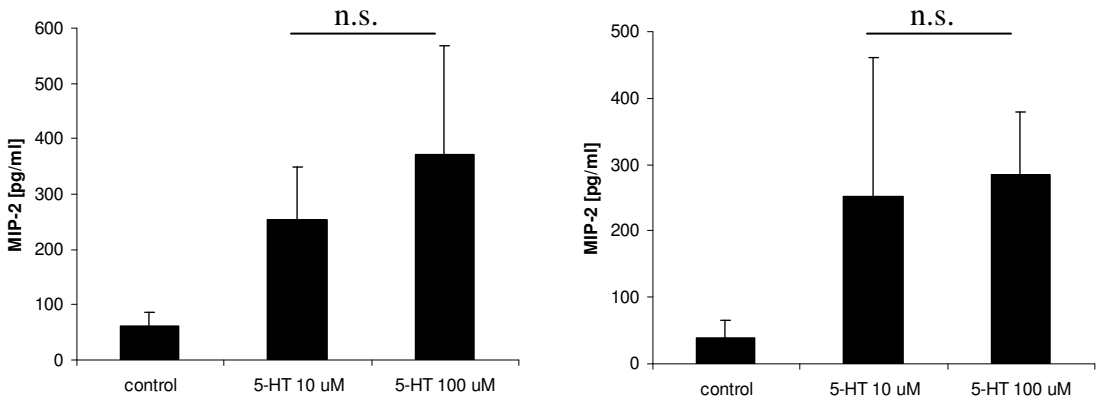

Figure 29. **MIP-2 production is increased in alveolar epithelial cells upon serotonin stimulation.** Alveolar epithelial cells (AEC) were stimulated with 10^{-5} M and 10^{-4} M serotonin (5-HT) and cultured for 24 h and 48 h. MIP-2 concentration was quantified by ELISA. Data represent 3-4 independent experiments per group. All differences between MIP-2 productions were statistically significant with $p < 0.05$ except where indicated by n.s. (not significant).

3.6.5 TNF-α production in alveolar macrophages is not modulated by presence of serotonin

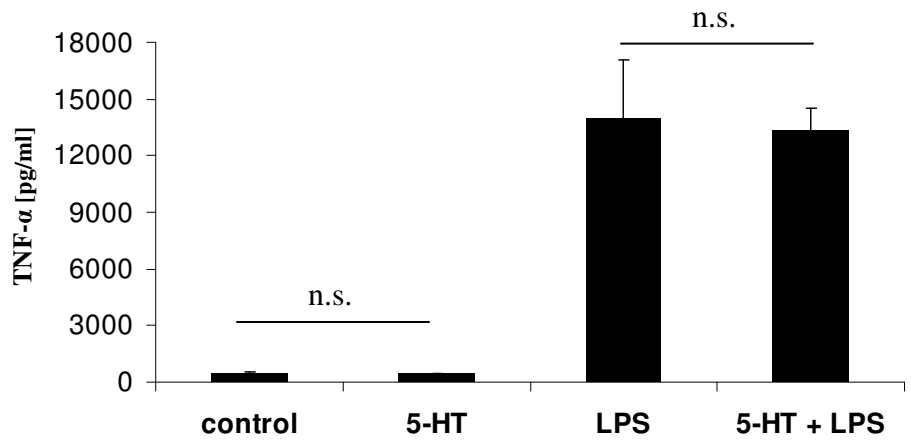

Figure 30. TNF-α protein level in bronchoalveolar lavage fluid is not modulated upon serotonin stimulation. Mice were intratracheally stimulated with 10^{-5} M serotonin (5-HT) in presence or absence of LPS. Mice were sacrificed after 6 h and bronchoalveolar lavage fluid was quantified by ELISA for the presence of TNF-α. Data represents 9 independent experiments per group. All differences between TNF-α production were statistically significant with $p < 0.05$ except where indicated by n.s. (not significant).

One of the first responses of rAMΦ to bacterial assault is increased TNF-α production. To assess the role of 5-HT in one of the first reactions of rAMΦ *in vivo* we treated mice with LPS in presence or absence of 5-HT and TNF-α production from BALF was assessed. After 6 h post LPS stimulation no significant difference in TNF-α level in BALF was observed between mice treated with or without 5-HT (Fig 30). Additionally, 5-HT alone did not influence TNF-α production. A similar experiment was conducted *in vitro* (Fig. 31). Freshly isolated rAMΦ were stimulated with LPS alone, or together with 5-HT, and TNF-α production was assessed after 6 h. Here, again no significant difference was observed between rAMΦ treated with LPS alone or together with 5-HT, suggesting that 5-HT does not play a role in rAMΦ TNF-α production upon LPS stimulation.

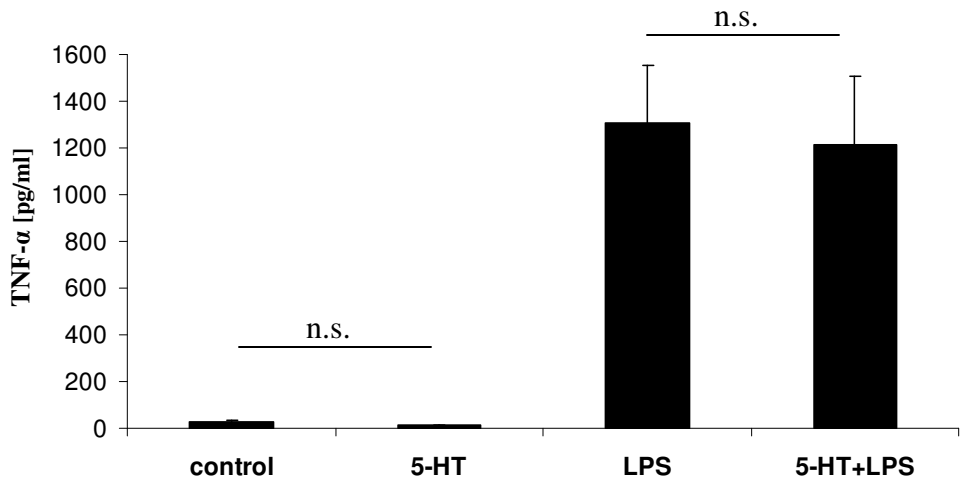

Figure 31. TNF-α protein production *in vitro* in alveolar macrophages is not modulated upon serotonin stimulation. Resident alveolar macrophages were stimulated with 10^{-5} M serotonin (5-HT) with presence or absence of LPS and cultured for 6 h. TNF-α production was quantified by ELISA. Data represents 6 independent experiments per group. All differences between TNF-α production were statistically significant with $p < 0.05$ except where indicated by n.s. (not significant).

3.7 Gramd3 as a potential cell surface marker for lung dendritic cells

Based on the present knowledge there is no single, specific marker that could discriminate between lung MΦ and DC. The need for such a marker comes from the fact that the isolation procedure, as well as analysis by flow cytometry of MΦ and DC would be much easier. These two cell types are visibly different assessed even by light microscopy, so there is a strong indication that such a marker, specific for just one type might exist.

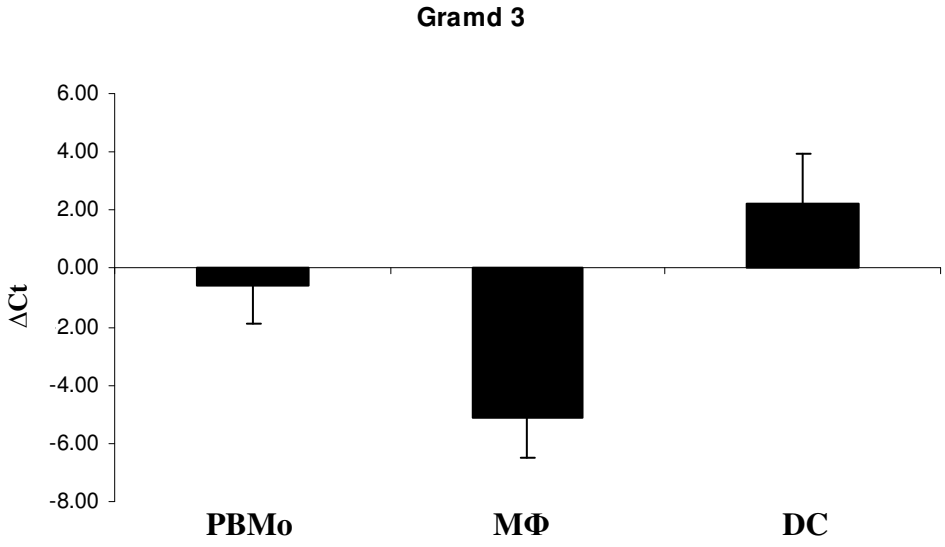

Figure 32. The expression of gramd3 in peripheral blood monocytes, lung macrophages and lung dendritic cells examined by qRT-PCR. Peripheral blood monocytes (PBMo), lung macrophages (MΦ) and dendritic cells (DC) mRNA expressions were assessed by qRT-PCR analysis for Gramd3. Data are presented as mean ± SD of 4 independent experiments per group. All differences between gene expressions were statistically significant with $p < 0.05$

Microarray data provided a list of known and unknown genes that code for proteins that are transmembrane and could be evaluated as markers. From the discovery point of view it would be more interesting to investigate an unknown gene and not only prove it as a DC marker but also assign it a biological function.

Microarray results were screened for unknown genes that were significantly upregulated on DC in comparison to PBMo and MΦ and additionally had transmembrane domains.

Gramd3 (NM_026240, GRAM containing domain 3) was the only gene from the selected genes that was validated by qPCR (Fig. 32). The GRAM domain is found in glucosyltransferases [85], myotubularins [86] and other putative membrane-associated proteins associated with membrane traffic and pathogenesis and signal transduction.

At this moment the next step in establishing Gramd3 as a new DC marker would be to raise antibodies against the protein produced by this gene and stain the lung sections to examine if Gramd3 is really specific for lung DC.

.

3.8 Expression of proteases on lung dendritic cells

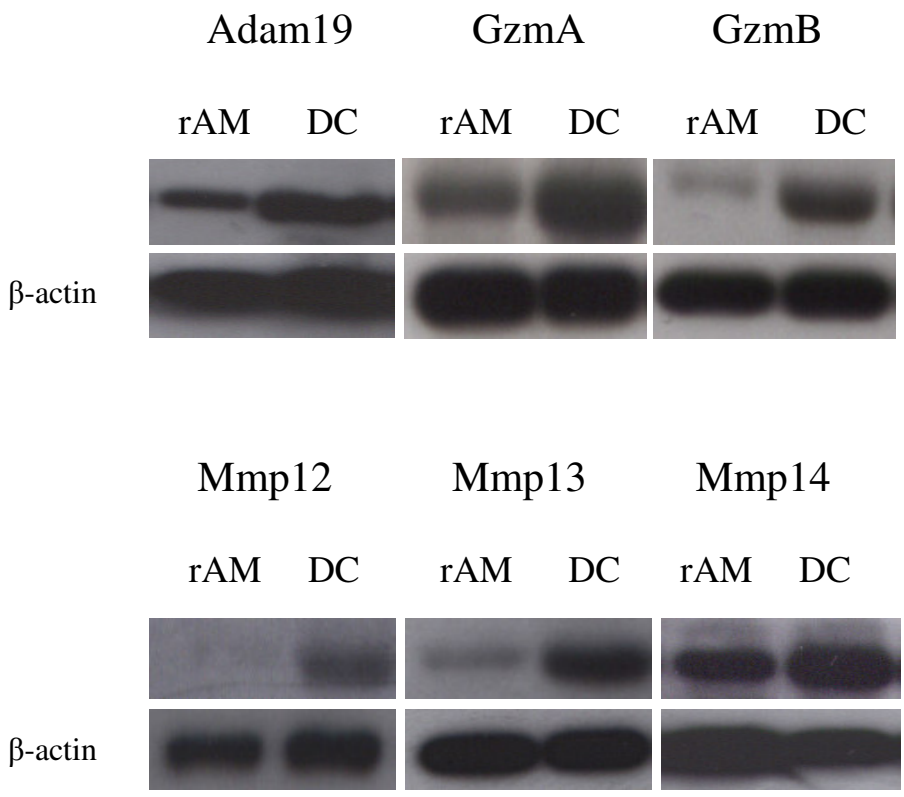

Figure 33. Protease expression is increased in lung dendritic cells in comparison with alveolar macrophages. Resident alveolar macrophages (rAM) and lung dendritic cells (DC) were flow sorted and their expression of proteases was measured by western blot analysis. Experiment was done in triplicate and figure shows a representative blot.

There were three groups of gene clusters in the microarray analysis that were involved in cell trafficking, namely MMPs, integrins and chemokines. A decision to continue with just one group had to be made, for practical reasons. Since chemokine and integrin involvement in the immune cell recruitment to the lung is well established, the research interest was narrowed to the expression of MMPs on lung DC. Dendritic cells in the lungs exhibited the highest expression of MMPs from cells compared in the microarray study.

The expression pattern of MMPs in rAMΦ and DC obtained from the microarray experiment was validated at the protein level by western blot analysis (Fig. 33). The expressions of all compared proteases were upregulated in DC in comparison with rAMΦ. The Mmp14 and GzmB expressions were slightly upregulated, while other proteases were strongly upregulated. Interestingly, Mmp12 was hardly detectable in rAMΦ.

3.9 Granzyme B is active in lung dendritic cells

The decision to continue research with granzymes was based on the fact that knockout animals were available, fertile, exhibited distinct phenotype and that difference in GzmB expression between rAMΦ and DC was one of the most significant of all compared proteases. Western blots could not answer the question if granzyme is active and functional in DC. To establish whether this was the case, flow sorted DC were cultured for 24 h in presence or absence of LPS. Subsequently, supernatants and cell lysates were examined for granzyme activity (Fig. 34). Only in cell lysates, and not in supernatant, granzyme activity was observed. The LPS stimulation did not modulate granzyme activity.

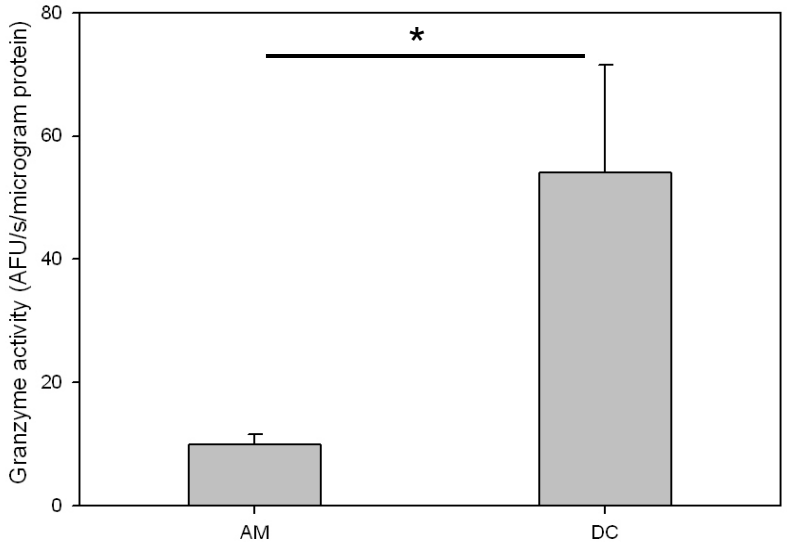

Figure 34. Granzyme B activity is increased in lung dendritic cells in comparison with alveolar macrophages assessed by a fluorescent substrate activity assay. Lung macrophages (AM) and dendritic cells (DC) were flow sorted and lysed. Lysates were incubated with granzyme B substrate for 30 s. Fluorescence was measured in a fluorometer at excitation wavelength 400 nm and at emission wavelength 505 nm. Data represent 3-4 independent experiments per group. * indicates $p<0.05$

4. Discussion

4.1 Microarray analysis as a tool for studying the mononuclear phagocyte system in the lung

The constant maintenance of both DC and MΦ cell pools in the lung is essential for effective immune surveillance in pulmonary tissue. Recent reports highlight the role of PBMo that emigrate into the lung and differentiate into both lung DC and MΦ, thereby serving as a constant supply for the renewal of the lung DC and MΦ pool [18]. While many studies have investigated monocyte recruitment under inflammatory conditions, little is known about the pathways mediating monocyte trafficking and differentiation in lung tissue under non-inflammatory conditions [81, 87, 88]. Since PBMo are believed to be precursors for lung MΦ and DC, a global gene expression profiling approach was chosen to reveal crucial differences between these cell types, to better understand their relation to one another, and to identify gene clusters relevant for the migration and differentiation process that takes place under steady-state conditions. Previous microarray studies investigating the relation, differentiation and/or maturation of monocytes, MΦ and DC have been mainly conducted *in vitro,* using both murine and human cells [89-91]. A study comparing primary human MΦ versus MΦ differentiated *in vitro* from PBMo has demonstrated significant differences in gene expression profiles [92], indicating the necessity of carefully elaborating the differences and similarities between *in vivo* and *in vitro* differentiation. A recent publication from our group compared gene expression profiles of murine mononuclear phagocytes recruited to the alveolar space under noninflammatory and inflammatory conditions using 1 K nylon arrays [93]. The present study was undertaken as the first *in vivo* investigation using cell specific whole genome expression profiling of key players in lung immunity, namely lung MΦ and lung DC and their circulating precursors PBMo, to define the gene expression differences between these three cell populations under non-inflammatory conditions in mice. By this, it could be demonstrated that approximately 5–10% of the transcriptome are differentially regulated between these three cell populations which are closely related with respect to origin, destination and function. Whether these expression differences represent

preformed, lineage-specific differentiation programs or are rather due to the interaction of migrating PBMo and specific micro-environmental factors of the lung must be addressed in detail in subsequent studies.

4.1.1 Differentially regulated genes between lung macrophages and lung dendritic cells are essential for cell migration

Lung DC and MΦ play diverse functional roles in the innate immunity, and their localization to different compartments of the lung suggests different migration properties of these cell types. Under steady-state conditions, DC largely reside in the interstitial compartment, with only minor parts located in the alveolar space, and ultimately they emigrate to the thoracic lymph nodes to present antigen to T cells. Conversely, MΦ readily pass through the epithelial barrier and enter the alveolar airspaces, which very likely represents a terminal destination. Hypothesizing that DC and MΦ residing in different environments most likely require different migration and tissue invasion capacities, differentially expressed genes were grouped into trafficking related clusters such as integrins, MMPs, chemokine and chemokine receptors, and interleukins and interleukin receptors. Integrins are key mediators of cell-cell interactions, and given their different tissue localization, DC and MΦ most likely have to interact with different cell types or the ECM. Indeed, the lack of integrin gene expression in rAMΦ suggest that these cells require less integrin-mediated cell-cell communication than both subsets of PBMo and lung DC, which is consistent with the view of rAMΦ being confined to the alveolar space, rather than possessing extensive migratory properties. Members of the MMP family can cleave components of the ECM, thereby facilitating cell migration [94]. Furthermore, MMPs can modulate the activity of chemokines [95], cytokines [96], and selectins [97]. Chemokines themselves also regulate MMPs and integrin avidity [98-100]. The different biological functions of DC and MΦ would imply that these cell types have different interactions with their direct environment, suggesting the differential expression of genes that regulate cell interaction with the ECM, and responses to chemokines and cytokines. Our data show that DC and MΦ express different clusters of MMP as well as cytokine and chemokine receptor genes, indicating distinct patterns of migration properties. Another important aspect of this study is the detailed delineation of the

expression pattern of chemokines and their receptors in PBMo, lung MΦ and lung DC under non-inflammatory conditions. The microarray and qRT-PCR analyses demonstrate that all three cell populations express a variety of both chemokines and receptors. The qRT-PCR analysis of the mRNA levels in iMΦ and rAMΦ, however, indicates a more active participation in chemokine production by the iMΦ than by the rAMΦ population.

4.1.2 Differentially regulated integrins: validation of microarray results at the protein level

The gene expression patterns obtained from our study suggest that lung DC are phenotypically more related to PBMo than lung tissue MΦ. When further comparing the transcriptional regulation of selected genes in the lung macrophage subpopulations by qPCR, the transcripts of CCR2, CCL2, CCR7 and CD61 all highly expressed in PBMo were found to be less downregulated in iMΦ compared to rAMΦ. This finding supports a recent report by Landsman *et al*., suggesting that iMΦ are an intermediate stage in the differentiation process to rAMΦ [17]. An important issue when interpreting DNA microarray data is whether mRNA expression levels demonstrates the same expression trends as the expression of the encoded proteins. Notably, the transcriptional expression patterns of selected integrins obtained by DNA array and qRT-PCR were found to demonstrate the same expression trend as the expression levels of the respective proteins on the cell surface as detected by flow cytometry.

4.2 Serotonin acts on alveolar macrophages through the 5-HT_{2C} receptor

4.2.1 Expression of serotonin receptors in the lung

In this study, the first evidence for functional expression of 5-HT_{2C} receptors on mouse lung MΦ is provided. In freshly isolated rAMΦ, 5-HT rapidly stimulates intracellular calcium elevation and leads to increased production of the monocyte chemoatractant CCL2, as well as changes in the transcriptional profile based on an unbiased microarray study.

While many studies have investigated effects of 5-HT on cytokine production in various immune cells, little is know about the action of 5-HT on lung MΦ. Acute effects of 5-HT on rAMΦ have not been investigated so far. Previous studies have pointed to the importance of 5-HT_2 receptors in a development of bleomycin-induced pulmonary fibrosis in mice [57] and monocrotaline-induced pulmonary hypertension in rats [58]. The first evidence of 5-HT_{2C} expression on MΦ was suggested by Zasłona *et al.* [84] based on microarray study. In the lung 5-HT_2 receptors are differentially expressed by rAMΦ and AEC. This finding supports a recent work by Fabre *et al.* which shows the expression of 5-HT_{2A} and 5-HT_{2B} on murine pneumocytes [57]. Interestingly, both alveolar and lung interstitial MΦs express high levels of 5-HT_{2C} mRNA, but they express lower quantities of other two 5-$HT_{2A/B}$ receptors.

4.2.2 Alveolar macrophages increase CCL2 production upon serotonin stimulation

To get general insights into physiological responses of rAMΦ upon 5-HT stimulation, secretion of inflammatory mediators by rAMΦ was measured with the use of a dot-blot based assay. Indeed, changes in the production of inflammatory mediators were observed. Mainly CCL2, but also CCL5, TNF-α, KC and MIP-2 production was increased by 5-HT stimulation. Increased CCL2 production in 5-HT stimulated rAMΦ was validated by ELISA. Importantly, KO cells do not increase CCL2 in response to 5-HT, proving involvement of the 5-HT_{2C} in those responses. In addition, CCL2 mRNA was increased upon 5-HT stimulation, and again this effect was 5-HT_{2C}-dependent.

The CCL2 production is induced by variety of cells upon infection and is responsible for the migration of immune cells to the site of infection [9] (Fig. 35). The CCL2 is a chemokine that drives monocytes recruitment to the lung under inflammatory conditions [101]. This phenomenon was confirmed in bacterial [102] and viral [103] models of lung inflammation, however in both settings AEC were responsible for CCL2 increase. According to the data generated in our group rAMΦ do not play a role in monocyte recruitment process in non-inflamed lung, e.g. elicited by CCL2 installation. However in a combined LPS/CCL2 challenge depletion of rAMΦ decreased alveolar neutrophil and monocyte recruitment [88]. Mouse rAMΦ carry CCR2 receptors, indicating potential binding of CCL2 [88] and are also known to produce CCL2 in response to different

stimuli, however in lower quantities than AEC. It has been shown that CCL2 production in rat NR8383 Macrophage cell line can be increased by ATP, and the release from induced cells can be attenuated after chelating intracellular Ca2+ with BAPTA [104]. Since CCL2 is stored in cytosolic granules [105], it is possible, that 5-HT promote release of stored CCL2 via exocytosis which is a Ca2+- and G-protein-dependent process [106]. To summarize one can comment that MΦ are not the main producers of CCL2 in the lung, but increase of CCL2 release by rAMΦ upon 5-HT stimulation may play a role in microenvironment, e.g. by promoting crosstalk between MΦ and AEC.

Since 5-HT levels are elevated in inflamed tissues [44] it is possible that MΦ and AEC have contact and react to 5-HT under local inflammatory conditions (Fig. 36, 37). It is also likely that AEC and MΦ reaction to 5-HT is quite different since 5-HT_{2C} is just present on AM. The serotonin 5-$HT_{2A/B}$ receptors, based on our study, are not responsible for CCL2 production in MΦ. Moreover, AEC which express 5-$HT_{2A/B}$ do not increase CCL2 production upon 5-HT stimulation (data not shown). It can be speculated that upon contact with 5-HT, CCL2 production starts in small levels in MΦ, and that facilitates AEC activation by CCR2-dependent mechanism [107].

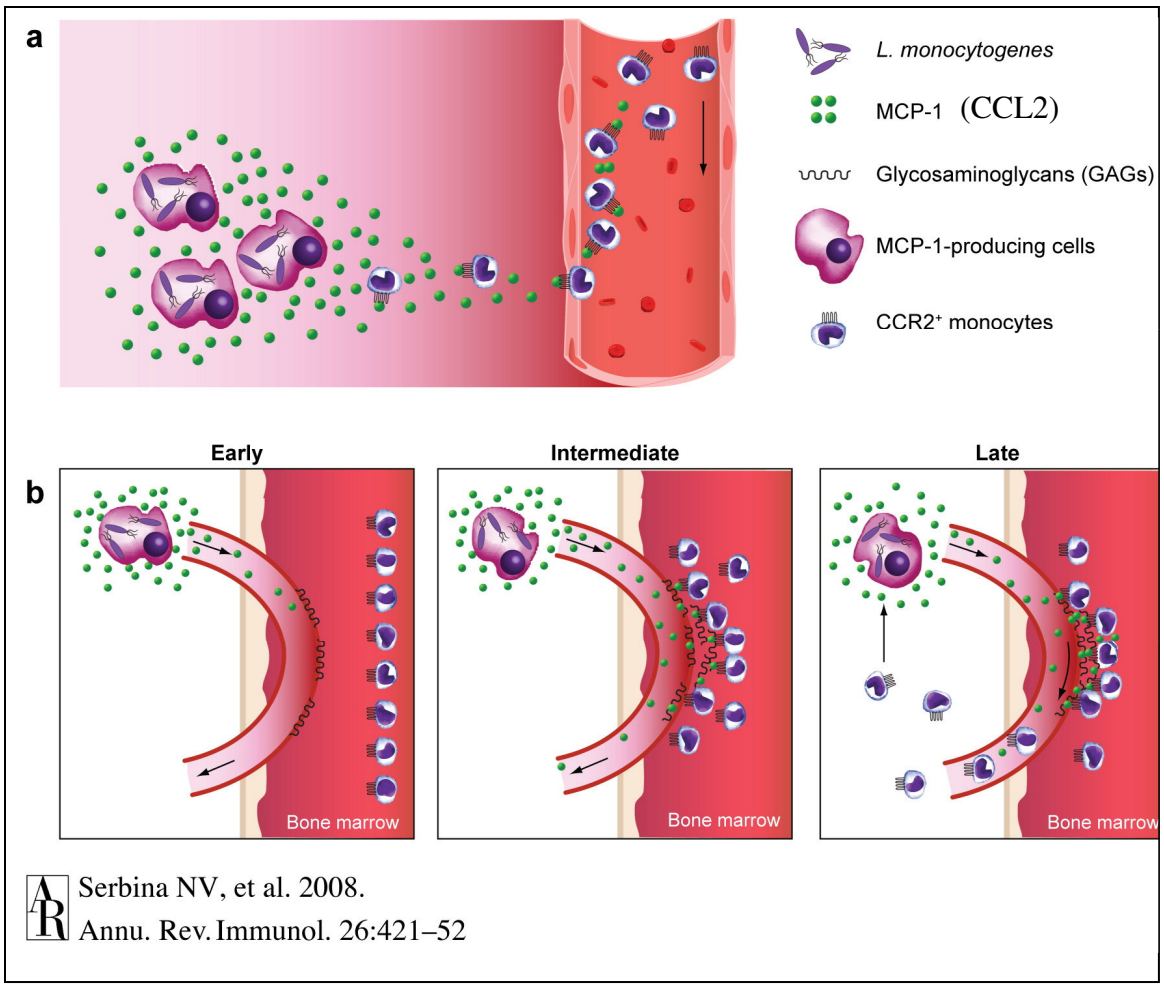

Figure 35. Models of CCL2 mediated monocyte recruitment. Adapted from Serbina *et al* .2008 [9]. During infection MCP-1 (CCL2) is produced and secreted by infected or cytokine stimulate non-infected cells. (a) In the first model secreted MCP-1 establishes a gradient across the distance from infection site and attracts monocytes to the infection sites. (b) In an alternative model MCP-1 gradient is established not by distance from chemokine production site but rather by chemokine binding with specific glycosaminoglycans (GAGs).

4.2.3 Serotonin changes the transcriptional profile of alveolar macrophages

To better understand transcriptional changes in rAMΦ upon 5-HT stimulation, a microarray analysis was performed on whole mouse genome. Experiments were performed on rAMΦ isolated from wild type and 5-HT_{2C}-deficient animals. Differentially expressed genes were present just in the first group, indicating that 5-HT acts on rAMΦ

exclusively through 5-HT_{2C}. Differentially regulated genes on rAMΦ cover a broad spectrum of functions important for rAMΦ biology. From upregulated genes on rAMΦ upon 5-HT stimulation osteopontin (*spp1*) is known to be involved in interstitial lung diseases [108] and airway remodeling [109]. Increased osteopontin production in the lungs is associated with airway collagen deposition in experimental model of allergen induced airway remodeling [110]. If transcriptional changes in osteopontin in rAMΦ translate to protein expression, it can be speculated that 5-HT can play a role in local lung remodeling by acting on rAMΦ through 5-HT_{2C}, as it was suggested by Fabre *et al*. for 5-$HT_{2A/B}$ on AEC [57]. At the same time *nt5e*, which was upregulated on rAMΦ in our study and which protein product converts AMP to adenosine is involved in the protection against ventilator induced lung injury assessed by decreased protein content in BAL, decreased water in lung [111] and decreased neutrophil influx in LPS-treated lungs [112]. Additionally *nt5e* was proved to be important in attenuating pulmonary inflammation and fibrosis in bleomycin induced injury model, where in *nt5e*-deficient animals osteopontin and other profibrotic mediators were increased [113]. Further study has to be conducted to confirm if 5-HT stimulated rAMΦ increase osteopontin and *nt5e* on protein level and an animal model has to be chosen to validate a role of 5-HT and complex interplay of listed above genes in lung pathology.

In conclusion, 5-HT was established as a novel modulator of rAMΦ function. In this study, the first evidence for 5-HT_{2C} exclusive role in rAMΦ activation is provided, assessed by transcriptional and functional changes.

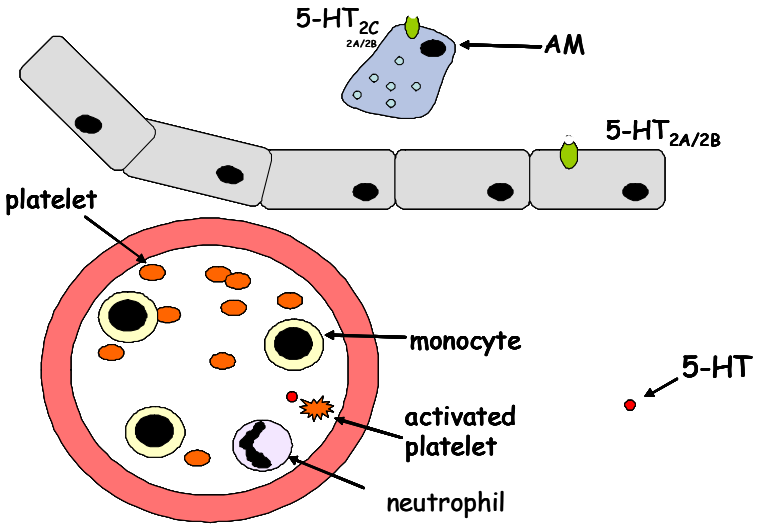

Figure 36. Serotonin under steady-state conditions in the lung. Under steady state conditions epithelial cells (in gray) and alveolar macrophages (AM) in blue do not have contact with high levels of serotonin (5-HT)

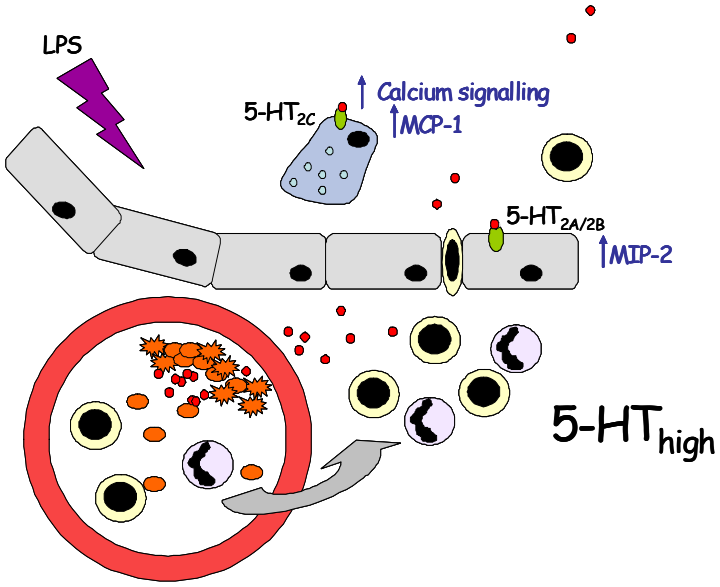

Figure 37. Serotonin in lung inflammation. During lung inflammation there is a recruitment of neutrophils (violet) and monocytes (yellow) from the blood together with platelets (red) that by aggregation in the lung release serotonin that acts on alveolar macrophages (AM) in blue through 5-HT_{2C} and epithelial cells (gray) through 5-$HT_{2A/B}$. AM start to produce MCP-1 (CCL2), while AEC produce MIP-2.

4.3 Expression of proteases in lung dendritic cells

4.3.1 Differential expression of MMPs among peripheral blood monocytes, lung dendritic cells and macrophages

It has previously been shown that Mmp2 and Mmp9 are critically required by DC for recruitment to the airways in a murine model of asthma [114] and for the migration of DC from the skin to the lymph nodes [115]. While a difference in gene expression of Mmp2 and Mmp9 between lung DC and lung AM could not be demonstrated by microarray, five members of the MMP family, Adam19, Adam23, Mmp12, Mmp13 and Mmp14 were identified, which were dramatically upregulated in lung DC versus MΦ; while Mmp19 was upregulated in both iMΦ and rAMΦ, compared to DC. In contrast, expression of MMPs except Mmp8, Mmp19 and Adam19 in PBMo was low or not detectable, indicating that the transcriptional upregulation of proteases is an important and immediate step in the differentiation process after PBMo emigration from the blood into the lung. However, the exact role played by these differentially expressed members of the MMP family in cell migration, phagocytosis and antigen processing has to be further delineated. Similarly, the mechanisms by which MMPs regulate the function of chemokines, cytokines, and integrin expression, which influence DC and MΦ migration and activity, needs to be addressed in further studies.

4.3.2 The expression of proteases assessed by western blot on lung dendritic cells

Of the differentially expressed proteases, the majority was upregulated on lung DC. These data are novel, since to date most of investigations concerning expression of MMPs in the lung were restricted to MΦ.

To validate the microarray results, western blot analysis was performed to examine whether expression of MMPs would also be altered at the protein level. Indeed, the expression of Adam19, Adam23, Mmp12, Mmp13, Mmp14 as well as GzmA and GzmB was upregulated in DC. The largest difference in the expression levels between lung DC

and MΦ was observed for GzmB and Mmp13. It has to be kept in mind that the western blot analysis did not demonstrate the activity level of the examined proteases.

Both Mmp13 [116] and Mmp14 [117] play a pivotal role in cell cancer metastasis and invasion, so it can be speculated that the expression of these enzymes on DC may also be important in the migration process. It is difficult, however, to identify inhibitors that would specifically inhibit individual MMP members. In addition, protease substrate specificities overlap within the MMP family. These were the main concerns in the continuation of research with one of the members of MMP family expressed in lung DC. Additionally, the role of MMP in cell migration was often addressed in many publications, including studies in lung DC migration. Conversely, a role of granzymes in DC biology has not been addressed, and to the present day no study has been conducted to demonstrate the expression of granzymes in lung DC.

4.3.3 Expression and role of granzymes in DC: future perspective

The information that granzymes are expressed by DC is not completely new. Previous studies have shown that human pDC [67, 118], as well as monocyte derived human DC [119] express granzyme B. Different studies have focused on mouse and human myeloid DC, presenting data on mRNA level, for both granzyme A and B [120]. The suggested function for granzymes expressed in DC is cytotoxicity, but since perforin was not expressed, this was not the obvious role. Although an alternative pathway of granzyme-mediated killing that does not involve perforin has been proposed [121], more probable is that DC express granzymes not for killing purpose, but rather for some extracellular functions. This idea is supported by the fact that there are non-cytotoxic cells expressing granzymes such as keratinocytes [122] or chondrocytes [123]. Additionally, in several diseases such as hypersensitivity pneumonitis [124], chronic allergic asthma [125], *Plasmodium falciparum* infection [126] or experimental endotoxemia [127] elevated granzymes levels are observed. It is unlikely that elevated extracellular granzymes levels are due to cell killing processes, where release of granzymes to target cell is not precise. The extracellular role for granzymes may not just be ECM remodeling, as discussed previously, but could also be cell signaling mediated by cytokine production, which is supported by *in vitro* data [128, 129].

Lung DC, according to data presented here, express active granzyme B. To answer the question of what granzyme B does, we have to look back at dendritic cell biology. Lung DC, in comparison to MΦ, are much more mobile under steady state conditions. These cells constantly migrate from the blood to lungs seeking antigen to process and present to T-cells in lymph nodes (Fig. 38). Most probably, granzyme B is active in one or more processes during this journey. Granzyme B is either involved in DC migration through different compartments in the lung that require digestion of matrix proteins and basement membranes, or it plays a role in antigen presentation in processing and fragmentation of antigen for MHC class II loading. The best model to address this question would be an *in vivo* assay to examine DC migration, such as in ovalbumin coupled to fluorescin model and T-cell proliferation assay facilitated by carboxyfluorescein succinimidyl ester dyes. With the help of flow cytometry, different populations of lung DC could be examined. The pulmonary DC migration could be studied in the presence and absence of inflammation. The DC specific role of granzymes can be further studied using adoptive transfer of granzyme-deficient labeled lung DC into wild type recipient lungs to observe their migration and function.

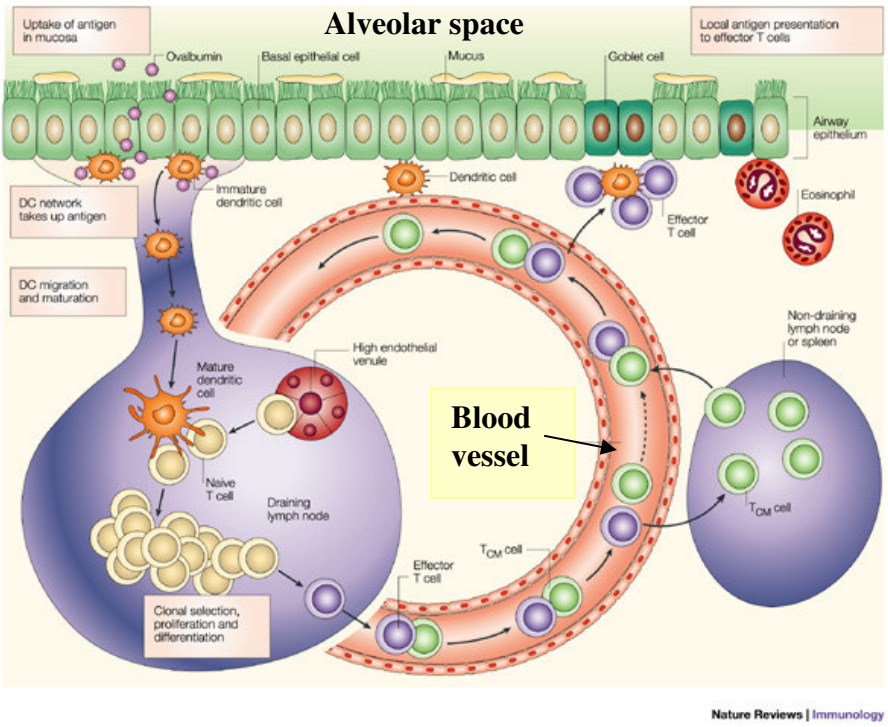

Figure 38. **Overview of lung dendritic cells migration.** Adapted from Lambrecht and Hammad 2003 [40]. Precursors of dendritic cells (DC) enter lungs from blood circulation. Immature DC search for antigen, and when antigen is taken up by DC, The DC mature and travel to the mediastinal lymph nodes, where DC select a specific T-cell from the polyclonal repertoire. If DC present antigen in a immunogenic manner, than within four days, this will lead to clonal expansion of antigen specific T-cell. This process is amplified in the presence of inflammation, increasing the possibility of pathogenic substances to be presented to naïve T-cells.

5. Summary

Peripheral blood monocytes (PBMo) originate from the bone marrow, circulate in the blood, and emigrate into various organs where PBMo differentiate into tissue resident cellular phenotypes of the mononuclear phagocyte system (MPS), including macrophages (MΦ) and dendritic cells (DC). As in other organs, this emigration and differentiation process is essential to replenish the mononuclear phagocyte pool in the lung under both inflammatory and non-inflammatory steady-state conditions. While many studies have addressed inflammation-driven monocyte trafficking to the lung, the emigration and pulmonary differentiation of PBMo under non-inflammatory conditions is comparatively poorly understood.

In order to assess the transcriptional profile of circulating and lung-resident MPS phenotypes, PBMo, lung MΦ and lung DC from naïve mice were flow-sorted to high purity, and cellular gene expression was compared by DNA microarray on a genome-wide scale. Differential regulation of selected genes was validated by quantitative polymerase chain reaction (qPCR) and at the protein level by flow cytometry.

Differentially-expressed genes related to cell trafficking were selected and grouped into three clusters: (i) matrix metallopeptidases, (ii) chemokines/chemokine receptors, and (iii) integrins. Expression profiles of gene clusters were further examined at the mRNA and protein levels in subsets of circulating PBMo ($GR1^-$ versus $GR1^+$) and lung MΦ (alveolar MΦ versus interstitial MΦ). These data identify differentially activated genetic programs in circulating monocytes and their lung descendents. Lung DC activate an extremely diverse set of genes, but largely preserve a mobile cell profile with high expression levels of integrins, chemokines and chemokine receptors. In contrast, interstitial and alveolar MΦ, downregulate gene expression of these traffic-relevant communication molecules, but strongly upregulate a distinct set of matrix metalloproteinases potentially involved in tissue invasion and remodeling.

In addition, in this study, the first evidence for functional expression of $5\text{-}HT_{2C}$ receptors on resident alveolar MΦ (rAMΦ) is provided. The inventory of 5-HT type 2 receptors in mouse lung MΦ and alveolar epithelial cells (AEC) was investigated by qPCR, which

revealed the expression of receptor subunits 5-HT_{2A} and 5-HT_{2B} on AEC and 5-HT_{2C} on rAMΦ. Upon 5-HT stimulation, freshly isolated rAMΦ increased expression of CCL2 mRNA as assessed by qPCR. Moreover, rAMΦ stimulated with 5-HT augmented production of CCL2 protein as indicated by dot-blot assay and enzyme-linked immunosorbent assay. In rAMΦ isolated from $5HT_{2C}$-deficient mice, CCL2 production at both the mRNA and protein level was not affected by 5-HT stimulation. The response of rAMΦ to 5-HT was also assessed at the whole mouse genome level, by microarray. Genes that were identified by microarray as being regulated were involved in cytokine activity, signal transduction, biosynthetic processes or cell differentiation. Taken together, these data demonstrate the presence of functional 5-HT_{2C} receptors on rAMΦ and identify 5-HT as a novel modulator of rAMΦ function.

Collectively, these data provide new insight into the changes of the genetic profiles of PBMo and their lung descendents, namely DC and MΦ under non-inflammatory, steady-state conditions. Genes involved in cell trafficking expressed on DC were validated at the protein level, while expression of the 5-HT_{2C} receptor in rAMΦ was investigated for its functionality. These findings will help to better understand the complex relations within the mononuclear phagocyte pool of the lung.

6. Zusammenfassung

Periphere Blut Monozyten (PBMo) entstammen dem Knochenmark, sie zirkulieren im Blut und können in verschiedene Organe einwandern, wobei sich PBMo im Gewebe zu Zellen des Mononukleären Systems (MPS), wie Makrophagen (MΦ) und dendritische Zellen (DC) differenzieren.

Wie in anderen Organen ist der Prozess des Auswanderns und Differenzierens von PBMo auch in der Lunge notwendig, um die Funktion des pulmonalen Monozyten-Makrophagen Systems unter entzündlichen und nicht-entzündlichen Bedingungen zu gewährleisten. Während sich viele Studien der Entzündungs-gerichteten Monozyten-Einwanderung in die Lunge gewidmet haben, ist über die Migration und pulmonale Weiterentwicklung von PBMo unter nicht-entzündlichen Bedingungen vergleichsweise wenig bekannt.

Um das Transkriptionsprofil von zirkulierenden und in der Lunge residenten Zellen des MPS zu untersuchen, wurden PBMo, Lungen-MΦ und Lungen-DC von gesunden Mäusen mittels Durchflusszytometrie hochrein sortiert und ihre zelluläre Genexpression durch DNA-Microarray in einem Genom-weiten Maßstab verglichen. Unterschiedlich expremierte Gene wurden durch quantitative Polymerase-Ketten-Reaktion (qPCR) und auf Protein-Ebene mittels Durchflusszytometrie bestätigt.

Differenziell regulierte Gene, die im Zusammenhang mit Zellmigration stehen, wurden ausgewählt und in drei Gruppen unterteilt: (i) Matrix Metalloproteinasen, (ii) Chemokine / Chemokin-Rezeptoren, und (iii) Integrine. Expressionsprofile dieser Gen-Cluster wurden in Subpopulationen von zirkulierenden PBMo ($GR1^-$ versus $GR1^+$) und Lungen MΦ (alveoläre MΦ versus interstitielle MΦ) auf mRNA und Proteine weiter untersucht. Diese Daten zeigten, dass in zirkulierenden Monozyten und ihren residenten Nachkommen in der Lunge unterschiedliche genetische Programme aktiviert werden. Pulmonale DC aktivieren eine äußerst heterogene Gruppe von Genen, erhalten jedoch weitgehend ein mobiles Zellprofil mit hoher Expression von Integrinen, Chemokinen und Chemokin-Rezeptoren. Im Gegensatz dazu regulieren interstitielle und alveoläre MΦ die Genexpression von Zellmigrations-relevanten Molekülen herunter, aktivieren hingegen

die Genexpression einer bestimmten Gruppe von Matrix Metalloproteinasen, die möglicherweise am Prozess des Gewebeumbaus und der Zellinvasion beteiligt sind.
Desweiteren wurde in dieser Studie der erste Beleg für die funktionelle Expression von 5-HT_{2C} Rezeptoren auf residenten alveolären MΦ (rAMΦ) erbracht. Die 5-HT Typ 2 Rezeptoren in MΦ und Alveolarepithelzellen (AEC) der Mauslunge wurden mittels qPCR untersucht, die die Expression von den Rezeptor-Untereinheiten 5-HT_{2A} und 5-HT_{2B} auf AEC-und von 5-HT_{2C} auf rAMΦ ergab. Frisch isolierte rAMΦ stimuliert mit 5-HT, erhöhten die Expression von CCL2 mRNA und die Produktion des CCL2 Proteins, gezeigt durch qPCR, Dot-Blot und Enzyme Linked Immunosorbent Assay.
In rAMΦ von $5HT_{2C}$-defizienten Mäusen wurde die CCL2 Produktion sowohl auf mRNA als auch auf Protein-Ebene durch 5-HT-Stimulation nicht gesteigert. Die transkriptionelle Reaktion von rAMΦ auf 5-HT wurde zusätzlich auf der Ebene des kompletten Mausgenoms mittels Microarray geprüft. Nach 5-HT Behandlung differenziell regulierte Gene, die mittels Microarray identifiziert wurden, sind an Zytokin-Aktivität, Signaltransduktion, Biosynthese-Prozessen und Zelldifferenzierung beteiligt. Diese Daten zeigen das Vorhandensein von funktionellen 5-HT_{2C} Rezeptoren auf rAMΦ und identifizieren 5-HT als neuartigen Modulator der Funktion von rAMΦ. Zusammengenommen bieten diese Daten neue Einblicke in die Veränderungen der genetischen Profile von PBMo und ihrer residenten Nachkommen (DC und MΦ) in der Lunge unter nicht-entzündlichen Bedingungen. Gene, die in die Zellmigration von DC involviert sind, wurden auf Protein-Ebene bestätigt, während für den 5-HT_{2C} Rezeptor auf rAMΦ gezeigt wurde, dass dieser funktionell aktiv ist und die zelluläre Antwort auf 5-HT vermittelt. Diese Ergebnisse werden dazu beitragen die komplexen Beziehungen innerhalb des Monozyten-Makrophagen-Pools in der Lunge besser zu verstehen.

7. Appendix

7.1 Reagents and source of supply

Acetic acid	Merck, Germany
Acetonitrile	Sigma-Aldrich, Germany
Acrylamide solution, Rotiphorese Gel 30	Roth, Germany
Agarose, low-melting	Sigma-Aldrich, Germany
Ammonium persulfate (APS)	Promega, Germany
Antibiotics (Penicillin/Streptomycin)	PAA Laboratories, Austria
Bovine serum albumin (BSA)	Sigma-Aldrich, Germany
Bromophenol blue	Sigma-Aldrich, Germany
Calibrate beads	BD Biosciences, Germany
Collagenase A	Roche, USA
DC protein assay	Bio-Rad, Germany
Distilled water	Braun, Germany
DifcoTM skim milk	BD Pharmingen, Germany
Dithiothreitol (DTT)	Invitrogen, UK
DNAse	Serva, Germany
dNTPs	Roche, USA
DMEM medium	PAA Laboratories, Austria
E.coli (0111:B4) ultrapure lipopolysaccharide (LPS)	Calbiochem, Germany
ECL Plus Western Blotting Detection System	Amersham Biosciences, UK
EDTA	Biochrom, Germany
ELISA kits	R&D Systems, Germany
Ethanol	Riedel-de-Hän, Germany
Ethidium bromide solution	Carl Roth, Germany
Octagam (human IgG for Fc-blocking)	Octapharma, Germany
Fetal calf serum (FCS)	PAA Laboratories, Austria
Glycine	Sigma-Aldrich, Germany

Hank's buffered saline solution (HBSS)	PAA laboratories, Austria
HEPES buffer	Invitrogen, UK
Hydrochloric acid (HCl)	Merck, Germany
Isoflurane	Abbott, Germany
Ketavet (Ketamine hydrochloride)	Pharmacia&Upjohn,Germany
M-MLV reverse transcriptase	Invitrogen, UK
N,N,N',N'-tetramethyl-ethane-1,2-diamine (TEMED)	Sigma-Aldrich, Germany
May-Grünwald/Giemsa staining solutions	Merck, Germany
Paraformaldehyde (PFA)	Sigma-Aldrich, Germany
Phosphate buffered saline (PBS)	PAA Laboratories, Austria
Platinum Taq DNA polymerase	Invitrogen, UK
Platinum SYBR Green qPCR SuperMix-UDG	Invitrogen, UK
Protease inhibitor cocktail	Roche, Germany
Random hexamers	Boehringer, Germany
RNA amplification/labeling kit	Agilent, USA
RNA isolation kit, RNeasy mini	Qiagen, Germany
RNA isolation kit, Rneasy mikro	Qiagen, Germany
RNase away	Molecular bioproducts, USA
RNase inhibitor	Promega, USA
Rompun (Xylazine hydrochloride)	Bayer, Germany
RPMI-1640 medium	PAA laboratories, Austria
Sodium chloride (0.9% NaCl solution)	Braun, Germany
Sodium dodecyl sulfate (SDS)	Sigma-Aldrich, Germany
β-mercaptoethanol	Sigma-Aldrich, Germany
Tris	Carl Roth, Germany
Trypan blue	Sigma-Aldrich, Germany
Tween 20	Sigma-Aldrich, Germany
5× first strand buffer for cDNA synthesis	Invitrogen, Germany

7.2 Equipment and source of supply

Abbocath	Abbott, Germany
Agilent Bioanalyzer 2100	Agilent Biosystems, USA
Autoradiography film	GE Healthcare, UK
BioDocAnalyse video system	Whatman-Biometra,Germany
Cell culture incubator	Heraeus, Germany
Cell-culture plates: 12, 24, 48 wells	BD Labware, USA
Centrifuges	Heraeus, Germany
Cytospin cytocentrifuge	Thermo Scientific, Germany
Developing machine for X-ray films, Curix 60	Agfa, Germany
EDTA coated tubes	Sarstedt, Germany
Electrophoresis apparatus	Keutz, Germany
ELISA reader	Molecular Devices, USA
ELISA 96-well plate autowasher	Tecan, Germany
Eppendorf tubes (0.6 ml; 1.5 ml; 2 ml)	Eppendorf, Germany
Falcons (15 ml; 50 ml)	BD Falcon, USA
FACSCanto	BD, Germany
FACSDiva Software Package	BD, Germany
FACSVantage	BD, Germany
Filter tip	Greiner bio-one, Germany
Filter units	Millipore, USA
Film cassette	Cronex, Germany
Fluorescence spectrophotometer	BD, USA
Hybridization oven	Stovall, USA
MACS cell isolation columns	Miltenyi Biotech, Germany
Magnetic stir bar	Roth, Germany
Microarray whole mouse genome 44k chip	Agilent, USA
Microarray chip scanner Genepix 4000A	Molecular Devices, USA
Mini Protean 3 cell	Bio-Rad, USA
Mini spin centrifuge	Eppendorf, Germany

Mini Trans Blot	Bio-Rad, USA
PCR tubes (0.2 ml)	Applied Biosystems, USA
Pipettes	Gilson, France
Pipette tips	BD, Germany
Power supply	Biometra, Germany
PVDF transfer membrane	GE Healthcare, UK
Serological pipettes	BD Falcon, USA
Sequence Detection System 7900 HT	Agilent Biosystems, USA
Stereomicroscope	Leica, Germany
Vortex machine	Scientific Industries,Germany

7.3 List of primers designed for qPCR

Gene	forward primers 5′→ 3′	reverse primers 3′→ 5′
adam23	GCTCCACGTATCGGTCAACT	CCCACGTCTGTATCATCGTCT
adamts2	AGTGGGCCCTGAAGAAGTG	CAGAAGGCTCGGTGTACCAT
adam19	GCTGGTCTCCACCTTTCTGT	CAGAACTGCCAACACGAAGA
adam8	TAGACCTGATCCTCCCACCA	ACCTTTGGCTCACCAGCTC
mmp12	TGATGCAGCTGTCTTTGACC	GTGGAAATCAGCTTGGGGTA
mmp13	ATCCCTTGATGCCATTACCA	AAGAGCTCAGCCTCAACCTG
mmp14	GCCCAATGGGAAGACCTACT	AGGGTACTCGCTGTCCACTG
mmp19	TCCAGTGACTGCAAAACCTG	AGTCGCCCTTGAAAGCATAA
Itgae	TGGCTCTCAATTATCCCAGAA	CATGACCAGGACAGAAGCAA
Itgam	GGACTCTCATGCCTCCTTTG	ACTTGGTTTTGTGGGTCCTG
Itgb3	GTCCGCTACAAAGGGGAGAT	TAGCCAGTCCAGTCCGAGTC
Itgb7	GAGGACTCCAGCAATGTGGT	GGGAGTGGAGAGTGCTCAAG
itga4	TTCGGAAAAATGGAAAGTGG	AACTTTTGGGTGTGGCTCTG
itgax	GAACCCCAAAAACCACCTTC	CGACCACACTGGTCTTCTCC
sell	AAACGAAAGGCAGCTCTCTG	CCCGTAATACCCTGCATCAC
ccl2	AGCATCCACGTGTTGGCT C	CCAGCCTACTCATTGGGATCAT
ccl5	CTGCTTTGCCTAGGTCTCCCT	CGGTTCCTTCGAGTGACAAAC
ccr2	TCTTTGGTTTTGTGGGCAACA	TCAGAGATGGCCAAGTTGAGC
ccr7	GTGGTGGCTCTCCTTGTCAT	GAAGCACACCGACTCGTACA
gapdh	TGGTGAAGGTCGGTGTGAAC	TGAATTTGCCGTGAGTGGAG
il18	CTGGCTGTGACCCTCTCTGT	CTGGAACACGTTTCTGAAAGAAT
htr2a	ATAGCCGCTTCAACTCCAGA	TCATCCTGTAGCCCGAAGAC
htr2b	GCAGATTTGCTGGTTGGATT	ATAACCAGGCAGGACACAGG
htr2c	GTTCAATTCGCGGACTAAGG	TCACGAACACTTTGCTTTCG
gzma	CTCCGTGGTGGAAAGGACT	GGCGATCTCCACACTTCTCT
gzmb	CCAAAGACCAAACGTGCTTC	GAAAGCACGTGGAGGTGAAC
gzmk	GATGCCAGAGGTCAAAAGGA	GCGATGCCACATTTATAGCC
gzmm	TTAAAGGCTGGGAGCAAGAG	GCAGGTTTTGGAGCTGAAAG
gramd3	GATCGCCCTTCGTCTCTGC	GATTCCGGAGTCTGGGATCC
sphk1	GATGCATGAGGTGGTGAATG	TGCTCGTACCCAGCATAGTG

Gene	**forward primers 5′→ 3′**	**reverse primers 3′→ 5′**
csf1	CCAAGAACTGCAACAACAGC	CACTGCTAGGGGTGGCTTTA
dpf1	TCCAAGAAGACTGGGTGTCC	CACCGTGAACTGTAAACACGA
nt5e	CACCCTGAAGAAGGCTTTTG	TCCAGGGCTTTCGGTTAATA
il20rb	CCAGCCTACGTGTGTGGAG	TCAGCATGAAGCCAACAAAC
myo1d	ATGAGCTGAAACGCAAGGAC	GGTGACGGTCAGTGACAAAA
flrt3	TACCTTTGGCTGCCATCATT	ACAGTGACCCGTTCCTATGC
tgfbi	CCATGCCTCCAGAAGAACTG	CTCCGCTAACCAGGATTTCA
ptges	ATGCGCTGAAACGTGGAG	GAAGCCGAGGAAGAGGAAAG
icosl	GGCATTCGTTTCCTTCATCA	AGGCGTGGTCTGTAAGTTCAA
slc7a2	AACCCTCTTCAGCCCCTCT	GGACGCCATACGTGGTTAGA
htra1	AGGGAAAGCTGTCACCAAGA	TGACGGTCCTTCAGCTCTTT
spp1	GCTTGGCTTATGGACTGAGG	CGCTCTTCATGTGAGAGGTG
actb	ACCCTAAGGCCAACCGTG A	CAGAGGCATACAGGGACAGCA
hmbs	TGGTGAAGGTCGGTGTGAAC	TGAATTTGCCGTGAGTGGAG

8. References

1. Gordon, S. and P.R. Taylor, *Monocyte and macrophage heterogeneity.* Nat Rev Immunol, 2005. 5(12): p. 953-64.
2. Herbomel, P., B. Thisse, and C. Thisse, *Ontogeny and behaviour of early macrophages in the zebrafish embryo.* Development, 1999. 126(17): p. 3735-45.
3. McCusker, K. and J. Hoidal, *Characterization of scavenger receptor activity in resident human lung macrophages.* Exp Lung Res, 1989. 15(4): p. 651-61.
4. Smythies, L.E., et al., *Human intestinal macrophages display profound inflammatory anergy despite avid phagocytic and bacteriocidal activity.* J Clin Invest, 2005. 115(1): p. 66-75.
5. Helmy, K.Y., et al., *CRIg: a macrophage complement receptor required for phagocytosis of circulating pathogens.* Cell, 2006. 124(5): p. 915-27.
6. Auffray, C., M.H. Sieweke, and F. Geissmann, *Blood monocytes: development, heterogeneity, and relationship with dendritic cells.* Annu Rev Immunol, 2009. 27: p. 669-92.
7. Geissmann, F., S. Jung, and D.R. Littman, *Blood monocytes consist of two principal subsets with distinct migratory properties.* Immunity, 2003. 19(1): p. 71-82.
8. Auffray, C., et al., *Monitoring of blood vessels and tissues by a population of monocytes with patrolling behavior.* Science, 2007. 317(5838): p. 666-70.
9. Serbina, N.V., et al., *Monocyte-mediated defense against microbial pathogens.* Annu Rev Immunol, 2008. 26: p. 421-52.
10. Libby, P., et al., *Diversity of denizens of the atherosclerotic plaque: not all monocytes are created equal.* Circulation, 2008. 117(25): p. 3168-70.
11. Serbina, N.V. and E.G. Pamer, *Monocyte emigration from bone marrow during bacterial infection requires signals mediated by chemokine receptor CCR2.* Nat Immunol, 2006. 7(3): p. 311-7.
12. Randolph, G.J., et al., *Differentiation of phagocytic monocytes into lymph node dendritic cells in vivo.* Immunity, 1999. 11(6): p. 753-61.
13. Nahrendorf, M., et al., *The healing myocardium sequentially mobilizes two monocyte subsets with divergent and complementary functions.* J Exp Med, 2007. 204(12): p. 3037-47.
14. Sunderkotter, C., et al., *Subpopulations of mouse blood monocytes differ in maturation stage and inflammatory response.* J Immunol, 2004. 172(7): p. 4410-7.
15. Fogg, D.K., et al., *A clonogenic bone marrow progenitor specific for macrophages and dendritic cells.* Science, 2006. 311(5757): p. 83-7.
16. Varol, C., et al., *Monocytes give rise to mucosal, but not splenic, conventional dendritic cells.* J Exp Med, 2007. 204(1): p. 171-80.
17. Landsman, L. and S. Jung, *Lung macrophages serve as obligatory intermediate between blood monocytes and alveolar macrophages.* J Immunol, 2007. 179(6): p. 3488-94.
18. Landsman, L., C. Varol, and S. Jung, *Distinct differentiation potential of blood monocyte subsets in the lung.* J Immunol, 2007. 178(4): p. 2000-7.

19. Becker, S., M.K. Warren, and S. Haskill, *Colony-stimulating factor-induced monocyte survival and differentiation into macrophages in serum-free cultures.* J Immunol, 1987. 139(11): p. 3703-9.
20. Sallusto, F. and A. Lanzavecchia, *Efficient presentation of soluble antigen by cultured human dendritic cells is maintained by granulocyte/macrophage colony-stimulating factor plus interleukin 4 and downregulated by tumor necrosis factor alpha.* J Exp Med, 1994. 179(4): p. 1109-18.
21. Taylor, P.R., et al., *Macrophage receptors and immune recognition.* Annu Rev Immunol, 2005. 23: p. 901-44.
22. Sibille, Y. and H.Y. Reynolds, *Macrophages and polymorphonuclear neutrophils in lung defense and injury.* Am Rev Respir Dis, 1990. 141(2): p. 471-501.
23. Holt, P.G., *Down-regulation of immune responses in the lower respiratory tract: the role of alveolar macrophages.* Clin Exp Immunol, 1986. 63(2): p. 261-70.
24. Thepen, T., N. Van Rooijen, and G. Kraal, *Alveolar macrophage elimination in vivo is associated with an increase in pulmonary immune response in mice.* J Exp Med, 1989. 170(2): p. 499-509.
25. Strickland, D.H., et al., *Regulation of T-cell function in lung tissue by pulmonary alveolar macrophages.* Immunology, 1993. 80(2): p. 266-72.
26. Holt, P.G., *Regulation of antigen-presenting cell function(s) in lung and airway tissues.* Eur Respir J, 1993. 6(1): p. 120-9.
27. Mizgerd, J.P., *Acute lower respiratory tract infection.* N Engl J Med, 2008. 358(7): p. 716-27.
28. Martin, T.R. and C.W. Frevert, *Innate immunity in the lungs.* Proc Am Thorac Soc, 2005. 2(5): p. 403-11.
29. Havenith, C.E., et al., *Separation of alveolar macrophages and dendritic cells via autofluorescence: phenotypical and functional characterization.* J Leukoc Biol, 1993. 53(5): p. 504-10.
30. Hammad, H. and B.N. Lambrecht, *Dendritic cells and epithelial cells: linking innate and adaptive immunity in asthma.* Nat Rev Immunol, 2008. 8(3): p. 193-204.
31. del Rio, M.L., et al., *CD103- and CD103+ bronchial lymph node dendritic cells are specialized in presenting and cross-presenting innocuous antigen to CD4+ and CD8+ T cells.* J Immunol, 2007. 178(11): p. 6861-6.
32. de Heer, H.J., et al., *Essential role of lung plasmacytoid dendritic cells in preventing asthmatic reactions to harmless inhaled antigen.* J Exp Med, 2004. 200(1): p. 89-98.
33. van Rijt, L.S., et al., *Allergen-induced accumulation of airway dendritic cells is supported by an increase in CD31(hi)Ly-6C(neg) bone marrow precursors in a mouse model of asthma.* Blood, 2002. 100(10): p. 3663-71.
34. Vermaelen, K. and R. Pauwels, *Pulmonary dendritic cells.* Am J Respir Crit Care Med, 2005. 172(5): p. 530-51.
35. Holt, P.G., et al., *Origin and steady-state turnover of class II MHC-bearing dendritic cells in the epithelium of the conducting airways.* J Immunol, 1994. 153(1): p. 256-61.

36. McWilliam, A.S., et al., *Rapid dendritic cell recruitment is a hallmark of the acute inflammatory response at mucosal surfaces.* J Exp Med, 1994. 179(4): p. 1331-6.
37. von Wulffen, W., et al., *Lung dendritic cells elicited by Fms-like tyrosine 3-kinase ligand amplify the lung inflammatory response to lipopolysaccharide.* Am J Respir Crit Care Med, 2007. 176(9): p. 892-901.
38. Vermaelen, K.Y., et al., *Specific migratory dendritic cells rapidly transport antigen from the airways to the thoracic lymph nodes.* J Exp Med, 2001. 193(1): p. 51-60.
39. Maus, U.A., et al., *Role of resident alveolar macrophages in leukocyte traffic into the alveolar air space of intact mice.* Am J Physiol Lung Cell Mol Physiol, 2002. 282(6): p. L1245-52.
40. Lambrecht, B.N. and H. Hammad, *Taking our breath away: dendritic cells in the pathogenesis of asthma.* Nat Rev Immunol, 2003. 3(12): p. 994-1003.
41. Berger, M., J.A. Gray, and B.L. Roth, *The expanded biology of serotonin.* Annu Rev Med, 2009. 60: p. 355-66.
42. Lesurtel, M., et al., *Platelet-derived serotonin mediates liver regeneration.* Science, 2006. 312(5770): p. 104-7.
43. Dale, G.L., et al., *Stimulated platelets use serotonin to enhance their retention of procoagulant proteins on the cell surface.* Nature, 2002. 415(6868): p. 175-9.
44. Mossner, R. and K.P. Lesch, *Role of serotonin in the immune system and in neuroimmune interactions.* Brain Behav Immun, 1998. 12(4): p. 249-71.
45. Shibazaki, M., M. Nakamura, and Y. Endo, *Biphasic, organ-specific, and strain-specific accumulation of platelets induced in mice by a lipopolysaccharide from Escherichia coli and its possible involvement in shock.* Infect Immun, 1996. 64(12): p. 5290-5294.
46. Yoshida, A., et al., *Accumulation of platelets in the lung and liver and their degranulation following antigen-challenge in sensitized mice.* Br J Pharmacol, 2002. 137(2): p. 146-152.
47. O'Connell, P.J., et al., *A novel form of immune signaling revealed by transmission of the inflammatory mediator serotonin between dendritic cells and T cells.* Blood, 2006. 107(3): p. 1010-1017.
48. Nakamura, K., et al., *Role of a Serotonin Precursor in Development of Gut Microvilli.* Am J Pathol, 2008. 172(2): p. 333-344.
49. Kushnir-Sukhov, N.M., et al., *Human mast cells are capable of serotonin synthesis and release.* J Allergy Clin Immunol, 2007. 119(2): p. 498-9.
50. Fazzino, F., et al., *Serotonin transporter is differentially localized in subpopulations of lymphocytes of major depression patients. Effect of fluoxetine on proliferation.* J Neuroimmunol, 2008. 196(1-2): p. 173-180.
51. Rudd, M.L., et al., *Peritoneal macrophages express the serotonin transporter.* J Neuroimmunol, 2005. 159(1-2): p. 113-118.
52. Idzko, M., et al., *The serotoninergic receptors of human dendritic cells: identification and coupling to cytokine release.* J Immunol, 2004. 172(10): p. 6011-9.

53. Durk, T., et al., *5-Hydroxytryptamine modulates cytokine and chemokine production in LPS-primed human monocytes via stimulation of different 5-HTR subtypes.* Int Immunol, 2005. 17(5): p. 599-606.
54. Cloez-Tayarani, I., et al., *Differential effect of serotonin on cytokine production in lipopolysaccharide-stimulated human peripheral blood mononuclear cells: involvement of 5-hydroxytryptamine2A receptors.* Int Immunol, 2003. 15(2): p. 233-40.
55. Freire-Garabal, M., et al., *Serotonin upregulates the activity of phagocytosis through 5-HT1A receptors.* Br J Pharmacol, 2003. 139(2): p. 457-63.
56. Hoyer, D., et al., *International Union of Pharmacology classification of receptors for 5-hydroxytryptamine (Serotonin).* Pharmacol Rev, 1994. 46(2): p. 157-203.
57. Fabre, A., et al., *Modulation of bleomycin-induced lung fibrosis by serotonin receptor antagonists in mice.* Eur Respir J, 2008. 32(2): p. 426-36.
58. Hironaka, E., et al., *Serotonin receptor antagonist inhibits monocrotaline-induced pulmonary hypertension and prolongs survival in rats.* Cardiovasc Res, 2003. 60(3): p. 692-9.
59. Wang, L., et al., *'Tuning' of type I interferon-induced Jak-STAT1 signaling by calcium-dependent kinases in macrophages.* Nat Immunol, 2008. 9(2): p. 186-93.
60. Russell, J.H. and T.J. Ley, *Lymphocyte-mediated cytotoxicity.* Annu Rev Immunol, 2002. 20: p. 323-70.
61. Simon, M.M., et al., *Release of biologically active fragments from human plasma-fibronectin by murine T cell-specific proteinase 1 (TSP-1).* Biol Chem Hoppe Seyler, 1988. 369 Suppl: p. 107-12.
62. Lieberman, J., *The ABCs of granule-mediated cytotoxicity: new weapons in the arsenal.* Nat Rev Immunol, 2003. 3(5): p. 361-70.
63. Bots, M. and J.P. Medema, *Granzymes at a glance.* J Cell Sci, 2006. 119(Pt 24): p. 5011-4.
64. Buzza, M.S. and P.I. Bird, *Extracellular granzymes: current perspectives.* Biol Chem, 2006. 387(7): p. 827-37.
65. Romero, V. and F. Andrade, *Non-apoptotic functions of granzymes.* Tissue Antigens, 2008. 71(5): p. 409-16.
66. Froelich, C.J., J. Pardo, and M.M. Simon, *Granule-associated serine proteases: granzymes might not just be killer proteases.* Trends Immunol, 2009. 30(3): p. 117-23.
67. Rissoan, M.C., et al., *Subtractive hybridization reveals the expression of immunoglobulin-like transcript 7, Eph-B1, granzyme B, and 3 novel transcripts in human plasmacytoid dendritic cells.* Blood, 2002. 100(9): p. 3295-303.
68. Tschopp, C.M., et al., *Granzyme B, a novel mediator of allergic inflammation: its induction and release in blood basophils and human asthma.* Blood, 2006. 108(7): p. 2290-9.
69. Pardo, J., et al., *Granzyme B is expressed in mouse mast cells in vivo and in vitro and causes delayed cell death independent of perforin.* Cell Death Differ, 2007. 14(10): p. 1768-79.
70. Strik, M.C., et al., *Human mast cells produce and release the cytotoxic lymphocyte associated protease granzyme B upon activation.* Mol Immunol, 2007. 44(14): p. 3462-72.

71. Buzza, M.S., et al., *Extracellular matrix remodeling by human granzyme B via cleavage of vitronectin, fibronectin, and laminin.* J Biol Chem, 2005. 280(25): p. 23549-58.
72. Knickelbein, J.E., et al., *Noncytotoxic lytic granule-mediated CD8+ T cell inhibition of HSV-1 reactivation from neuronal latency.* Science, 2008. 322(5899): p. 268-71.
73. Chowdhury, D. and J. Lieberman, *Death by a thousand cuts: granzyme pathways of programmed cell death.* Annu Rev Immunol, 2008. 26: p. 389-420.
74. Metkar, S.S., et al., *Human and mouse granzyme A induce a proinflammatory cytokine response.* Immunity, 2008. 29(5): p. 720-33.
75. Tecott, L.H., et al., *Eating disorder and epilepsy in mice lacking 5-HT2c serotonin receptors.* Nature, 1995. 374(6522): p. 542-6.
76. Vermaelen, K. and R. Pauwels, *Accurate and simple discrimination of mouse pulmonary dendritic cell and macrophage populations by flow cytometry: methodology and new insights.* Cytometry A, 2004. 61(2): p. 170-77.
77. Maus, U., et al., *Monocytes recruited into the alveolar air space of mice show a monocytic phenotype but upregulate CD14.* Am J Physiol Lung Cell Mol Physiol, 2001. 280(1): p. L58-68.
78. Chiang, C.S., et al., *Functional phenotype of macrophages depends on assay procedures.* Int Immunol, 2008. 20(2): p. 215-22.
79. Schneider, J., et al., *Systematic analysis of T7 RNA polymerase based in vitro linear RNA amplification for use in microarray experiments.* BMC Genomics, 2004. 5(1): p. 29.
80. Wilhelm, J., et al., *Systematic comparison of the T7-IVT and SMART-based RNA preamplification techniques for DNA microarray experiments.* Clin Chem, 2006. 52(6): p. 1161-7.
81. Imhof, B.A. and M. Aurrand-Lions, *Adhesion mechanisms regulating the migration of monocytes.* Nat Rev Immunol, 2004. 4(6): p. 432-44.
82. Crowell, R.E., et al., *Alveolar and interstitial macrophage populations in the murine lung.* Exp Lung Res, 1992. 18(4): p. 435-46.
83. Sung, S.S., et al., *A major lung CD103 (alphaE)-beta7 integrin-positive epithelial dendritic cell population expressing Langerin and tight junction proteins.* J Immunol, 2006. 176(4): p. 2161-72.
84. Zaslona, Z., et al., *Transcriptome profiling of primary murine monocytes, lung macrophages and lung dendritic cells reveals a distinct expression of genes involved in cell trafficking.* Respir Res, 2009. 10: p. 2.
85. Oku, M., et al., *Peroxisome degradation requires catalytically active sterol glucosyltransferase with a GRAM domain.* EMBO J, 2003. 22(13): p. 3231-41.
86. Tsujita, K., et al., *Myotubularin regulates the function of the late endosome through the gram domain-phosphatidylinositol 3,5-bisphosphate interaction.* J Biol Chem, 2004. 279(14): p. 13817-24.
87. Maus, U., et al., *Molecular pathways of monocyte emigration into the alveolar air space of intact mice.* Am J Respir Crit Care Med, 2002. 165(1): p. 95-100.
88. Maus, U., et al., *The role of CC chemokine receptor 2 in alveolar monocyte and neutrophil immigration in intact mice.* Am J Respir Crit Care Med, 2002. 166(3): p. 268-73.

89. Lehtonen, A., et al., *Gene expression profiling during differentiation of human monocytes to macrophages or dendritic cells.* J Leukoc Biol, 2007. 82(3): p. 710-20.
90. Chen, Z., et al., *Analysis of the gene expression profiles of immature versus mature bone marrow-derived dendritic cells using DNA arrays.* Biochem Biophys Res Commun, 2002. 290(1): p. 66-72.
91. McIlroy, D., et al., *Profiling dendritic cell maturation with dedicated microarrays.* J Leukoc Biol, 2005. 78(3): p. 794-803.
92. Li, J., et al., *cDNA microarray analysis reveals fundamental differences in the expression profiles of primary human monocytes, monocyte-derived macrophages, and alveolar macrophages.* J Leukoc Biol, 2007. 81(1): p. 328-35.
93. Srivastava, M., et al., *The inflammatory versus constitutive trafficking of mononuclear phagocytes into the alveolar space of mice is associated with drastic changes in their gene expression profiles.* J Immunol, 2005. 175(3): p. 1884-93.
94. Brinckerhoff, C.E. and L.M. Matrisian, *Matrix metalloproteinases: a tail of a frog that became a prince.* Nat Rev Mol Cell Biol, 2002. 3(3): p. 207-14.
95. McQuibban, G.A., et al., *Matrix metalloproteinase processing of monocyte chemoattractant proteins generates CC chemokine receptor antagonists with anti-inflammatory properties in vivo.* Blood, 2002. 100(4): p. 1160-7.
96. Schonbeck, U., F. Mach, and P. Libby, *Generation of biologically active IL-1 beta by matrix metalloproteinases: a novel caspase-1-independent pathway of IL-1 beta processing.* J Immunol, 1998. 161(7): p. 3340-6.
97. Preece, G., G. Murphy, and A. Ager, *Metalloproteinase-mediated regulation of L-selectin levels on leucocytes.* J Biol Chem, 1996. 271(20): p. 11634-40.
98. Klier, C.M. and P.J. Nelson, *Chemokine-induced extravasation of MonoMac 6 cells: chemotaxis and MMP activity.* Ann N Y Acad Sci, 1999. 878: p. 575-7.
99. Okada, T., et al., *Chemokine requirements for B cell entry to lymph nodes and Peyer's patches.* J Exp Med, 2002. 196(1): p. 65-75.
100. Yamamoto, T., et al., *Monocyte chemoattractant protein-1 enhances gene expression and synthesis of matrix metalloproteinase-1 in human fibroblasts by an autocrine IL-1 alpha loop.* J Immunol, 2000. 164(12): p. 6174-9.
101. Maus, U.A., et al., *Monocytes are potent facilitators of alveolar neutrophil emigration during lung inflammation: role of the CCL2-CCR2 axis.* J Immunol, 2003. 170(6): p. 3273-8.
102. Winter, C., et al., *Lung-specific overexpression of CC chemokine ligand (CCL) 2 enhances the host defense to Streptococcus pneumoniae infection in mice: role of the CCL2-CCR2 axis.* J Immunol, 2007. 178(9): p. 5828-38.
103. Herold, S., et al., *Alveolar epithelial cells direct monocyte transepithelial migration upon influenza virus infection: impact of chemokines and adhesion molecules.* J Immunol, 2006. 177(3): p. 1817-24.
104. Stokes, L. and A. Surprenant, *Purinergic P2Y2 receptors induce increased MCP-1/CCL2 synthesis and release from rat alveolar and peritoneal macrophages.* J Immunol, 2007. 179(9): p. 6016-23.
105. Nakayama, T., et al., *Prostaglandin E2 promotes degranulation-independent release of MCP-1 from mast cells.* J Leukoc Biol, 2006. 79(1): p. 95-104.

106. Di, A., B. Krupa, and D.J. Nelson, *Calcium-G protein interactions in the regulation of macrophage secretion.* J Biol Chem, 2001. 276(40): p. 37124-32.
107. Christensen, P.J., et al., *Expression and functional implications of CCR2 expression on murine alveolar epithelial cells.* Am J Physiol Lung Cell Mol Physiol, 2004. 286(1): p. L68-72.
108. Prasse, A., et al., *Essential role of osteopontin in smoking-related interstitial lung diseases.* Am J Pathol, 2009. 174(5): p. 1683-91.
109. Kohan, M., R. Breuer, and N. Berkman, *Osteopontin induces airway remodeling and lung fibroblast activation in a murine model of asthma.* Am J Respir Cell Mol Biol, 2009. 41(3): p. 290-6.
110. Kohan, M., et al., *Enhanced osteopontin expression in a murine model of allergen-induced airway remodelling.* Clin Exp Allergy, 2007. 37(10): p. 1444-54.
111. Eckle, T., et al., *Identification of ectonucleotidases CD39 and CD73 in innate protection during acute lung injury.* J Immunol, 2007. 178(12): p. 8127-37.
112. Reutershan, J., et al., *Adenosine and inflammation: CD39 and CD73 are critical mediators in LPS-induced PMN trafficking into the lungs.* FASEB J, 2009. 23(2): p. 473-82.
113. Volmer, J.B., L.F. Thompson, and M.R. Blackburn, *Ecto-5'-nucleotidase (CD73)-mediated adenosine production is tissue protective in a model of bleomycin-induced lung injury.* J Immunol, 2006. 176(7): p. 4449-58.
114. Vermaelen, K.Y., et al., *Matrix metalloproteinase-9-mediated dendritic cell recruitment into the airways is a critical step in a mouse model of asthma.* J Immunol, 2003. 171(2): p. 1016-22.
115. Ratzinger, G., et al., *Matrix metalloproteinases 9 and 2 are necessary for the migration of Langerhans cells and dermal dendritic cells from human and murine skin.* J Immunol, 2002. 168(9): p. 4361-71.
116. Zigrino, P., et al., *Stromal Expression of MMP-13 Is Required for Melanoma Invasion and Metastasis.* J Invest Dermatol, 2009.
117. Moss, N.M., et al., *Ovarian cancer cell detachment and multicellular aggregate formation are regulated by membrane type 1 matrix metalloproteinase: a potential role in I.p. metastatic dissemination.* Cancer Res, 2009. 69(17): p. 7121-9.
118. Matsui, T., et al., *CD2 distinguishes two subsets of human plasmacytoid dendritic cells with distinct phenotype and functions.* J Immunol, 2009. 182(11): p. 6815-23.
119. Korthals, M., et al., *Monocyte derived dendritic cells generated by IFN-alpha acquire mature dendritic and natural killer cell properties as shown by gene expression analysis.* J Transl Med, 2007. 5: p. 46.
120. Bonmort, M., et al., *Killer dendritic cells: IKDC and the others.* Curr Opin Immunol, 2008. 20(5): p. 558-65.
121. Motyka, B., et al., *Mannose 6-phosphate/insulin-like growth factor II receptor is a death receptor for granzyme B during cytotoxic T cell-induced apoptosis.* Cell, 2000. 103(3): p. 491-500.

122. Hernandez-Pigeon, H., et al., *UVA induces granzyme B in human keratinocytes through MIF: implication in extracellular matrix remodeling.* J Biol Chem, 2007. 282(11): p. 8157-64.
123. Horiuchi, K., et al., *Expression of granzyme B in human articular chondrocytes.* J Rheumatol, 2003. 30(8): p. 1799-810.
124. Tremblay, G.M., et al., *Granzyme activity in the inflamed lung is not controlled by endogenous serine proteinase inhibitors.* J Immunol, 2000. 165(7): p. 3966-9.
125. Bratke, K., et al., *Increase in granzyme B+ lymphocytes and soluble granzyme B in bronchoalveolar lavage of allergen challenged patients with atopic asthma.* Clin Exp Immunol, 2004. 136(3): p. 542-8.
126. Hermsen, C.C., et al., *Circulating concentrations of soluble granzyme A and B increase during natural and experimental Plasmodium falciparum infections.* Clin Exp Immunol, 2003. 132(3): p. 467-72.
127. Lauw, F.N., et al., *Soluble granzymes are released during human endotoxemia and in patients with severe infection due to gram-negative bacteria.* J Infect Dis, 2000. 182(1): p. 206-13.
128. Sower, L.E., et al., *Extracellular activities of human granzyme A. Monocyte activation by granzyme A versus alpha-thrombin.* J Immunol, 1996. 156(7): p. 2585-90.
129. Sower, L.E., et al., *Extracellular activities of human granzymes. I. Granzyme A induces IL6 and IL8 production in fibroblast and epithelial cell lines.* Cell Immunol, 1996. 171(1): p. 159-63.

9. Declaration

Ich erkläre: Ich habe die vorgelegte Dissertation selbständig ohne unerlaubte fremde Hilfe und nur mit den Hilfen angefertigt, die ich in der Dissertation angegeben habe. Alle Textstellen, die wörtlich oder sinngemaß aus veröffentlichten oder nicht veröffentlichten Schriften entnommen sind, und alle Angaben, die auf mündlichen Auskünften beruhen, sind als solche kenntlich gemacht. Bei den von mir durchgeführten und in der Dissertation erwähnten Untersuchungen habe ich die Grundsätze guter wissenschaftlicher Praxis, wie sie in der „Satzung der Justus-Liebig-Universität Gießen zur Sicherung guter wissenschaftlicher Praxis“ niedergelegt sind, eingehalten.“

Zbigniew Jan Zasłona

Der Lebenslauf wurde aus der elektronischen Version der Arbeit entfernt.

The curriculum vitae was removed from the electronic version of the paper.

Publications:

1. **Zbigniew Zasłona,** Jochen Wilhelm, Lidija Cakarova, Leigh M. Marsh, Werner Seeger, Jürgen Lohmeyer, Werner von Wulffen. "Transcriptome profiling of primary murine monocytes, lung macrophages and lung dendritic cells reveals a distinct expression of genes involved in cell trafficking." *Respiratory Research* 2009 Jan 16;10:2.

2. Maciej Cabanski, Jochen Wilhelm, **Zbigniew Zasłona**, Mirko Steinmüller, Ludger Fink, Werner Seeger, Juergen Lohmeyer. "Genome-wide transcriptional profiling of mononuclear phagocytes recruited to mouse lungs in response to alveolar challenge with the TLR2-agonist Pam3CSK4." *American Journal of Physiology – Lung Cellular and Molecular Physiology* 2009 Oct;297(4):L608-18. Epub 2009 Jul 17.

3. Zbigniew Mikulski, Petra Hartmann, Gitte Jositsch, **Zbigniew Zasłona**, Katrin S. Lips, Uwe Pfeil, Hjalmar Kurzen, Jürgen Lohmeyer, Wolfgang G. Clauss, Veronika Grau, Martin Fronius, and Wolfgang Kummer. "Nicotinic receptors on rat alveolar macrophages dampen ATP-induced increase in cytosolic calcium concentration." The manuscript is under revision in *Journal of Leukocyte Biology* and has been assigned the number J0908-558R.

4. Matthias Hecker, **Zbigniew Zasłona**, Grażyna Kwapiszewska, Anna Zakrzewicz, Jochen Wilhelm, Leigh M. Marsh, Daniel Sedding, Walter Klepetko, Jürgen Lohmeyer, Werner Seeger, Norbert Weissmann, Ralph T. Schermuly, Oliver Eickelberg, Rory E. Morty. "Dysregulation of the interleukin 13 receptor system: a novel pathomechanism in pulmonary arterial hypertension." The manuscript is under revision in *American Journal of Respiratory and Critical Care Medicine* and has been assigned the number Blue-200909-1367OC.

5. Zbigniew Mikulski*, **Zbigniew Zasłona***, Lidija Cakarova, Petra Hartmann, Jochen Wilhelm, Laurence Tecott, Juergen Lohmeyer, Wolfgang Kummer. "Serotonin activates murine alveolar macrophages through 5-HT2C receptor." The manuscript is under revision in *American Journal of Physiology – Lung Cellular and Molecular Physiology* and has been assigned the number L-00032-2010. *both authors contributed equally to the study

Poster presentations:

1. **Zbigniew Zasłona**, Jochen Wilhelm, Lidija Cakarova, Leigh M. Marsh, Werner Seeger, Jürgen Lohmeyer, Werner von Wulffen. "Transcriptome profiling of primary murine monocytes, lung macrophages and lung dendritic cells reveals a distinct expression of genes involved in cell trafficking." *114 Kongress der Deutschen Gesellschaft für Innere Medicine, Wiesbaden, Germany, 29 March – 2 April 2008.*

2. **Zbigniew Zasłona**, Jochen Wilhelm, Lidija Cakarova, Leigh M. Marsh, Werner Seeger, Jürgen Lohmeyer, Werner von Wulffen. "Transcriptome profiling of primary murine monocytes, lung macrophages and lung dendritic cells reveals a distinct expression of genes involved in cell trafficking." *ECCPS Symposium on Remodeling and Reverse Remodeling in the Cardiopulmonary System, Bad Nauheim, Germany, 29 June – 2 July 2008.*

3. **Zbigniew Zasłona**, Zbigniew Mikulski, Lidija Cakarova, Petra Hartmann, Werner von Wulffen, Jürgen Lohmeyer, Wolfgang Kummer. "Serotonin acutely elevates intracellular calcium concentration and augments CCL2 production in murine alveolar macrophages." *World Immune Regulation Meeting III, Davos, Switzerland, 22 – 25 March 2009.* **Best Poster Prize "Late breaking abstracts"**

4. **Zbigniew Zasłona**, Zbigniew Mikulski, Lidija Cakarova, Petra Hartmann, Jochen Wilhelm, Laurence Tecott, Juergen Lohmeyer, Wolfgang Kummer. "Serotonin acutely elevates intracellular calcium concentration and augments CCL2 production in murine alveolar macrophages." *Keystone Meeting, The Macrophage: Intersection of Pathogenic and Protective Inflammation, Banff, Canada, 12 – 17 February 2010*

Oral presentations:

1. **Zbigniew Zasłona** "Transcriptome profiling of primary murine monocytes, lung macrophages and lung dendritic cells reveals a distinct expression of genes involved in cell trafficking." *MBML annual retreat, Rauischholzhausen, Germany, 9 – 11 July 2007.*

2. **Zbigniew Zasłona** "Defining the role of proteinases in the biology of lung dendritic cells." *MBML annual retreat, Rauischholzhausen, Germany, 28 – 30 July 2008.*

3. **Zbigniew Zasłona** "Transcriptome profiling of primary murine monocytes, lung macrophages and lung dendritic cells reveals a distinct expression of genes involved in cell trafficking." *First GGL Conference on Life Sciences, Giessen, Germany, 30 September – 1 October 2008.*

4. **Zbigniew Zasłona** "Can biology of lung dendritic cells be a model for studying non-apoptotic role of granzymes?" *MBML annual retreat, Rauischholzhausen, Germany, 27 – 29 July 2009.*

Conferences attended as a non-presenting delegate:

1. International Symposium Frontiers in Allergy and Autoimmunity, Mainz, Germany, 30 –31 May 2008

2. First Von Behring-Röntgen Symposium. Neurotransmission then, now and tomorrow – The lessons of Loewi, Marburg, Germany 18-19 November 2009

Workshops:

1. 7th Workshop: "Animal Models of Asthma" held at the Fraunhofer Institute of Toxicology and Experimental Medicine, Hannover, Germany, 18 – 19 January 2008.

11. Acknowledgements

I would like to specially acknowledge Prof. Jürgen Lohmeyer, who gave me the opportunity to do PhD in his group and provided me with many helpful suggestions and important advices during the course of this work.

I would like to thank to my co-supervisor Dr. Werner von Wulffen, who helped me to come up with my thesis topic and introduced me to the world of flow cytometry.

Special thanks to Dr. Rory Morty for all the help that I got from him whenever it was needed, even if I did not know that it was needed.

I am grateful to my lab colleagues that worked with me: Dr. Lidija Cakarova, Katrin Högner, Dr. Susanne Herold, Dr. Leigh Marsh, Dr. Maciej Cabański, Dr. Mirko Steinmüller for help and support and working together in a friendly atmosphere. The technicians Dagmar Hensel and Petra Janssen are thanked for their help in everyday lab work and being assistance in many experiments.

I would like to say thank you to Zbigniew Mikulski and Prof. Wolfgang Kummer for starting with me the serotonin project.

I also have to say thank you to guys from judo and football especially Harald, 2×Martin, Abdul, Yunus, Kristopher, Doro, Julia, Patrick, Mo, Daniel, Sergei, Holger and others so I could enjoy sport and have strength to work in the lab without back pain.

I would like to say thank you to Prof. Krzysztof Dołowy and Prof. Huub Savelkoul, who showed me how interesting science can be and basically inspired me with their work and attitude to do PhD.

Finally my parents, brother and sister, who are far away, but I feel their support, as if they are here with me. Grandparents, those that I lost and those that are still with me.

And Magda who is with me all the time whenever I go and whatever I do.